



Summary of the Impact of Launch Vehicle Exhaust and Deorbiting Space and Meteorite Debris on Stratospheric Ozone

Prepared for:

U.S. Air Force Space and Missile Systems Center
Environmental Management Branch
SMC/AXFV

Under

Contract F09603-95-D-0176-0007

Prepared by:

Tyrrel W. Smith, Jr., Ph.D.
TRW Space & Electronics Group

and

John R. Edwards
Daniel Pilson
Environmental Management Branch

30 September 1999



Summary of the Impact of Launch Vehicle Exhaust and Deorbiting Space and Meteorite Debris on Stratospheric Ozone

Prepared for:

U.S. Air Force Space and Missile Systems Center
Environmental Management Branch
SMC/AXFV

Under

Contract F09603-95-D-0176-0007

Prepared by:

Tyrrel W. Smith, Jr., Ph.D.
TRW Space and Electronics Group

and

John R. Edwards
Daniel Pilson
Environmental Management Branch

Approved by:

John J. Lamb, Ph.D.
Program Manager

30 September 1999

Acknowledgement

The authors acknowledge the contributions of the following colleagues for their input to enhance the technical detail of this document: R. Disselkamp, M. Molina, P. Lohn, E. Wong, M. Ko, and M. Prather. We thank V. Lang, E. Beiting, B. Brady, and P. Zittel of The Aerospace Corporation for their support and their editorial comments.

CONTENTS

EXECUTIVE SUMMARY.....	1
1 INTRODUCTION.....	8
1.1 PURPOSE OF THIS REPORT.....	8
1.1.1 <i>Background</i>	8
1.1.2 <i>Impact of Launch Vehicles</i>	8
1.1.3 <i>Ozone Depleting Chemicals</i>	9
1.2 SCOPE OF THIS REPORT.....	10
1.3 TRW.....	11
1.4 STRUCTURE AND OVERVIEW.....	11
2 STRATOSPHERIC CHEMISTRY.....	12
2.1 CHEMISTRY OF THE STRATOSPHERE.....	12
2.2 STRUCTURE OF THE ATMOSPHERE.....	12
2.3 STRATOSPHERIC OZONE.....	13
2.3.1 <i>Ozone Production</i>	13
2.3.2 <i>Ozone Depletion</i>	14
2.3.3 <i>The Antarctic Ozone Hole</i>	15
2.4 ADDITIONAL STRATOSPHERIC INPUTS.....	16
2.4.1 <i>Aerosols</i>	16
2.4.2 <i>Measurement Techniques</i>	17
2.4.3 <i>Montreal Protocol</i>	17
2.5 LAUNCH VEHICLES.....	18
2.5.1 <i>Impact on the Stratosphere</i>	18
2.5.2 <i>Launch Vehicle Emissions</i>	18
2.5.3 <i>Launch Vehicles and Stratospheric Chemistry</i>	19
2.6 SUMMARY.....	20
3 MODELING OBSERVATIONS OF SRM EXHAUST.....	21
3.1 MODELING OBSERVATIONS OF SRM EXHAUST.....	21
3.2 THE EXHAUST PLUME.....	21
3.2.1 <i>Launch Vehicle Characteristics</i>	22
3.2.2 <i>Launch Rates and Stratospheric Chemical Composition</i>	22
3.2.3 <i>Chemical Emissions into the Stratosphere</i>	27
3.3 LOCAL AND REGIONAL EFFECTS.....	32
3.3.1 <i>Plume Effects from Single and Multiple Rocket Motors</i>	33
3.4 GLOBAL SCALE EFFECTS.....	38
3.4.1 <i>Stratosphere/Troposphere Exchange</i>	38
3.4.2 <i>Homogeneous Modeling Efforts</i>	38

3.4.3	<i>Heterogeneous Modeling Efforts</i>	39
3.5	EFFECTS OF STRATOSPHERIC PARTICULATE	41
3.5.1	<i>Sedimentation Velocity</i>	41
3.5.2	<i>Removal by collision with sulfate aerosol</i>	42
3.5.3	<i>Reaction Probability</i>	42
3.6	STRATOSPHERIC PLUME DIFFUSION.....	44
3.6.1	<i>Plume Diffusion Models</i>	45
3.6.2	<i>Comparison and Discussion</i>	46
3.7	SUMMARY	49
4	LABORATORY MEASUREMENTS OF SRM EMISSION PRODUCTS.....	50
4.1	LABORATORY MEASUREMENTS OF SRM EMISSION PRODUCTS	50
4.2	LABORATORY SIMULATIONS	50
4.3	CHEMICAL PROCESSES AND YIELDS	51
4.4	ROCKET EXHAUST HETEROGENEOUS PROCESSES.....	52
4.4.1	<i>Rocket Exhaust Chemistry</i>	52
4.4.2	<i>Heterogeneous chlorine activation reaction mechanism</i>	53
4.4.3	<i>Measurement of the reaction probability for the $ClONO_2 + HCl$ reaction</i>	53
4.5	PARTICULATE CHEMISTRY	54
4.5.1	<i>Adsorption of water vapor on alumina surfaces</i>	54
4.5.2	<i>Effect of sulfuric acid vapor on the alumina surface</i>	55
4.6	ALUMINUM OXIDE/NITROGEN OXIDE AEROSOL CHEMISTRY	57
4.6.1	<i>Laboratory Studies of Al_2O_3-NO_x Aerosols</i>	57
4.6.2	<i>NO_2/γ-Al_2O_3 Aerosol Samples</i>	57
4.6.3	<i>NO/γ-Al_2O_3 Aerosol Samples at 298 K</i>	58
4.6.4	<i>NO/γ-Al_2O_3 Aerosol Samples at 183 K</i>	59
4.7	SUMMARY OF Al_2O_3/NO_x CHEMISTRY	60
5	IN-SITU MEASUREMENTS OF SRM EXHAUST PRODUCTS.....	61
5.1	IN-SITU MEASUREMENTS OF SRM EXHAUST PRODUCTS.....	61
5.2	IN-SITU OBSERVATIONS.....	61
5.3	ROCKET IMPACTS ON STRATOSPHERIC OZONE (RISO) EXPERIMENT	62
5.3.1	<i>RISO Program Science Objectives</i>	62
5.3.2	<i>Ultraviolet Network Instrumentation</i>	63
5.3.3	<i>Plume In-Situ Measurement</i>	63
5.3.4	<i>Ozone In-Situ Measurements</i>	64
5.3.5	<i>Aerosol In-Situ Measurements</i>	66
5.3.6	<i>Plume LIDAR Experiment and Plume's Vertical Extent</i>	67
5.4	IN-SITU VIDEO OBSERVATIONS	68
5.5	IN-SITU SATELLITE OBSERVATIONS	69
5.6	HIGH RESOLUTION OZONE IMAGER.....	72
5.7	SUMMARY	73
6	PROPELLANTS – CURRENT USAGE AND PROPOSED ALTERNATIVE FUELS ...	75
6.1	PROPELLANTS.....	75
6.2	LIQUID PROPELLANTS.....	75

6.2.1	<i>Calculations of Ozone Depletion from Conventional Liquid Propellants</i>	76
6.2.2	<i>Local Stratospheric Impact from Liquid Engines</i>	77
6.2.3	<i>NTO Oxidizer Used in Liquid Engines</i>	77
6.3	ALTERNATE PROPELLANTS TO REDUCE PRODUCTION OF PORS.....	78
6.4	IDENTIFICATION OF CHEMICAL SPECIES RELEVANT TO OZONE DEPLETION	78
6.5	IDENTIFICATION OF ALTERNATE PROPELLANTS WHICH REDUCE OR ELIMINATE FORMATION OF SELECTED PORS	79
6.5.1	<i>Mitigation of Ozone Depletion by Reducing Cl Production</i>	83
6.5.2	<i>Mitigation of Ozone Depletion by Removal of HCl</i>	84
6.5.3	<i>Mitigation of Ozone Depletion by Removal of Al₂O₃ and H₂O</i>	85
6.5.4	<i>Mitigation of Ozone Depletion by Removal of CO₂</i>	85
6.5.5	<i>Hardware Technology Status</i>	86
6.6	DEVELOPMENT AND SCALE-UP OF A REDUCED HCL PROPELLANT.....	88
6.7	LIQUID VERSUS SOLID FUEL COMPARISONS.....	91
6.8	FUTURE U.S. LAUNCH VEHICLE PROGRAMS AND PROPELLANT USAGE	93
6.8.1	<i>Sea Launch Limited Partnership (SLLP)</i>	93
6.8.2	<i>Evolved Expendable Launch Vehicle (EELV)</i>	96
6.8.3	<i>Reusable Launch Vehicles (RLVs): the Experimental X-33 and VenturestarTM</i>	103
7	CONCLUSIONS & RECOMMENDATIONS	104
7.1	CONCLUSIONS & RECOMMENDATION.....	104
7.2	CONCLUSIONS	104
7.2.1	<i>Modeling, In-situ, and Laboratory Investigations</i>	104
7.2.2	<i>Alternative Propellants</i>	106
7.2.3	<i>Deorbiting Debris</i>	108
7.3	RECOMMENDATIONS	108
	CONCLUSIONS & RECOMMENDATIONS	112
	APPENDIX A - List of Acronyms & Abbreviations.....	127
	APPENDIX B - List of Chemical Formulae and Nomenclature.....	133
	APPENDIX C – Description of Launch Vehicles by Country of Origin.....	138

TABLES

TABLE 2-1. ALTITUDE RANGE FOR VARIOUS ATMOSPHERIC LAYERS.	12
TABLE 2-2. MAIN EXHAUST PRODUCTS	19
TABLE 3-1. EXAMPLES OF LAUNCHERS, CHEMICAL PROPULSION SYSTEMS, AND MAJOR EXHAUST PRODUCTS	23
TABLE 3-2. OZONE DEPLETING CHEMICALS FROM LAUNCH VEHICLES	28
TABLE 3-3. WORLDWIDE SUCCESSFUL SPACE LAUNCHES.....	29
TABLE 3-4. ACTUAL AND PROJECTED STATUS OF ANNUAL ROCKET PLATFORM LAUNCHES.....	30
TABLE 3-5. ANNUAL STRATOSPHERIC DEPOSITION RATES (TONS/YEAR) FOR CHLORINE AND ALUMINA PARTICULATE FOR U. S. AND FOREIGN LAUNCHES; 1991-2010	32
TABLE 3-6. OZONE HOLE SIZE (RADIUS) AND LIFETIME IN THE STRATOSPHERE.....	37
TABLE 3-7. DIFFUSION DATA-MODEL COMPARISON.....	48
TABLE 3-8. SUMMARY OF PLUME EXPANSION RATE & DIFFUSION DATA	48
TABLE 4-1. MAJOR EXHAUST GASES AND MOLE FRACTIONS OF A TITAN IV SRM	50
TABLE 4-2. ANALYSIS OF AL ₂ O ₃ AEROSOL SAMPLES WITH NO ₂ REACTANT GAS	58
TABLE 4-3. ANALYSIS OF AL ₂ O ₃ AEROSOL SAMPLES WITH NO	58
TABLE 5-1. PLUME EXPANSION OR DIFFUSION RATE AS MEASURED BY BEITING [1999]	69
TABLE 5-2. SUMMARY OF IN-SITU EXPANSION OR DISPERSION RATE.....	69
TABLE 6-1. SPECIFICATIONS OF LIQUID ROCKET MOTOR	76
TABLE 6-2. SUMMARY OF OZONE DEPLETION MITIGATION APPROACHES UTILIZING ADVANCED PROPELLANTS	80
TABLE 6-3. TYPICAL MOLE FRACTIONS NECESSARY TO ACHIEVE AFTERBURNING INITIATION	83
TABLE 6-4. INGREDIENTS CONSIDERED FOR USE IN REDUCED HCL PROPELLANTS	90
TABLE 6-5. COMPARISON OF PORS PRODUCTION FROM LIQUID AND SOLID ENGINES (IN KG S ⁻¹)	91
TABLE 6-6. LAUNCH VEHICLES MODELED IN BRADY ET AL., [1997]	92
TABLE 6-7. SEA LAUNCH ZENIT-3SL FUEL PROFILE.....	94
TABLE 6-8. ZENIT-3SL KEROSENE-LOX	94
TABLE 6-9. SOLID FUEL SEPARATION ROCKETS.....	95
TABLE 6-10. UPPER STAGE CONTROL/ULLAGE MOTORS	95
TABLE 6-11. OZONE DESTRUCTION BY CHEMICAL COMPOUNDS	96
TABLE 6-12. FLIGHT TRAJECTORY TIMES FOR ATLAS V AND DELTA IV	97
TABLE 6-13. SUMMARY OF ATLAS & DELTA EMISSIONS IN UPPER ATMOSPHERE.....	98
TABLE 6-14. VEHICLE DEPOSITION RATES IN THE STRATOSPHERE.....	99
TABLE 6-15. OZONE DEPLETION TIME & HOLE SIZE AT ALTITUDES OF 20 KM.....	99
TABLE 6-16. PEAK ANNUAL COMBINED EELV LAUNCH EMISSIONS INTO UPPER ATMOSPHERE.....	100
TABLE 6-17. NO-ACTION PEAK ANNUAL LAUNCH EMISSIONS INTO UPPER ATMOSPHERE.....	102

EXECUTIVE SUMMARY

Assessments of the current understanding of the stratospheric ozone layer and its depletion by natural and anthropogenic sources have been published in various joint reports from the World Meteorological Organization and the United Nations Environment Program. However, the effects of rocket exhaust on stratospheric ozone have not been updated in these assessments since 1991(*WMO [1991]*), and many questions have been left unanswered. The objective of this report is to compile and present current computer modeling calculations, laboratory data, and *in-situ* observations on the effects of rocket exhaust on stratospheric ozone. This report also describes the impact of deorbiting debris from satellites and launch vehicles on stratospheric ozone and compares this with the impact of meteorite debris. The information in this document is provided as a record of accomplishments and as a resource, and will serve as the current assessment report on the impact of rocket emissions and debris on stratospheric ozone.

Since the space program began in the late 1950's, space missions have been conducted using liquid propellants in a variety of launch vehicles. The requirement for instant readiness for the strategic missiles demanded that a storable type of fuel be used; that fuel was solid propellants. While all launch vehicle rocket engines produce effluents that may potentially affect the environment, effluents from solid rocket motors have received special scrutiny, since they contain chlorine, which is known to catalytically destroy ozone in the stratosphere. It is essential to understand the environmental effects of the effluents from solid rocket motors to: (1) be in compliance with the National Environmental Policy Act (NEPA) of 1969, and Executive Order 12114 - Environmental Effects Abroad of Major Federal Actions; (2) assist in maintaining current systems so that any deleterious environmental effects are minimized without affecting their reliability; and (3) assist in the design of new systems with improved performance that meet cost, reliability, and environmental requirements.

Studies performed by TRW, The Aerospace Corporation, and others have reported on several facets of launch vehicles that may have deleterious effects on stratospheric ozone. Among the U.S. launch vehicles addressed in this review are the Evolved Expendable Launch Vehicle (EELV), SEA Launch, Space Shuttle, and the Titan, Delta, and Atlas rocket platforms. While the primary focus of this work has been the effects of rocket exhaust, another area of concern reported on here is the effects of deorbiting space and meteorite debris on ozone. Also addressed in this review are potential alternative chemical propellants that may show diminished environmental impact. Ground-based sources of ozone depleting chemicals used in launch preparations are not included in this report.

The combustion of current conventional rocket fuels is known to produce chemical species that may be harmful to the environment in several ways, including destruction of stratospheric ozone. Solid-fuel rocket motor launch vehicles deposit chlorine directly in the stratosphere. Prudence, as well as consistency, requires that these sources should be evaluated under the same criteria as emission sources on the ground (for example, ozone depleting chemicals or ODCs) to determine their contributions, if any, to ozone depletion. The components of rocket exhaust (e.g., HCl, Al₂O₃, etc.) have not been listed as a Class I ODCs, and the Environmental Protection Agency (EPA) has made no move to reclassify them. However, this does not preclude them

being listed in the future, particularly if it were aggressively petitioned to do so (*SRS [1995]*). Accordingly, the terms ODC and ODP (Ozone Depletion Potential) will not be employed to describe the components of rocket exhaust, but instead the term PORS (Potential Ozone Reactive Species) will be introduced and used throughout the remainder of this report.

Assessment of the impact of space launch operations on the environment is now an integral part of launch operations and launch system acquisition. There are numerous published modeling studies dealing with the effect on the ozone layer by ozone reactive compounds that are exhausted into the stratosphere by solid rocket motors. Chlorine and chlorine oxides are present only in the exhaust of solid rocket motors such as those found on the Titan IV, the Space Shuttle, and many smaller launch vehicles. There are two other classes of compounds commonly found in rocket exhaust that can cause ozone destruction. These are the oxides of nitrogen and hydrogen, and they are present to some extent in the exhaust of every launch vehicle. This is due in part to entrainment of ambient atmospheric oxygen, nitrogen, and hydrogen. There are also species such as alumina from solid rocket boosters and aerosol particulate and soot from LOX/Kerosene fuel in rocket exhaust. Particulate may promote heterogeneous reactions with ozone and ambient chlorine containing compounds (*Lohn et al., [1999]*).

Validation of computer models is essential to understanding the full ramifications of rocket exhaust on the atmosphere, and this validation is accomplished by laboratory investigations and by *in-situ* measurements of SRM exhaust plumes. In the Laboratory Measurements chapter of this report, chemical processes and yields are described. Heterogeneous processes are discussed, including rocket exhaust laboratory simulations, chlorine activation reaction dynamics, and reaction probability determinations for ozone depleting chemical reactions involving the effects of sulfuric acid vapor, the adsorption of water vapor on the surface of alumina, and the aerosol chemistry of aluminum oxide and nitrogen oxide.

The modeling results on the impacts of SRM exhaust products on stratospheric ozone are validated further with *in-situ* observations of the exhaust plume. Stratospheric ozone measurements are described. A variety of plume measurement campaigns are described, including RISO, the Rocket Impacts on Stratospheric Ozone experiment. Also described are a variety of plume measuring techniques, including specific ozone and aerosol measurements, LIDAR remote sensing, measurements of plume dispersion via electronic imaging, Total Ozone Mapping Spectrometer (TOMS) satellite observations, and a new instrument with the acronym High Resolution Ozone Imager (HIROIG) which may be used to study the plume chemistry in a local plume environment.

Local Effects on Ozone Depletion

Rocket launches have the potential to affect the atmosphere both in an immediate, episodic manner, and in a long-term, cumulative manner. When the stratosphere is affected immediately after launch, the perturbation occurs along or near the flight trajectory. Emissions from some types of launch vehicles significantly perturb the atmosphere along the launch trajectory at an approximate range of 10 kilometers or less from the rocket passage. Ozone concentration is temporarily reduced, an aerosol plume may be produced, and combustion products such as chlorinated compounds, alumina, NO_x, and reactive radicals can temporarily change the normal chemistry along the vehicle path.

Rocket launches can have a significant local effect on the stratosphere by reducing ozone substantially within the expanding exhaust plume up to 2 hours after launch. An ozone hole is observed within this plume and found to increase in size during this period. Ozone concentrations recover to background levels as time passes and ozone back-fills into the hole by diffusive processes. The extent of the hole depends on the quantity of emissions released and the thrust (size) of the launch vehicle. The time for this hole to refill to ambient ozone levels was 3000 seconds at 15-20 km and 6000 seconds at 40 km, based on measurement (*Ross et al., [1997]*) and modeling (*Lohn et al., [1999]*) studies.

It was long thought that hydrogen chloride, a relatively inactive form of chlorine, was the only SRM chlorine containing emission species. Calculations and laboratory experiments (*WMO [1991, 1995]*) have shown that chlorine is present also as Cl₂ or Cl radical. This is significant, because, while hydrogen chloride primarily adds to the global chlorine burden and, hence the global ozone depletion, the extremely active Cl (Cl₂ photolyzes rapidly to Cl) can participate in immediate, local destruction of ozone.

The process of ozone destruction is controlled by the rate at which plume species diffuse into the ambient atmosphere and by the reaction of ozone with chlorine (with ClO as a product) and the subsequent reproduction of chlorine by photoreactions, and reactions associated with chlorine chemistry. These model simulations of dramatic ozone losses in the first couple of hours after launch have been corroborated by measurements taken after the launch of a variety of SRM vehicles, namely Titan III, Titan IV, and Space Shuttle (*Ross [1997], Jackman [1998], Lohn et al., [1999], McKenzie [1998], WMO [1991]*).

Global Effects on Ozone Depletion

In addition to local effects, the effluents from rockets may have long term or global impacts on stratospheric ozone. These potential global impacts derive from the relatively long lifetimes of alumina particulate and chlorine (primarily as HCl) in the stratosphere. Although rocket motor emissions appear to represent a small fraction of the total anthropogenic impact on stratospheric chemistry, prudence requires a careful evaluation of this impact, particularly on stratospheric ozone (*Ko [1999], WMO [1991]*).

Jackman *et al.*, [1998] carried out detailed stratospheric modeling calculations of ozone depletion caused by a launch rate of nine Space Shuttle launches and three Titan IV launches per year using the reaction probability measurement of ClONO₂ with HCl on alumina surfaces by Molina [1999]. Their results indicate that the effect on the annually averaged global total ozone is a decrease of 0.025% by the year 1997; about one-third of this decrease results from the SRM-emitted alumina and the remaining two-thirds results from the SRM-emitted hydrogen chloride. These results were confirmed independently by the modeling efforts of both Lohn *et al.*, [1999] and Ko *et al.*, [1999].

Potential long-term effects utilizing solid rocket propellants include a global reduction in stratospheric ozone, an increase in the chlorine loading of the stratosphere, and an increase in the particulate burden. Based on the modeling efforts of Jackman *et al.*, [1998] and others, the global implications appear to be extremely minor at current launch rates, but are nonetheless real and long-lived.

***In-Situ* Measurement Studies**

In-situ measurement results clearly suggest that SRM launch vehicles produce transient ozone loss following launch. A comparison of *in-situ* data to recent modeling efforts has confirmed that the models only slightly underestimate both the size and the duration of the region of ozone removal in the wake of large and medium launch vehicles. However, even when such reductions occurred, the reduction in column ozone was found to exist over an area a few kilometers by a few tens of kilometers and was generally much smaller. The local-plume ozone reductions decrease to near zero over the course of a day, and the regional effects were smaller than could be detected by TOMS satellite observations.

Laboratory Studies

Laboratory investigations by Disselkamp [1999] assessed the uptake of NO and NO₂ onto the surface of Al₂O₃. These reactions have two potential implications in atmospheric chemistry. First, a decrease in atmospheric NO_x concentrations could enhance the catalytic destruction of ozone by halogen species. Considering that the ambient stratospheric NO_x concentration was approximately 10 ppbv (parts per billion volume), or 2.5×10^{10} molecules/cm³, it would take an Al₂O₃ particle density of 640 particles/cm³ to deplete all the NO_x species. Aluminum oxide chemistry is not expected to be important in the exhaust plume because the particulate concentration is far too low to be significant in comparison with the homogeneous chlorine chemistry. A second potential atmospheric implication of this chemistry was to consider the uptake of halogen species onto the surface of aluminum oxide particles. Disselkamp [1999] suggests that the uptake of active halogen species by aluminum oxide to liberate NO would have the effect of increasing the ozone concentration by reducing the contribution of halogen catalyzed ozone destruction. There is no evidence to date to support this hypothesis; additional studies are needed to characterize this halogen chemistry.

The reaction probability (γ) for the reaction of ClONO_2 with HCl on alumina surfaces was measured by Molina [1999]. The result was $\gamma = 0.02$ under conditions similar to those which would be encountered at mid-latitudes in the lower stratosphere. The result is in good agreement with other published measurements on alumina and on glass surfaces conducted with larger reactant concentrations. The reaction was found to be nearly zero-order in HCl, and the mechanism was dependent on the presence of absorbed water layers not on the detailed nature of the refractory oxide surface itself. Furthermore, it was determined that a significant fraction of the injected alumina surface area would be catalytically active and would remain unaffected in the stratosphere by sulfuric acid vapor. The time required for the alumina particulate to be covered by a monolayer of sulfuric acid was estimated at 8 months, assuming an accommodation coefficient of 0.1. Finally, coalescence with stratospheric sulfuric acid aerosols would most likely be unimportant for the alumina particles larger than about $0.1 \mu\text{m}$ in diameter before they settle out of the stratosphere. For particle distributions less than $0.13 \mu\text{m}$, the mass-weighted atmospheric lifetime is about 0.3 years with or without sedimentation and collision removal, because reactivity for particles smaller than $0.13 \mu\text{m}$ is small. These results were confirmed by 3-D model calculations of Ko *et al.*, [1999].

Propellants

A methodology for the systematic removal of PORS from rocket plume exhaust streams using alternate propellants is presented. The changes to launch vehicles vary from a minimum of a reformulated conventional solid propellant containing ammonium perchlorate, but with afterburning suppressant chemicals added, to a completely reformulated solid propellant that incorporated nitrate/carbonate oxidizers, to new engines based on fluorine oxidizers or redeveloped engines burning conventional liquid propellants. Reformulated solids with afterburning suppressants could be implemented as a direct response to Cl_2 production; conventional liquid engines utilizing LOX/LH₂ and/or LOX/RP-1 could be implemented to remove HCl; and fluorine systems (solids and/or gels) could be implemented to eliminate H₂O and CO₂.

Among launch vehicles utilizing the following propellants LOX/LH₂, LOX/RP-1, NTO/Amine, solid, and solid with chlorine, Brady *et al.*, [1997] concluded that LOX vehicles generated the least amount of ozone depletion (a hole which lasted less than 5 minutes) and that solid rocket motors with chlorine generated the most ozone destruction (a depleted region which persisted for 3 to 10 hours, depending on dilution parameters).

Deorbiting Space and Meteorite Debris

A discussion of the impact on stratospheric ozone from deorbiting debris is presented. Consideration of the individual studies assessed in this document leads to the conclusion that the physical and chemical phenomena associated with deorbiting debris and meteoroids do not have a significant impact on global stratospheric ozone. The reasons are twofold: slow reaction rate and low particle density. However, it was noted that a large deposition of particles in the

stratosphere due to volcanic eruptions could have a significant impact on the local ozone column density. The effect of meteoroids on the stratospheric ozone layer also was investigated. The meteoroid population for micron to millimeter size objects was found to be comparable to the orbital debris flux. Meshishnek [1995] presented data from the Interplanetary Dust Experiment (IDE) which measured impact fluxes on six sensors on the Long Duration Exposure Facility (LDEF). The LDEF sensors measured impacts due to particles greater than roughly 0.2 μm and up to 100 μm in diameter. There was no way to differentiate between debris and micrometeoroid impacts; however, the vast majority (>80%) of the particle impacts were presumed to be from debris since the sensors must have been in the 25- μm and below range, where debris clearly dominates (Meshishnek [1995]). To the extent that they are comparable, it may be concluded that meteoroids pose little or no threat to global stratospheric ozone.

Summary

Depletion of stratospheric ozone locally within the exhaust plume of a launch vehicle is real as measured by *in-situ* and other field techniques, but is short-lived. On a global scale, depletion of ozone from a rocket launch is calculated in theoretical models, but is found to be well below the detection limits of current measurement techniques. Should the frequency of rocket launches using solid propellants increase (i.e., from both commercial and government launches on a global scale), the extent of ozone depletion will increase. As the United States and other governments move toward more reliable and more “ozone friendly” propellants in its rocket programs, the levels of global ozone depletion will be minimized.

Perhaps the single most important parameter in modeling stratospheric ozone depletion by rocket exhaust plumes is the rate of dispersion in an expanding plume parcel. The plume expansion rates measured in the fly-through of a NASA WB57F aircraft (Ross *et al.*, [1997]), as well as that determined by LIDAR (Dao *et al.*, [1997]) and electronic imaging (Beiting [1999]) of several different launch vehicles are in reasonable agreement with modeling efforts (Brady *et al.*, [1997], Beiting [1999], Denison *et al.*, [1994], Lohn *et al.*, [1994], Watson *et al.*, [1978]). As explained in Beiting [1999], the WB-57 and LIDAR observations cannot measure the aggregate plume dispersion; they can detect the existence of parcels at later times and the parcels can have a higher concentration of PORS than that inferred from the aggregate dispersion rate. To understand the spatial extent of the plume as a function of time, the aggregate dispersion rate should be used. Higher concentrations of PORS than predicted by the aggregate dispersion rate will exist in parcels – as noted by LIDAR (Dao *et al.*, [1997]) and WB-57 aircraft (Ross *et al.*, [1997]). The models give reasonable answers when correct dispersion rates are used in them. Watson *et al.*, [1978] and Lohn *et al.*, [1994] calculated diffusion constants for large scales. The model of Brady *et al.*, [1997] uses an experimental value for the diffusion parameter and will give correct concentrations for the correct parameters – which may vary greatly depending on atmospheric conditions and altitude. Again, all of the differences between modeling efforts and *in-situ* measurements may be explained if each plume parcel is expanding at its own rate, a complexity which must be incorporated into future modeling efforts.

Future Work

Despite the conclusions presented in this report, there are still opportunities for further work. These opportunities include increased fidelity in the models employed, thorough assessments of potential alternative propellants, the effect of deposition of large amounts of water in the stratosphere, more detailed *in-situ* assessments, and deployment of the HIROIG instrument for monitoring the local effects of rocket exhaust in locations which are geographically inaccessible or have restricted access.

1 INTRODUCTION

1.1 Purpose of this Report

1.1.1 Background

Since the space program began in the late 1950's, space missions have been conducted using a variety of launch vehicles. Originally, strategic missiles used a variety of liquid propellant engines. Commencing with the German V-2, these liquid propelled strategic missiles have included the Atlas, Titan 1, and Thor, and the rocket-powered airplanes, such as the Me-262 and X-15. But the requirement for instant readiness for the strategic missiles demanded that an alternate type of fuel be used; that fuel comprises a variety of solid propellants. Increased carrying capacity for liquid-powered vehicles resulted in the requirement for strap-on solid propellant boosters, most notably on the SST (Space Shuttle), but also on the Delta (upgraded Thor), Titan, and Ariane. The large Saturn vehicles provided the launch capability for the manned lunar exploration program (Apollo), the manned space station missions (Skylab), and the joint U.S.- USSR Apollo-Soyuz Test Project. The smaller Atlas, anti-Scout launch vehicles are currently used by the United States to launch a variety of automated spacecraft (e.g., communication satellites, weather satellites, Earth-orbiting scientific satellites, and interplanetary exploratory spacecraft).

In October 1998, the United States Air Force (USAF) awarded contracts for 29 Evolved Expendable Launch Vehicle (EELV) launches. EELV was envisioned to replace all Titan IV, Delta II and Atlas launch vehicles on a fairly short phase-out schedule as part of the U.S. government National Mission Model to provide cleaner, cheaper and more efficient access to space, both for commercial ventures and government programs. To determine the feasibility of the EELV, a half-scale Advanced Technology Demonstrator Vehicle, Experimental-Thirty-Three (X-33), and a Delta V Prototype Reusable Launch Vehicle will be tested as part of NASA's Reusable Launch Vehicle Program in early 2000. The first EELV commercial launch is scheduled for the 2001-2002 time frame (*X-33 [1996]*, *EELV [1998]*).

1.1.2 Impact of Launch Vehicles

It is well known that solid-fuel rocket motors of large space launch vehicles release gases and particles that may significantly affect stratospheric ozone densities along the vehicle's path (*EIS [1977]*, *Potter [1977]*, *Cour-Palais [1977]*, *Potter [1978]*). Solid rocket exhaust products deplete ozone in the stratosphere in the following way. Solid propellants, which contain large amounts of chlorine containing substances, have the potential to chemically destroy ozone in the stratosphere. Normally the release of active chlorine from the solid-fuel exhaust would be slow, and most of this harmful substance would leave the atmosphere in the tropopause through natural processes such as rain. However, a series of chemical reactions at the extremely high temperatures in the rocket plume cause the immediate release of large amounts of active chlorine into a small area of the stratosphere local to the rocket plume. On a global scale, each chlorine atom released eventually causes the destruction of many thousands of ozone molecules in what is

known as a catalytic cycle. In a rocket plume, each chlorine atom destroys an ozone molecule in an approximately 1:10,000 ratio. Rocket exhaust also contains aluminum oxide particles that may further accelerate ozone depletion, similar to the depletion that occurs over Antarctica due to polar stratospheric clouds. Assessments of the state of knowledge about ozone depletion have been published in various joint reports from the World Meteorological Organization and the United Nations Environment Program (*WMO [1985]*, *WMO [1988]*, *WMO [1991]*, *WMO [1995]*, *WMO [1998]*). Portions of these reports pertaining to the rocket exhaust issue are summarized in the subsequent sections of this report.

1.1.3 Ozone Depleting Chemicals

The Montreal Protocol established international policy and requirements controlling the industrial use of ozone depleting chemicals (ODCs) or substances (ODSs). Each year, the parties to the protocol meet to identify additional industrial materials that deplete ozone, and as appropriate, establish timetables for their curtailment or phase-out. In the United States, the Clean Air Act Amendments of 1990 implement this protocol and call for an elimination of the worst “Class I” ODCs within several years. These Class I ODC chemicals typically are released in the troposphere, but are sufficiently long-lived that they can be transported to the stratosphere, where most are broken down by ultraviolet radiation, producing highly reactive Cl and Br radicals that are chiefly responsible for the catalytic destruction of stratospheric ozone. Because the time scale of mixing in the troposphere is less than the residence time of these halocarbons, the effect on ozone (as measured by the ozone depletion potential or ODP) does not depend exactly on where, when and how they are released (*Ko et al., [1994]*).

First defined for CFCs a decade ago, the ODP is an index measuring the time-integrated ozone depletion caused by specific quantity of a chemical relative to that caused by the same quantity of the chlorofluorocarbon, CFC-11 (the fully substituted methane, CFCl_3). The definition presumes the chemical is ultimately released into the atmosphere. Total chlorine loading of the atmosphere (*Prather et al., [1990]*) has also been used to assess the global ozone loss caused by these chemicals, either separately or in combination for specific emissions predictions. The amount of chlorine in the stratosphere not still tied up in the parent halocarbon is defined as the stratospheric chlorine loading (*WMO [1991]*).

There are more direct and effective ways that chlorine can enter the stratosphere. These include solid-fuel rocket motors in the Space Shuttle launches, which deposit chlorine directly in the stratosphere. Prudence, as well as consistency, requires that these sources should also be evaluated under the same criteria (for example, ODPs) to determine their contributions, if any, to ozone depletion. A complete description of this subject may be found in *Ko et al., [1994]*. It should be mentioned that rocket exhaust has not been listed as a Class I ODC, and the Environmental Protection Agency (EPA) has made no move to reclassify it. However, this does not preclude its being listed in the future, particularly if it were aggressively petitioned to do so (*SRS [1995]*). Accordingly, the terms ODC and ODP will not be employed to describe the components of rocket exhaust, but instead the term PORs, which stands for Potential Ozone Reactive Species, will be introduced and used throughout the remainder of this report.

The Air Force is investigating several areas where there is insufficient information to determine environmental impact from space programs. This information includes the contribution of rockets to ozone depletion in the stratosphere and the impact of deorbiting debris from satellites and other anthropogenic sources on stratospheric ozone. The Space and Missile Systems Center's (SMC) environmental analysis arm is the Environmental Management Division (AXAF). It is responsible for assuring that all SMC federal actions having potential environmental impacts are evaluated in accordance with the National Environmental Policy Act (NEPA) of 1969, and Air Force Regulations 19-2 and 19-3, which implement NEPA in the United States and overseas, respectively (*EELV [1998]*).

The National Environmental Policy Act requires SMC, as a government agency, to analyze the environmental impacts of its programs. Because space launch programs on some level contribute to depletion of stratospheric ozone, SMC is required to characterize this effect. In addition, the relative impacts of liquid-fueled and solid-fueled rockets and alternative propellants need to be quantified for the design of future launch systems.

1.2 Scope of this Report

In compliance with the National Environmental Policy Act, NASA and the Air Force are actively engaged in studies to determine the effects of launch vehicles on the atmosphere. This report is provided to SMC to document the current knowledge of the environmental impact on stratospheric ozone depletion from solid-fuel rocket launches for the purpose of establishing potential constraints on launch activities. It includes a comprehensive review of modeling efforts, both the local stratospheric ozone impact of rocket exhaust from launch vehicles, as well as global and long-term effects. Additionally, detailed laboratory studies concerning the heterogeneous effects of SRM exhaust particulate including aluminum oxide are described. Limited data exists on *in-situ* sampling of exhaust plumes. These data are presented which validate the modeling efforts. Furthermore, a variety of fuels and propellants are analyzed to provide less harmful alternatives for future launch vehicle manufacturing. Finally the effects of deorbiting space and meteorite debris on stratospheric ozone are summarized. Detailing information in this manner enhances the usability of this report.

It should be mentioned that this report does not identify manufacturing processes that require ODS use and quantities of ODSs used in solid rocket motor manufacturing. This information may be found elsewhere (*SRS [1995]*). Additionally, this report does not concern itself with the impact of SRM exhausts and the "green house effect" (the potential to warm the global temperature of the Earth). This effect is minimal and is discussed elsewhere (*EELV [1998]*).

1.3 TRW

TRW Space & Electronics Group (S&EG) builds communications, scientific and defense spacecraft for military, civil and commercial customers; produces, integrates and tests payloads; develops advanced space instruments; and integrates experiments into spacecraft. It is an operating unit of TRW Inc., which provides advanced technology products and services for the global automotive, aerospace and information systems markets.

TRW S&EG is currently preparing for a test of its Ultra Low Cost Engine (ULCE) at NASA Stennis Space Center (SSC) E1 test facility. TRW's ULCE design concept consists of a 650-klbf sea level LOX/LH₂ thrust chamber assembly. The test results will demonstrate if this engine is ready to continue on to full engine testing or whether additional research must be conducted. TRW's ULCE will burn cryogenic O₂ (LOX) with either cryogenic H₂ (LH₂) or kerosene (RP-1) at relatively low combustion pressures (300 psia to 1400 psia). One complete thrust chamber assembly (TCA) has been delivered to NASA SSC while a second is being prepared for delivery. Testing is scheduled to commence in January 2000.

1.4 Structure and Overview

Section 1 of this report introduces the issue of solid rocket motor (SRM) exhaust and its potential impact on stratospheric ozone depletion. Section 2 presents a discussion of the structure and chemistry of the stratosphere, and the chemicals emitted there. Section 3 presents an overview of the modeling efforts to date on the effects of these SRM emissions on stratospheric ozone. These studies include both global and regional to local effects of the exhaust plume. Section 4 describes the laboratory investigations of the homogeneous and heterogeneous chemistry that occurs in the exhaust plume and serves to validate the model studies in section 3. Section 5 summarizes the limited data available on *in-situ* measurements made within actual exhaust plumes. Section 6 describes propellants that may be utilized as replacements for current ozone depleting propellants. Section 7 summarizes the effects of deorbiting space debris and meteorites. Section 8 presents concluding remarks and summarizes future investigations that should be conducted to study launch vehicle emissions in the future. A complete list of references is included at the end of the report. In addition to the references listed in this document, a recent bibliography on the environmental impacts of launch vehicles is available and should be consulted (*Cocchiaro [1999]*). Included in the Appendices are a list of acronyms and abbreviations (Appendix A); a list of chemical formulae and nomenclature (Appendix B); and a description of launch vehicles by country of origin (Appendix C). Finally a complete reference section is included at the end of the document.

2 STRATOSPHERIC CHEMISTRY

2.1 Chemistry of the Stratosphere

Because launch vehicles pass through and affect the stratosphere, Section 2 serves as a brief introduction to the structure of the stratosphere, the chemistry of ozone, and the impact of rocket exhaust on the depletion of ozone. Because the primary activity of ozone depletion occurs in the stratosphere, it is necessary to provide an overview of the structure of the Earth's atmosphere. This is addressed in Section 2.2. Section 2.3 examines the chemical composition of the stratosphere. Ozone production and destruction mechanisms in the natural stratosphere are described here and concluded with a brief description of the "Ozone Hole" which forms annually over Antarctica. Section 2.4 considers additional stratospheric inputs to the stratosphere in the form of particulate. These inputs may be both natural (i.e., from volcanic activity) or anthropogenic (i.e., from the activities of man). Also considered in this section are stratospheric *in-situ* ozone measurement techniques, and a brief description of Montreal Protocol, an international treaty to ban substances that are known to deplete ozone. In Section 2.5, the impact of launch vehicles is described. These include both emissions and chemistry in the stratosphere. A summary is included in Section 2.6.

2.2 Structure of the Atmosphere

There are four principal layers in the earth's atmosphere: the troposphere, stratosphere, mesosphere, and the ionosphere. Generally, these atmospheric layers are defined by temperature, structure, density, composition, and degree of ionization (*DOT [1992]*). The approximate altitude of these layers is provided in Table 2-1. The troposphere is the turbulent and weather region containing 75 percent of the total mass of the earth's atmosphere. The troposphere is critical because any rocket emissions could potentially increase ambient pollution in the air or could fall back or be rained back to earth. Both the stratosphere and the troposphere are of most concern when considering greenhouse gases and global warming. The stratosphere is also the region where the majority of the atmospheric ozone is located and is the focus of this section (*Warneck, [1988]*).

Table 2-1. Altitude Range for Various Atmospheric Layers.

Atmospheric Layer	Altitude Range (km)
Troposphere	Surface to 10
Stratosphere	10 – 50
Mesosphere	50 – 80
Ionosphere	80 – 100

The lower boundary of the stratosphere lies between altitudes of approximately 10 and 18 km above the Earth's surface (with an atmospheric pressure in the range of 100 to 200 millibars [mb]) at a temperature inversion known as the tropopause. The stratosphere extends up to nearly 50 km (with an atmospheric pressure of about 1 mb), at a temperature inversion known as the stratopause. Both the tropopause and stratopause serve as a boundary inhibiting the mass transfer (i.e., the transfer occurs over months) of gases and particulate between layers (*Brasseur et al., [1984]*). Although containing less than 20 percent of the atmosphere's mass, and despite having relatively little direct impact on weather at the surface, the composition of the stratosphere can strongly influence the attenuation of solar radiation reaching the Earth's surface. Perturbations in the trace gas composition of the stratosphere can potentially affect how the stratosphere absorbs and scatters the sun's radiation incident at its top. The environment at the Earth's surface is affected by both changes in UV radiation and by changes in the balance of outgoing and incoming long- and short- wave solar radiation, which maintains the Earth's present climate. The stratospheric ozone burden is of key importance because it has a major influence on the surface UV flux and is a significant contributor to the global climatic heat budget. Nearly as important as ozone is the stratosphere's aerosol burden, which also determines the degree of solar attenuation. Because it contains halogens (e.g., chlorine, bromine), the aerosol can also perturb the stratosphere's ozone mass budget. Other trace gases such as water vapor and CO₂ are greenhouse gases, which absorb solar radiation.

2.3 Stratospheric Ozone

2.3.1 Ozone Production

The term ozone comes from the Greek word meaning "smell," a reference to ozone's distinctively pungent odor. Each molecule contains three oxygen atoms (O₃) bonded together in a "bent" shape. Ozone exists through all levels of the atmosphere, from the surface to about 100 kilometers (km) altitude. The concentration profile of ozone varies with latitude. Most ozone is photochemically produced in the equatorial atmosphere and is transported towards the Polar region and downwards with time (*Brasseur et al., [1984]*). At 30° N latitude, which corresponds approximately to the latitude of the two main U. S. launch facilities (i.e., Vandenberg Air Force Base in California and Cape Canaveral in Florida), the annual ozone peak concentrations occur at an altitude of approximately 20 km. Ozone concentration varies seasonally, so that at 30° N latitude, the seasonal change in columnar ozone is on the order of 10-20 out of an average of 290 Dobson units (*WMO [1991]*).

The mechanism represented in reactions (2-1) to (2-4) is referred to as the Chapman Mechanism, so named after its discoverer (*Chapman [1930]*). It illustrates the chemical and photochemical processes that are important in the natural formation of ozone from molecular oxygen in the stratosphere, and the reactions associated with the natural destruction of ozone.



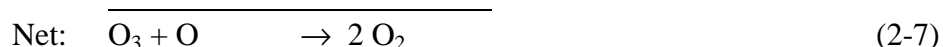
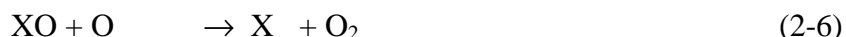
Ozone is continuously being produced in the stratosphere by solar ultraviolet radiation. Radiation at wavelengths less than 242 nm dissociate molecular oxygen (O₂) into atoms of oxygen (O) that reattach to nearby O₂ to form an ozone molecule. The majority of ozone is concentrated in the lower stratosphere at altitudes between about 20 and 25 km, in a region known as the ozone layer (*i.e.*, *Stolarski et al.*, [1992]). The distribution of ozone is maintained by a balance between its' production and destruction and by the transport of ozone from regions of net production to those of net loss. The transport of ozone is driven by the variable stratospheric wind fields, which give rise to daily fluctuations, seasonal variations, and inter-annual variability in ozone amounts.

The ozone layer is critical to life on Earth because it absorbs biologically damaging solar ultraviolet radiation. The amount of solar UV radiation received at any particular location on the Earth's surface depends upon the position of the Sun above the horizon, the amount of ozone in the atmosphere, and local cloudiness and pollution. Scientists agree that, in the absence of changes in clouds or pollution, decreases in atmospheric ozone lead to increases in ground-level UV radiation (*Martin [1998]*, *WMO [1998]*). Prior to the late 1980s, instruments with the necessary accuracy and stability for measurement of small long-term trends in ground-level UV-B were not available. Therefore, the data from urban locations with older, less-specialized instruments provide much less reliable information, especially since simultaneous measurements of changes in cloudiness or local pollution are not available. When high-quality measurements were made in other areas far from major cities and their associated air pollution, decreases in ozone have regularly been accompanied by increases in UV-B (*WMO [1998]*). Therefore, this increase in ultraviolet radiation received at the Earth's surface would likely increase the incidence of skin cancer and melanoma, as well as possibly impairing the human immune system (*Kerr et al.*, [1993]). Damage to terrestrial and aquatic ecosystems also may occur (*Martin [1998]*, *WMO [1998]*).

2.3.2 Ozone Depletion

Even though the energy from the sun produces new ozone, these gas molecules are destroyed continuously by natural compounds containing nitrogen, hydrogen, and chlorine. Such chemicals were all present in the stratosphere - in small amounts - long before humans began polluting the air. Nitrogen comes from soils and oceans, hydrogen comes mainly from atmospheric water vapor, and chlorine comes from the oceans.

The original emphasis, and still the main thrust for prevention of stratospheric ozone depletion is based on prevention of accumulation of tropospheric-stable, stratospheric-photo-decomposable chlorine and bromine species in the stratosphere. These originally included a number of CFCs (chlorofluorocarbons) used as aerosol propellants, foam plastic blowing agents, cleaning solvents, and refrigerants, some bromine analogs (Halons), and methyl chloroform. Later additions have included HCFCs (hydrochlorofluorocarbons), and heavily chlorinated or brominated aliphatic hydrocarbons such as carbon tetrachloride, perchloroethylene, methyl bromide, and bromoform. A general mechanism for ozone destruction in the upper stratosphere is described in reactions (2-5) to (2-7) below.



Where X = Cl, H, OH, NO, Br, etc.

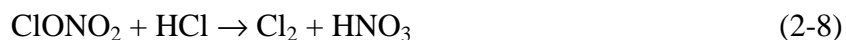
Because human activity has significantly contributed to the chlorine and bromine load levels in the stratosphere, chlorine and bromine have been of most concern. Rocket launches are one of the anthropogenic sources of chlorine in the stratosphere. Of the ozone-depleting chemicals mentioned above - oxygen, nitrogen, hydrogen, iodine, sulfur, chlorine (Cl), and bromine (Br) -- chlorine is responsible for the greatest amount of ozone destruction within the rocket plume. In response to continuing depletion of the ozone layer and the Antarctic ozone hole, the Parties to the Montreal Protocol (approximately 160 countries) have implemented a production ban in 1994 on halons, and in 1996 on CFCs (*WMO [1998]*). More information on this effort to reduce global emissions of ozone depleting chemicals will be presented in Section 2.4.3.

2.3.3 The Antarctic Ozone Hole

The search for evidence of downward trends in the thickness of the ozone layer was inconclusive until the discovery of the Antarctic ozone hole in 1985 (*Farman et al., [1985]*). Since that time, the concentration of stratospheric ozone has been observed to be decreasing throughout much of the globe. Ozone decreases during the Antarctic spring are now well documented (*Solomon [1988]*). Ozone decreases outside the Antarctic, at southern mid-latitudes, have been reported, as well as over the heavily populated northern mid-latitudes (*Bojkov et al., [1990]*; *Stolarski et al., [1991]*). Observations have demonstrated that the Antarctic ozone depletion is due to man-made chemicals, and the weight of evidence suggests that these chemicals likely cause much of the mid-latitude depletion as well. Heterogeneous chemistry (mixed-phase reactions), involving increased amounts of chlorine and bromine in the stratosphere, are key to the ozone decline. The sources of chlorine are largely chlorofluorocarbons, human-produced chemicals that are used as refrigerant, foaming, and cleaning agents. Bromine also has a large anthropogenic source. It is found in halons (e.g.,

Halon-1211, CF₂ClBr) that are used in various types of fire extinguishers and in some agricultural fumigation (e.g., Methyl bromide, CH₃Br).

Considerable monitoring has found evidence of significant ozone decreases in both the Arctic and Antarctic Polar Regions (*WMO [1988]*, *WMO [1998]*). The most pronounced reductions, the so-called ozone "hole," occur during the spring near Antarctica. This ozone hole is caused by the appearance of at least one type of polar stratospheric cloud (PSC). Polar stratospheric clouds form when the ambient air is sufficiently cold, sufficient water vapor is present, and when there is a sufficient lack of polewards mixing of warmer and drier air. A PSC acts to destroy ozone by freeing chlorine bound up in the chloronitrate pool via direct activation on frozen or supercooled liquid surfaces within the cloud. Current understanding of the mechanisms for polar ozone depletion emphasizes the participation of nitric acid, HNO₃, hydrogen chloride or hydrochloric acid, HCl, and ice crystals as necessary ingredients. Ice crystals that contain nitric acid trihydrate, HNO₃·3 H₂O, (NAT), absorb a film of liquid HCl or its hydrate: molecules of chlorine nitrate, ClONO₂, impinge on the film and react to form elemental chlorine and nitric acid.



Gaseous chlorine compounds can also be sequestered in the stratosphere in a form that at some later date can be converted and contribute to ozone destruction anywhere over the globe. Chlorine nitrate (ClONO₂) and hydrogen chloride (HCl) are two of these reservoir species. As the mechanisms and the reaction sequences that affect ozone in the stratosphere have been more clearly elucidated, the various nitrogen, fine particles and droplets that serve as reaction sites have drawn attention. Both aerosol droplets of SO₂ and fine ice crystals are implicated. Artificial injection of any of the three into the stratosphere is considered undesirable. More information on this and on stratospheric ozone depletion in general may be found in two excellent reviews by Rowland [*1991*] and Johnston [*1992*].

2.4 Additional Stratospheric Inputs

2.4.1 Aerosols

Injections of water and sulfur compounds can also play a role in perturbing lower stratospheric ozone in the tropics and mid-latitudes without requiring extremely low temperatures for PSC formation. Water vapor, which can form PSCs, can also be injected into the lower stratosphere through the agency of intense cumulonimbus cloud systems. A single cloud can temporarily inject up to 100 metric tons of water or ice hydrometeors immediately above the tropopause (*AF [1996]*, *AF [1990]*). Much of the water and ice immediately precipitates out; however, some of the very smallest particles with very low fall velocities (e.g., sub-micron range) can persist for weeks.

Stratospheric aerosols can also originate from a number of terrestrial sources such as the sulfate produced by the oxidation of carbonyl sulfide diffusing up from the troposphere (*Warneck*

[1988]). Volcanoes also directly inject aerosols and SO₂, which oxidizes to form a sulfate aerosol. Although the surface reactivity of such stratospheric aerosols may be relatively inefficient in catalyzing ozone destruction, the large mass injections by volcanic eruptions, such as El Chichón, can produce substantial temporary reductions in columnar ozone over the entire northern hemisphere (*WMO [1995], WMO [1991]*).

2.4.2 Measurement Techniques

Ozone measurements can be divided into two important types: those that measure the total thickness of the ozone layer and those that measure the ozone concentration as a function of altitude. Historically, the most important instrument for the measurement of the total thickness of the ozone layer has been the Dobson spectrophotometer, designed in the 1920s and still in use today. The Dobson instrument, located on the ground, measures the solar radiation transmitted through the ozone layer at pairs of wavelengths near 300 nm. One wavelength is chosen so that it is significantly absorbed by ozone while the other is attenuated in the instrument by a calibrated optical wedge. The wedge position is adjusted until equal signals for the two beams are obtained. Measurements are made for two separate pair of wavelengths to allow cancellation of errors due to aerosols in the atmosphere (*Dobson [1957]*). New evidence indicates that significant ozone decreases are also occurring in the spring and summer in both hemispheres and during the Southern Hemisphere winter. These decreases are observed mainly in the lower stratosphere, below 25 km, at middle and high latitudes, where heterogeneous chemistry occurs as in the Antarctic. The increased abundance of chlorine and bromine in the stratosphere is likely at the root of the ozone depletion. Evidence suggests that heterogeneous chemical reactions, similar to those involving ice crystals over Antarctica, can occur on the surface of sulfate aerosol particles that reside in the stratosphere. Another cause for part of the observed decrease in ozone levels could be the transport of ozone-depleted air from the Polar region into the middle latitudes (*WMO [1995], WMO [1998]*).

2.4.3 Montreal Protocol

The Montreal Protocol on Substances that Deplete Stratospheric Ozone is an international treaty that has been signed by many countries including the United States. This treaty calls for the phase-out of chlorofluorocarbons by the year 2000, although there are provisions for a faster phase-out if the science warrants. Because new advances in scientific understanding are occurring constantly, major scientific assessments of the state of knowledge about ozone depletion have been published in a variety of joint reports from the World Meteorological Organization and the United Nations Environment Program. The purpose of these reports has been to determine if stricter environmental provisions are necessary (*WMO [1985], WMO [1988], WMO [1991], WMO [1995], WMO [1998]*).

The ozone-depleting chemicals are being phased out of production in most countries, under the terms of the Montreal Protocol. Several countries, including the United States, have sped up

the timetable for ceasing production to mid- 1990's. Because of the important functions these ozone-depleting substances perform, substitutes are being developed. Some of the most likely substitutes do contain chlorine, but are more apt to react in the lower atmosphere so less chlorine would enter the stratosphere. Much research remains to be done to develop completely ozone-safe substitutes.

2.5 Launch Vehicles

2.5.1 Impact on the Stratosphere

Beginning in the early 1970s, predictions have been made that human activities will lead to a diminishing of the earth's protective ozone layer (*Johnston [1971], Molina et al., [1974], Rowland et al., [1975]*). Depletion of stratospheric ozone resulting from the catalytic effect of nitrogen oxides, or NO_x, emitted from a proposed fleet of supersonic transports was first predicted by Johnston (*Johnston [1971]*). A few years later, the deleterious effects of chlorine on stratospheric ozone from chlorofluorocarbons were predicted by M. J. Molina and F. S. Rowland [*Molina et al., [1974], Rowland et al., [1975]*]. The possible impact of the exhausts of solid-fuel rockets on the ozone layer were considered in the early 1970's as part of the Climatic Impact Assessment Program (*see Hoshizaki [1975]*). At that time, the effects of the Space Shuttle exhausts were considered to be small; model computations led to the conclusion that (with a launch rate of 60 Space Shuttles per year) the total ozone concentrations would be reduced by about 0.25 percent in the Northern Hemisphere and by about 0.025-0.05 percent in the Southern Hemisphere with an uncertainty factor of about three (*Potter [1978]*). Since that study, there has been new knowledge of the chemical reaction rates and changing perceptions of the role of homogeneous and heterogeneous chemical reactions. Accordingly, in this section more recent assessments are reviewed.

2.5.2 Launch Vehicle Emissions

The major chemical emissions and afterburning products from launch vehicle (LV) activities depend on the types of propellants used. Table 2-2 provides the main emissions/afterburning products from various propellants that are currently used in space flight or are under development (*AF [1990, 1991, 1994, 1996], Versar [1991], Jones [1996], NSWC [1996], WMO [1991], Lewis et al., [1994], DOT [1992]*).

The term hypergolic is used to characterize a propellant based on whether or not spontaneous ignition occurs when the propellants are brought into contact (this does not apply to solid propellants). A cryogenic propellant is one whose boiling point is below -130 °C. Finally, liquid propellant systems are usually categorized into the following types: monopropellant (both the oxidizer and fuel are combined into one system), bipropellant (both the oxidizer and fuel flow separately to each other), etc.

Table 2-2. Examples of Propellant Types and Potential Exhaust Products

Propellant Type	Example Propellants	Exhaust Products
Solid	CTPB, HTPB, Al, NH_4ClO_4	CO, CO_2 , NO_x , H_2O , HCl, Cl, Al_2O_3
Liquid Hydrocarbon	RP-1, Kerosene	CO, CO_2 , H_2 , H_2O , OH
Hypergolic	N_2O_4 , N_2H_4 (Aerozine-50), MMH	CO, CO_2 , NO_x , N_2 , H_2 , H_2O
Cryogenic	LOX/ LH_2	H_2 , H_2O
Hybrid Propellant	LOX/ Butyl Rubber	CO, CO_2 , NO_x , H_2 , H_2O , OH

2.5.3 Launch Vehicles and Stratospheric Chemistry

Rocket launches can affect the atmosphere both in an immediate, episodic manner, and in a long-term, cumulative manner. The stratosphere is affected immediately after launch along the flight trajectory of the launch vehicle (LV) for about 60 to 120 seconds, the time required for the LV to pass through the stratosphere. Formed either directly or indirectly from rocket exhaust, radicals, such as Cl, ClO, H, OH, HO_2 , NO, and NO_2 , can cause the catalytic destruction of stratospheric ozone. Other exhaust compounds that presumably could lead to ozone destruction either by direct reaction with ozone or by providing a surface for heterogeneous processes include Al_2O_3 and ice (*Hanning-Lee et al., [1996]*). While no experimental evidence exists and no work to date has been performed, Lohn *et al., [1999]* has suggested that soot may contribute to catalytic ozone destruction in rocket plumes. The emissions from some types of launch vehicles significantly perturb the atmosphere along the launch trajectory at a range of a kilometer or less from the rocket passage. Ozone is temporarily reduced, an aerosol plume may be produced, and combustion products such as NO_x , chlorinated compounds, and reactive radicals can temporarily change the normal chemistry along the vehicle path.

The stratosphere exchanges mass with the troposphere beneath it at a relatively low rate. With no rainout or other removal mechanisms, the rocket combustion products can build up in the stratosphere over time if there is a sufficient launch rate. When deposited into the stratosphere, ideally sized particulate (0.15 to 0.4 microns in size) such as alumina aerosols can persist for months and circle the globe. Aerosols that exist in the stratosphere can assist in catalyzing the destruction of ozone.

The stratospheric chemistry of alumina surfaces under stratospheric conditions has also been studied (*Meads et al., [1994]*). The results of this study indicated that the reaction probabilities for critical chlorine reactions are typically an order of magnitude less than for ice and water-rich nitrate aerosols. However, the alumina surfaces are considerably more reactive than the sulfuric acid aerosols found in the lower stratosphere in mid-latitudes. As a result, for regions where PSCs and water or ice aerosols are rare, such as in the tropical and mid-latitudes, the alumina aerosol surfaces may play an important role in expediting ozone destruction by halogen species if

a sufficient atmospheric loading occurs. However, compared with the sulfate aerosol loading, the alumina loading from rocket launches is less than 1 percent of the sulfate aerosol even when there have not been any recent volcanic eruptions (*Beiting [1997b]*).

2.6 Summary

There has been extensive research on the potentially harmful effects of large solid rocket exhaust on ozone depletion by the Air Force and the National Aeronautics and Space Administration (NASA). Hydrogen chloride emissions from SRMs are of primary concern. Most of the studies focus on HCl because the other emitted chemicals, such as Al_2O_3 , have been shown to have a much smaller effect on ozone depletion. These studies are generally based on a high launch rate to provide an upper limit to ozone depletion, which allows for evaluation of large HCl and Cl loads to the stratosphere. The following section will assess modeling efforts to characterize the local and global impact of SRMs on stratospheric ozone.

3 MODELING OBSERVATIONS OF SRM EXHAUST

3.1 Modeling Observations of SRM Exhaust

In this section, modeling efforts on the impact of SRM exhaust on stratospheric ozone are considered. The exhaust plume, including exhausted products and heights of release, is described in Section 3.2. The exhaust plume spreads out such that effects need to be considered at various time and space scales. Local and regional scale effects are considered in Section 3.3. These include plume effects from single and multiple rocket motors. Section 3.4 describes global scale effects, including both homogenous and heterogeneous chemical reaction mechanisms. The effects of particulate on stratospheric ozone are detailed in Section 3.5. Plume dispersion characteristics and model comparisons are made in Section 3.6. A summary of modeling efforts is presented in Section 3.7.

3.2 The Exhaust Plume

Assessment of the impact of space launch operations on the environment is now an integral part of launch operations and launch system acquisition. There are numerous published studies dealing with the effect on the ozone layer by ozone reactive compounds that are exhausted into the stratosphere by solid rocket motors (*i.e.*, Jackman *et al.*, [1996a,b, 1998], Denison *et al.*, [1994], Karol *et al.*, [1992], Kruger *et al.*, [1992], Danilin [1993], Brady *et al.*, [1994, 1995a,b,c, 1997a,b], Jones [1995], Prather *et al.*, [1990a,b, 1994], Zittel [1992, 1994], Ross *et al.*, [1996a,b, 1997a,b,c], WMO [1991], AIAA [1991], Lohn *et al.*, [1994, 1999], Ko *et al.*, [1994, 1999]). Chlorine and chlorine oxides are present only in the exhaust of solid rocket motors such as those found on the Titan IV, the Space Shuttle, and many smaller launch vehicles. There are two other classes of compounds commonly found in rocket exhaust that can cause ozone destruction. These are the oxides of nitrogen and hydrogen, and they are present to some extent in the exhaust of every launch vehicle. There are also species such as alumina and soot from LOX/Kerosene fuel in rocket exhaust that may promote heterogeneous reactions with ozone and ambient chlorine containing compounds.

Although rocket motor emissions appear to represent a small fraction of the total anthropogenic impact on stratospheric chemistry, prudence requires a careful evaluation of this impact, particularly on stratospheric ozone (Ko *et al.*, [1999], WMO [1991]). Increasingly sophisticated modeling efforts have converged on the view that the present fleet of solid-fueled rockets contributes only negligibly to ozone depletion on a global scale (Jackman *et al.*, [1996a]). While Jackman *et al.*, [1998] considered the potential impact of heterogeneous chemistry on ozone depletion expected from rockets, there still are unanswered questions.

Several countries have major space launch vehicles including the U.S. (*e.g.*, Space Shuttle, Centaur, Atlas, Titan, and Delta), the former USSR (*e.g.*, Energy and Proton), European Space Agency, ESA (*e.g.*, Ariane), Japan (*e.g.*, H-1, H-2, N-2, M-5), and China (*e.g.*, Long March) to name a few. Some of these launch vehicles depend on solid fuel, some depend on liquid fuel, and

others rely on a combination of solid and liquid (*e.g.*, Space Shuttle). The major exhaust products of various solid and liquid systems were reported in AIAA [1991, 1994] and are shown in Table 3-1. Included in Appendix C is a brief condensed description of these various launch platforms and serves as an aid in reading Table 3-1. A complete and detailed description of these various space launch systems may be found in the reference AIAA [1994].

3.2.1 Launch Vehicle Characteristics

The two solid-fueled motors used in the seven-segment Titan IV were the strap-on booster (T4/SRM), and the scheduled upgrade (T4/SRMU). These motors have a propellant composition ranging from 16% to 19% aluminum (Al), 68% ammonium perchlorate (AP), and polymeric binders and catalysts (PBAN or HTPB). The propellants used in the Titan IIIB first-stage (T3B) were an amine fuel and NTO (N_2O_4) oxidizer. The Aerozine-50 (or A-50) fuel in the second stage was a 50/50 mixture by weight of hydrazine and 1,1-dimethylhydrazine. The core stage used in the Delta space launcher (Delta core) is a 270 klb thrust motor using kerosene (RP-1) and liquid oxygen (LOX) propellants. Finally, the Space Shuttle main engine (SSME) utilizes a 520-klb thrust motor propelled by liquid hydrogen (LH_2) and LOX. The Space Shuttle actually employs a cluster of three SSME motors, with solid strap-on boosters at low altitude.

3.2.2 Launch Rates and Stratospheric Chemical Composition

The worldwide successful space launches for all government and commercial missions are presented in Table 3-3; the actual number of launches is given for 1957 through 1995 (*TRW Space Log [1996]*). Over the last decade, the total number of launches has stabilized to a mean value of approximately 84 worldwide launches per year (See also the space launches for 1996 to 1999 in Table 3-4).

Table 3-1. Compilation of Launch Vehicle Descriptions by Country, Vehicle Type or Configuration, Propellant Used and Probable Propellant Mass (lb.). Taken and condensed from *International Reference Guide to Space Launch Systems, Second Edition, Steven J. Isakowitz, AIAA, 1994.*

Country	Vehicle	Configuration	Propellant	Propellant Mass (lb.)	
China					
	Long March	CZ-2E or 3B (LB40) Liquid Strap-On	UDMH/N ₂ O ₄	84,000	
		CZ-1D Stage 1 (L60) Stage 2 (L10) Stage 3	UDMH/HNO ₃ UDMH/N ₂ O ₄ Solid	132,000 26,900 1,380,000	
		CZ-2C Stage 1 (L140) Stage 2 (L35)	UDMH/N ₂ O ₄ UDMH/N ₂ O ₄	317,000 77,000	
		CZ-2E or 3B Stage 1 (L180) Stage 2 (L80)	UDMH/N ₂ O ₄ UDMH/N ₂ O ₄	4,123,000 190,000	
		CZ-3 Stage 1 (L140) Stage 2 (L35) Stage 3 (H8)	UDMH/N ₂ O ₄ UDMH/N ₂ O ₄ LOX/LH ₂	313,000 77,000 18,700	
		CZ-3A Stage 1 (L180) Stage 2 (L35) Stage 3 (H18)	UDMH/N ₂ O ₄ UDMH/N ₂ O ₄ LOX/LH ₂	375,000 65,300 38,800	
		CZ-4 Stage 1 (L180) Stage 2 (L35) Stage 3 (L15)	UDMH/N ₂ O ₄ UDMH/N ₂ O ₄ UDMH/N ₂ O ₄	404,000 78,400 31,200	
Europe					
		Ariane	Ariane-4 Solid Strap-On (P9.5 or PAP) Liquid Strap-On (L40 or PAL) Stage 1 (L220) Stage 2 (L33) Stage 3 (H10)	CTPB	20,900
				N ₂ O ₄ /UH25	86,000
				N ₂ O ₄ /UH25	514,000
				N ₂ O ₄ /UH25	77,600
				LOX/LH ₂	23,800
	Ariane-5 Solid Booster (P230) Core Stage (H155) Upper Stage (L9)		HTPB LOX/LH ₂ N ₂ O ₄ /MMH	506,000 342,000 21,400	
Israel					
	Shavit	3 Stage	Solid	n/a	

Table 3-1. Compilation of Launch Vehicle Descriptions by Country, Vehicle Type or Configuration, Propellant Used and Probable Propellant Mass (lb.). Taken and condensed from *International Reference Guide to Space Launch Systems, Second Edition, Steven J. Isakowitz, AIAA, 1994. (Continued)*

Country	Vehicle	Configuration	Propellant	Propellant Mass (lb.)
India				
SLV	SLV-3	Stage 1	PBAN	19,100
		Stage 2	PBAN	6,940
		Stage 3	HEF-20	2,340
		Stage 4	HEF-20	578
	ASLV	Stage 0 (AS0)	HTPB	19,040
		Stage 1 (AS1)	HTPB	19,600
		Stage 2 (AS2)	HTPB	7,050
		Stage 3 (AS3)	HEF-20	2,340
		Stage 4 (AS4)	HEF-20	700
	PSLV	Strap-Ons (PSOM or S9)	HTPB	19,700
		Stage 1 (PS1 or S125)	HTPB	284,400
		Stage 2 (PS2 or L37.5)	UDMH/N ₂ O ₄	82,700
		Stage 3 (PS3 or S7)	HTPB	15,900
		Stage 4 (PS4 or L2)	MMH/N ₂ O ₄	4,400
	GSLV	Stage 0 (L40 or GS0)	UDMH/N ₂ O ₄	4 x 88,200
		Stage 1 (S-125 or GS1)	HTPB	284,000
Stage 2 (L-374 or GS2)		UDMH/N ₂ O ₄	82,700	
Stage 3 (CS or GS3)		LOX/LH ₂	27,600	
Japan				
H-2	SRB	Stage 1	HTPB	131,000
		Stage 2	LOX/LH ₂	190,000
		Stage 2	LOX/LH ₂	37,000
J-1		Stage 1	HTPB	130,500
		Stage 2	HTPB	22,900
		Stage 3	HTPB	7,300
M-3SII	Strap-On Booster (SB-735)	Stage 1 (M-13)	CTPB	8,800
		Stage 2 (M-23)	CTPB	59,700
		Stage 3 (M-38)	HTPB	22,900
		Stage 3 (M-38)	HTPB	7,230
	Stage 4 (Optional)	KM-P	HTPB	923
		KM-D	HTPB	617
		KM-M	HTPB	1,113
M-V		Stage 1 (M-14)	HTPB	157,600
		Stage 2 (M-24)	HTPB	68,500
		Stage 3 (M-34)	HTPB	22,000
		Stage 4 (Optional)	HTPB	2,890
CIS (Russia)				
Energia		Stage 1 (Strap-Ons)	LOX/Kerosene	705,000
		Stage 2 (Core)	LOX/LH ₂	1,810,000
		EUS – Optional	LOX/LH ₂	154,000
		RCS – Optional	LOX/Kerosene	33
Kosmos		Stage 1	HNO ₃ + 27%	180,300
		Stage 2	UDMH/N ₂ O ₄	41,900

Table 3-1. Compilation of Launch Vehicle Descriptions by Country, Vehicle Type or Configuration, Propellant Used and Probable Propellant Mass (lb.). Taken and condensed from *International Reference Guide to Space Launch Systems, Second Edition, Steven J. Isakowitz, AIAA, 1994. (Continued)*

Country	Vehicle	Configuration	Propellant	Propellant Mass (lb.)
CIS (Russia) (Continued)	Proton	Stage 1	UDMH/N ₂ O ₄	924,400
		Stage 2	UDMH/N ₂ O ₄	344,100
		Stage 3	UDMH/N ₂ O ₄	102,600
		Stage 4 (D-1-e only) Block D	LOX/RP-1	33,200
	Rokot	Stage 1	UDMH/N ₂ O ₄	N/A
		Stage 2	UDMH/N ₂ O ₄	N/A
		Briz	Solid?	N/A
	Soyuz/ Molniya	Strap-Ons	LOX/Kerosene	86,400
		Core Stage 1	LOX/Kerosene	208,000
		Core Stage 2	LOX/Kerosene	50,700
		Stage 3 (for Molniya)	LOX/Kerosene	7,600
Start	Multiple Stages	Solid	n/a	
CIS (Ukraine)	Ikar	Ikar-1 and Ikar-2 3 Stages	UDMH/N ₂ O ₄	n/a
	Tsyklon	F-1-m / F-2 Stages		
		Stage 1	UDMH/N ₂ O ₄	261,700
		Stage 2	UDMH/N ₂ O ₄	106,900
		Stage 3 (F-2 Only)	UDMH/N ₂ O ₄	6,600
	Zenit	Zenit 2		
		Stage 1	LOX/Kerosene	719,400
		Stage 2	LOX/Kerosene	180,800
		Zenit-3		
		Stage 1	LOX/Kerosene	703,000
	Stage 2	LOX/Kerosene	180,800	
	Stage 3	LOX/Kerosene	31,300	
United States	Atlas	E	LOX-RP1	248,800
		I	LOX-RP1	305,500
		II	LOX-RP1	344,500
		IIA	LOX-RP1	344,500
		Castor IVA (strap-on, 4 segments)	HTPB	89,200
		IIAS	LOX-RP1	344,500
	Conestoga	IVA (strap-on)	HTPB	22,300
		IVB (strap-on)	HTPB	22,000
		IVB (core)	HTPB	22,000
	Delta	6925 (Castor IVA) SRM	HTPB	22,300
		6925 (stage 1)	LOX-RP1	211,300
		6925 (stage 2)	N ₂ O ₄ -A50	13,364
		6925 (stage 3)	HTPB	4,430,000
		7925 (GEM) SRM	HTPB	25,800
		7925 (stage 1)	LOX-RP1	222,100
		7925 (stage 2)	N ₂ O ₄ -A50	13,367
		7925 (stage 3)	HTPB	4,430,000
	Space Shuttle	SRB	PBAN	2,650,000
		External Tank		1,589,000

Table 3-1. Compilation of Launch Vehicle Descriptions by Country, Vehicle Type or Configuration, Propellant Used and Probable Propellant Mass (lb.). Taken and condensed from *International Reference Guide to Space Launch Systems, Second Edition, Steven J. Isakowitz, AIAA, 1994. (Continued)*

Country	Vehicle	Configuration	Propellant	Propellant Mass (lb.)
United States (Continued)	Athena	Castor 120 LLV1 - Stage 1 LLV2 - Stage 1 LLV3(X) - Stage 1	HTPB	107,381
		Castor 120 LLV1 - LLV2 - Stage 2 LLV3(X) - Stage 2	HTPB	107,381
		Castor 120 LLV1 - LLV2 - LLV3(X) - Stage 1 strap-ons	HTPB	22,268
		Castor 120 LLV1 - Stage 2 LLV2 - Stage 3 LLV3(X) - Stage 3	HTPB	21,560
	Pegasus	Stage 1	HTPB	26,809
		Stage 2	HTPB	6,670
		Stage 3	HTPB	1,699
	Pegasus XL	Stage 1	HTPB	33,176
		Stage 2	HTPB	8,633
		Stage 3	HTPB	1,699
	Taurus	Stage 0	HTPB	108,000
		Stage 1	HTPB	26,809
		Stage 2	HTPB	6,670
		Stage 3	HTPB	1,699
	Titan	Titan II-SLV		
		Stage 1	N ₂ O ₄ -Aerozine 50	260,000
		Stage 2	N ₂ O ₄ -Aerozine 50	59,000
		Titan III		
		Stage 0 (SRM)	84% PBAN	463,000
		Stage 1	N ₂ O ₄ -Aerozine 50	294,000
		Stage 2	N ₂ O ₄ -Aerozine 50	77,200
		Titan IV		
		Stage 0 (SRM)	84% PBAN	600,000
Stage 0 (SRMU)		HTPB	688,000	
Stage 1		N ₂ O ₄ /Aerozine 50	340,000	
Stage 2		N ₂ O ₄ -Aerozine 50	77,000	
Titan III, Upper Stages				
PAM-DII [BA]	Solid	7,140		
OSC [LMT]	Solid/HTPB	21,400		
Titan IV, Upper Stages				
IUS (Stage 1) [BA]	Solid/HTPB	21,400		
IUS (Stage 2) [BA]	Solid/HTPB	6,060		
Centaur [LMT]	LOX/LH ₂	44,880		

HTPB - hydroxy-terminated polybutadiene n/a - Data Not Available [BA] is Boeing [LMT] is Lockheed Martin

3.2.3 Chemical Emissions into the Stratosphere

Each Shuttle launch vehicle uses about 1,000 tons of solid propellant and about 730 tons of liquid propellant (*Bennett et al., [1991]*). The solid boosters exhaust their effluents of HCl, Al₂O₃, CO, CO₂, H₂, and H₂O below 50 km, whereas the exhaust products H₂O and H₂ from the main engine (based on liquid propulsion) are primarily injected above 50 km. Most of the constituents exhausted below the tropopause, typically at a height of 15 km for the launch latitudes, are washed out rapidly before they can reach the stratosphere and hence have negligible effect on the ozone layer (*WMO [1991], Prather et al., [1990a,b], and Pyle et al., [1991]*). An estimate of the mass of chlorine and aluminum oxide solid particulate deposited in the stratosphere may be described as Potential Ozone Reactive Species (PORS). Annual deposition of PORS from U.S. and foreign space launch activities has been reported by *Brady et al., [1994]*. The U.S. contribution was further divided into the Air Force Space and Missile Systems Center (SMC), NASA, and commercial space launches.

Table 3-2 illustrates the amount of chlorine directly deposited in the stratosphere by various launch vehicles as a function of altitude. These exhaust data were provided by T. A. Bauer and K. P. Zondervan of The Aerospace Corporation (*Brady et al., [1994]*). The total mass of exhaust was calculated by an Aerospace simulation code, and the amounts of chlorine and alumina were calculated from their known percentages in the exhaust. The data were tabulated in tons. In addition, alumina particulate was thought to affect ozone by providing a site for the chlorine reactions. The particles can destroy ozone directly, as reported in the literature (*Klimovskii et al., [1983], Keyser [1976], Hanning-Lee et al., [1996], Brady et al., [1997a,b]*), or may catalyze chlorine chemistry analogous to that in the Antarctic clouds. The exhaust particles contain iron and chlorine, which may make them more reactive.

While individual space launches release only a small percentage of the total PORS loading in the stratosphere, the cumulative effect of all launches worldwide may be significant, see Table 3-2 (*Brady et al., [1994, 1997a,b], Lohn et al., [1999]*). For completeness, MX and Minuteman III data are included. Foreign space launch vehicles with solid rocket motors are also considered. PORS generated by the MX and Minuteman III were small compared to most space launch vehicles. In addition, ballistic missile tests are conducted less frequently than space launches. Thus, it is likely that the uncertainty in the PORS contribution from large launch vehicles is greater than the entire contribution from ballistic missiles (*Brady et al., [1994]*).

The Long March class of launch vehicles was not included in Table 3-2 because none of those vehicles use solid propellants, and therefore, their exhaust contains no chlorine or alumina. Similarly, the former Soviet Union has several large launch vehicles capable of commercial and military missions, Energia and Proton for example, but none of the vehicles uses solid propellants and their launch activity has been minimal and is likely to remain so. Data is not available on Soviet ballistic missile launch exhaust profiles or launch rates.

In addition, while chlorofluorocarbon (CFC) emissions are responsible for the largest fraction of global ODC, CFC usage will be curtailed sharply in the near future and the effect of

PORS from launch vehicles is expected to increase. CFC release has been estimated to add 300 kilotons of active chlorine to the stratosphere annually (*Prather et al., [1990]*). Natural sources of stratospheric chlorine are ten to one hundred times smaller (*Rowland [1993], Mankin et al., [1983], Martin [1994]*).

Table 3-2. Ozone Depleting Chemicals from Launch Vehicles

Chlorine in Stratosphere, tons per launch

Altitude, km Vehicle	15-25	25-45	45-60	Total in Stratosphere
Titan IV	20	27	2	48
Titan IV w/ SRMU	23	30	2	55
Delta II	2	5	1	8
Atlas IIAS	2	2	0	3
MX	2	3	1	6
MM III	1	1	0	2
Shuttle	40	39	0	79
Ariane 5	n/a	n/a	n/a	57
H1	1	2	0	3
H2	3	7	1	11

Alumina in Stratosphere, tons per launch

Altitude, km Vehicle	15-25	25-45	45-60	Total in Stratosphere
Titan IV	28	38	2	69
Titan IV w/ SRMU	39	51	3	93
Delta II	3	8	1	12
Atlas IIAS	3	2	0	5
MX	3	4	2	9
MM III	1	1	1	3
Shuttle	57	55	0	112
Ariane 5	N/a	n/a	n/a	81
H1	1	3	1	4
H2	4	10	2	16

n/a-data not available

Table 3-3. Worldwide Successful Space Launches

(Reference: TRW Space Log, Volume 31, TRW Space & Electronics Group,
One Space Park, Redondo Beach, CA 90278.)

Year	USSR/ CIS	USA	France	Australia	China	Japan	UK	Europe	India	Israel	Total
1957	2										2
1958	1	7									8
1959	3	11									14
1960	3	16									19
1961	6	29									35
1962	20	52									72
1963	17	38									55
1964	30	57									87
1965	48	63	1								112
1966	44	73	1								118
1967	66	58*	2	1							127
1968	74	45									119
1969	70	40									110
1970	81	29*	2		1	1					114
1971	83	32*	1		1	2	1				120
1972	74	31*				1					106
1973	86	23									109
1974	81	24*				1					106
1975	89	28*	3		3	2					125
1976	99	26			2	1					128
1977	98	24				2					124
1978	88	32			1	3					124
1979	87	16				2		1			106
1980	89	13				2			1		105
1981	98	18			1	3		2	1		123
1982	101	18			1	1					121
1983	98	22 ⁺			1	3		2 ⁺	1		127
1984	97	22			3	3		4			129
1985	98	17			1	2		3			121
1986	91	6			2	2		2			103
1987	95	8			2	3		2			110
1988	90	12*			4	2		7		1	116
1989	74	18				2		7			101
1990	75	27			5	3		5		1	116
1991	59	18			1	2		8			88
1992	54	28			4	1		7	1		95
1993	47	23			1	1		7			79
1994	48	26			5	2		6	2		89
1995	32	27			2	1		11		1	74
Total	2496	1057	10	1	41	48	1	74	6	3	3737

- Italy has launched nine spacecraft from its San Marco platform. U.S. Scout rockets were used for these launches, so NASA includes them in the U.S. launch total
- ** Launches through March 1984 were ESA sponsored. Arianspace, a private company jointly held by European companies has had launch responsibility since May of that year.
- + ESA launch from WSMC used U.S. Delta 3914 and is included in U.S. total.

Table 3-4. Actual and Projected Status of Annual Rocket Platform Launches

(^ Reference <http://www.flatoday.com/space/today/index.htm>,
 \$ <http://hea-www.harvard.edu/~jcm/space/log/launch.htm>)

Platform	1996 ^{\$}	1997 ^{\$}	1998 [^]	1999* [^]	1991 ^{&}	1992 ^{&}	1998-2010 [#]
Ariane	11	12	11	14	11	11	11
Athena			1	3			
Atlas	7	8	6	12	1	4	10
Delta	10	11	13	21	5	11	13.5
H1					1	1	1
H2	1	1	1				2
Kosmos	4	2	0	1			
LMLV-1	1						
Long March	4	6	6	1			
M5	0	1	1				
Molniya 3	3	3	1				
Pegasus	5	5	6	6			
Proton	8	9	5	8			
PSLV	1						
Soyuz	9	10	8	7			
Space Shuttle	7	8	5	5	8	8	8
Start-1	0	2					
Taurus			2	2			
Titan	4	5	3	8	2	2	4.5
Tsyklon 3	2	2	1				
VLS	1						
Zenit	1	1	3	1			
Total Launches	73	86	73	89	28	37	50

[^] Actual Number of Worldwide Launches – see web reference above

^{\$} Actual Number of Worldwide Launches – see web reference above

[&] Actual Number of Commercial and Government Launches from Brady *et al.*, [1993].

^{*^} Projected Worldwide Launches for 1999 Calendar Year from [^] Reference.

[#] Projected based on Brady *et al.*, [1993] National Mission Model

Presented in Table 3-4 is the actual and projected launch status of various rocket platforms. The launch vehicle is presented in the first column. The actual number of worldwide launches is presented for 1996 and 1997 (*Hea-Harvard [1999]*), as well as 1998 (*Flatoday [1999]*). The projected launches are listed for 1999 (*Flatoday [1999]*). The data for the remaining three

columns were taken from Brady *et al.*, [1994]. The data for 1991 and 1992 is the actual launch status for the respective vehicles and is used in model calculations presented in the next section. The data for 1998-2010 is the projected launch status based on the National Mission Model (Brady *et al.*, [1994]), and is in fairly good agreement with the actual data from the previous columns.

In Table 3-5, Brady *et al.*, [1994] calculated the annual deposition of chlorine and alumina particulate for the period 1991-2010. The sources considered are U.S. Government (i.e., NASA, U.S. Air Force (including SMC), etc.), U.S. Commercial ventures, and foreign launches, broken down by type of vehicle, and launch year. These numbers are simply the exhaust products deposited in the stratosphere for each vehicle type (shown in Table 3-1) times the respective launch rate (shown in Table 3-4). This table helps to give some feel for the total extent and rate of deposition. Although individual launches may be negligible compared to the massive ODC releases from non-launch sources, and individual programs may have a small impact on stratospheric ozone each year, the total amount of launch activity worldwide may be significant and will become more so. This is important because regulation of launches may be mandated by international agreement based on the total PORS deposition rate; restrictions imposed will apply to each individual program.

The Ariane-5 launch vehicle exhausts approximately 57 tons of chlorine in the form of HCl per launch above the tropopause (based on Pyle *et al.*, [1991] with the tropopause assumed at 14 km). The comparable value for Energy is zero tons (Pyle *et al.*, [1991]). The data in Table 3-5 give an idea of the extent of the future deposition rate, and may be useful for planning purposes. Based on predicted launch rates, the military and civilian government launches put about half or a third as much PORS in the stratosphere as the commercial launches.

The total PORS flux to the stratosphere from all types of vehicles and organizations in the years 1998-2010, based on estimates by Brady *et al.*, [1994], is presented in the last column of Table 3-5. These numbers were yearly averages and represented projections over the entire period. In short, space launches currently contribute over two thousand tons of chlorine and alumina particulate to the stratosphere annually. This represents two-thirds of one percent of the total PORS in the stratosphere if all launches worldwide are considered and are weighted the same for chlorine (Brady *et al.*, [1994]). The impact of this contribution will be examined in subsequent sections.

Table 3-5. Annual Stratospheric Deposition Rates (tons/year) for Chlorine and Alumina Particulate for U. S. and Foreign Launches; 1991-2010

<u>Organization</u>	1991	1992	1993-1997	1998-2010
<u>SMC</u>				
Titan IV	234	117	397	666
Delta II	20	51	67	67
Atlas IIAS	0	17	34	51
Shuttle	383	383	0	0
Total	637	567	499	784
<u>NASA</u>				
Shuttle	574	765	1531	1531
Total	574	765	1531	1531
<u>Commercial</u>				
Titan	0	117	0	0
Delta	82	102	102	112
Atlas	8	17	17	34
Shuttle	574	383	0	0
Total	664	619	119	146
<u>Foreign</u>				
Ariane	0	0	760	1520
H1	8	8	8	8
H2	0	0	27	53
Total	8	8	794	1581
World Total	1883	1959	2943	4042

3.3 Local and Regional Effects

The substances emitted from rocket exhausts are initially confined to a small volume of atmosphere a few hundred meters wide extending the length of the flight path. This affected volume is then moved away from the vicinity of the launch site by the wind systems and simultaneously distorted and mixed with the surrounding air, so that the contaminated volume increases, while the concentrations of pollutants decrease. This raised the possibility that restricted areas of severely reduced columnar ozone amounts may be found downwind of launch sites for a short period after each launch (*WMO [1991]*).

These local and regional effects are more difficult to calculate than global effects, being dependent on the meteorological situation prevailing at the time of launch and involving small-scale mixing processes. Nonetheless, plausible assumptions are possible that should permit estimates to be made that indicate the order of magnitude of the reductions. Predictions of the extent of local transient ozone loss in the expanding exhaust plume of a Space Shuttle or Titan IV rocket vary from a few tens of percent (*Kruger [1994]*) to 100% (*Ross et al., [1996b]*) over horizontal distances of several kilometers.

Karol et al., [1991] modeled ozone reductions that may be expected during the 24 hours following the launch of both NASA's Shuttle and the Soviet Energy rocket. Their model allowed the plume to diffuse horizontally for different stages of plume-spread. In addition to gases directly emitted by the exhaust, the possibility that nitrogen oxides are produced as a result of the mixing of hot exhaust gases with the surrounding air and that some HCl emitted by the Shuttle is converted rapidly to Cl_2 was considered. Effects of Al_2O_3 particles and heterogeneous chemistry were not included. *Karol et al., [1991]* concluded that the areas affected by the plume are of restricted horizontal extent. To illustrate this, for the Shuttle passing through a height of 24 km, the dispersion distance (i.e., from the center within which the ozone is destroyed by 10 percent or more) is slightly over 1 km for the first hour, increasing to 4 km over the next 2 hours, after which it shrinks rapidly to zero, as the plume recovers to the extent that the reductions nowhere exceed 10 percent. A criticism was that no heterogeneous chemistry was included in the calculations.

Aftergood [1991] suggested that there could be a significant "soft spot" or a local decrease in total ozone after a Space Shuttle launch. *Aftergood [1991]* observed that ozone reductions greater than 40 percent were detected in the exhaust trail of a Titan III solid rocket at an altitude of 18 km were observed only 13 minutes after launch (*Pergament et al., [1977a,b]*). Because rocket trajectories through the atmosphere are curved rather than straight-up, the calculations of *Karol et al., [1991]* indicated that the maximum depletion of the total ozone column never exceeded 10 percent at any point under the Shuttle plume in the first 2 hours, and subsequently diminished to much smaller values. Consistent with these model computations, *McPeters et al., [1991]* found no evidence of ozone depletion in a study of TOMS images taken at varying times after eight separate Shuttle launches. Because of this debate, a significant number of studies were undertaken to determine the extent of this localized ozone depletion.

3.3.1 Plume Effects from Single and Multiple Rocket Motors

Brady et al., [1997a,b] used the SURFACE CHEMKIN model to determine the time evolution of a point on the centerline of a dispersing plume from a launch vehicle in the stratosphere. The analysis was confined to an altitude of 20 km, the altitude where the majority of the stratospheric ozone distribution is located. The SURFACE CHEMKIN code was developed by R. J. Kee of Sandia, Livermore (*Coltrin et al., [1991]*, *Kee et al., [1991a,b]*). *Brady et al., [1997a,b]* analyzed a sampling of hypothetical large rocket motors in a model that

included 34 chemical species and over 100 gas phase chemical and photochemical reactions, and two heterogeneous reactions: the direct loss of ozone on alumina and catalysis of the reaction of chlorine nitrate with HCl. These chemical species were loosely based on the following propulsion systems from existing single and multi-engine launch vehicles, both single and multiple engine launch vehicles. Multiple engine effects are described in a subsequent section.

3.3.1.1 Single Engine Effects

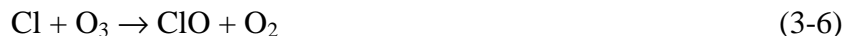
Afterburning occurs as the combustion gas leaves the rocket motor, converting a substantial amount of the effluent into potential ozone reacting species. Afterburning of plume exhaust was first realized as an important source of stratospheric ozone depletion at TRW (*see Denison et al., [1994]*). At approximately the same time, The Aerospace Corporation was examining different rocket motors and came to a similar conclusion (*Zittel [1994]*). Since this report, a variety of plume models have confirmed afterburning to be a significant source of local ozone depletion (*Martin [1994], Brady et al., [1994, 1997a,b], Lohn et al., [1994, 1999], Ross et al., [1997]*). Afterburning chemistry may occur when a substantial amount of the HCl in the exhaust stream is converted to the more reactive Cl and Cl₂ species (i.e., from 21-71%, depending on altitude). The chemistry occurs through reactions such as:



The chlorine radical immediately reacts with ozone present in the stratosphere to begin a catalytic destruction cycle. Two possible ozone destruction mechanisms may occur. At higher altitudes (e.g., 30 km) the sequence will be:



At lower altitudes (e.g., 20 km) a more complex ozone destruction cycle may take place involving the chlorine oxide dimer (ClO)₂ (*Martin [1994], Ross et al., [1997a], Molina [1999]*).



This lower altitude cycle is similar to that which causes the Antarctic ozone depleted region, except that the chlorine oxide dimer forms because of the high concentrations of chlorine in the rocket plume (six orders of magnitude above background), and not because of low temperatures. *Brady et al., [1997a,b]* reported the principal route for generation of atomic chlorine from the

dimer was not photolysis of the dimer (which is the route in the Antarctic), but was the branched chain reaction of the dimer with atomic chlorine as shown above. Because the two reaction cycles shown above regenerate atomic chlorine, these cycles continue to destroy ozone until the Cl and ClO return to HCl by reactions with hydrogen containing molecules such as methane or hydrogen.



Under normal ambient stratospheric conditions, the Cl and ClO are converted to HCl by this process in a few minutes, with HCl returning very slowly to the active form. In a rocket plume, however, there is sufficient Cl and ClO to deplete the methane and hydrogen concentration so that substantial local depletion of ozone may take place on short time scales.

Oxides of nitrogen (i.e., NO_x or NO and NO₂) in the rocket exhaust can come from two different sources, depending on the motor used. NO_x can come from the propellant; nitrogen tetroxide (N₂O₄, or NTO) that has not fully reacted remains as NO or NO₂ in the plume. Similarly, nitrogen in the fuel, from the amine fuels or impurities in the hydrocarbon fuels can be converted to NO_x upon oxidation. The second source of NO_x comes from afterburning that occurs in essentially all rocket plumes in the lower stratosphere. As air mixes into the hot exhaust, nitrogen and oxygen from the ambient atmosphere can combine to create NO_x in regions of high flame temperature (*Zittel [1995], Brady et al., [1997a,b]*). Several of these important reactions in this process, including the Zeldovich mechanism in reactions (3-12) through (3-14), follow.



Once the NO_x has formed, it can react with ozone in a cycle similar to that for chlorine.



Nitrogen oxides in the plume can be converted into the non-destructive reservoir species ClONO₂ and HNO₃ by reaction (3-21) and (3-22). As in the case of HCl, the reservoir species are very slowly converted back to active species and may be removed by mixing with the troposphere.



Brady *et al.*, [1997a,b] concluded that the observed ozone depletion in the exhaust gas plume was due to chlorine in the solid rocket motor exhaust, not NO_x as was originally suggested (Pergament *et al.*, [1977]). For launch vehicles utilizing LOX as a fuel, the ozone depleted region persisted (greater than 10% ozone depletion) for less than 5 minutes; for the solid rocket motors with chlorine, the depleted region persisted for 3 to 10 hours, depending on the dilution parameters. Other modeling efforts on single engine effects were performed by Danilin [1993], Denison *et al.*, [1994], Lohn *et al.*, [1994], and Prather *et al.*, [1994] and are presented later in this modeling section.

3.3.1.2 Multiple Engine Effects

Lohn *et al.*, [1999] used a Standard Plume Flowfield (SPF) model to simulate the effects on stratospheric ozone caused by launch vehicles with multiple solid rocket motors, such as the U.S. Space Shuttle main engine and Titan III & IV rocket motors. Lohn *et al.*, [1999] calculated the exhaust plume (“hot plume”) from the nozzle exit plane to the location where the plume (by mixing with the ambient atmosphere) reaches dynamic and thermal equilibrium with the atmosphere. Specifically, ozone loss caused by an SRM passing through the stratosphere was evaluated by calculation at altitudes of 15, 20, 25, 30, 35, and 40 kilometers. Inputs to the SPF “hot plume” calculation were vehicle altitude and nozzle exit plane conditions (species concentrations, velocity, temperature, pressure, and relative speed between the ambient atmosphere and the exhaust plume velocity). The relative speed drives mixing in the shear layer (the mixing layer between the atmospheric gas and the exhaust plume). Mixing with the atmosphere spreads the plume and brings it to rest and results in a “cold wake” that is in thermal and dynamic equilibrium with the ambient gases. Mixing of the burnable plume species with ambient oxygen (after-burning) produces thermal decomposition of HCl into chlorine. The chlorine mechanism is the main cause of ozone destruction by SRM exhaust. The production of chlorine by after-burning is thus a key step towards ozone destruction and requires careful evaluation of the “hot plume” dynamics and chemistry. The after-burning mechanism is described in detail elsewhere (Denison [1994], Lohn [1996], Burke [1998]).

Lohn *et al.*, [1999] determined that the “early to medium time” diffusion-driven behavior which occurs within two hours after launch. As the ozone hole increases in size ozone back-fills (as caused by diffusion processes) into the hole as time passes and the ozone concentration at the axis eventually recovers the ambient value. The process is controlled by the rate at which plume species diffuse into the ambient atmosphere. The process of ozone loss was controlled by the reaction of ozone with chlorine (with ClO as a product) and the subsequent re-production of chlorine by photoreactions and reactions associated with ClO. It is this cyclic regeneration of Cl that caused the generation of an ozone hole (for the present SRM chlorine has a far greater effect on local ozone depletion than NO and NO_2 or aluminum oxide particles). In short, approximately ten ozone molecules were consumed by each chlorine atom in the original plume during the time before diffusion filled-up the hole (The time to refill to ambient ozone levels was 3000 seconds at 15-20 km and 6000 seconds at 40 km). This 1:10 Cl: O_3 ratio is based on diffusion and production rates within the plume and differs from the 1:10,000 ratio which exists under background stratospheric conditions (Lohn *et al.*, [1999]). The total loss of ozone is

somewhat greater than the size of the hole indicates since the hole begins to fill when the radially inward diffusion of ozone exceeds the ozone loss.

The plume dynamics are controlled by the rate at which plume species diffuse into the ambient atmosphere (a process slowed by the stretching caused by cross winds). The initial cold wake size (radius) varied from 150 m at 15 km to 650 m at 40 km. The combination of size differences and ambient atmosphere pressure lead to a larger local ozone hole that lasted longer at higher altitude. Ozone loss was observed at the “diffusion interface” where the process of ozone loss is controlled by the reaction of ozone with Cl (with production of ClO and Cl₂O₂) and the subsequent reproduction of chlorine atoms by photo-reactions and reactions associated with ClO and Cl₂O₂ (both found in high concentration in the ozone hole region). Table 3.6 summarizes the ozone hole dynamics modeled by Lohn *et al.*, [1999].

Table 3-6. Ozone hole size (radius) and lifetime in the stratosphere.

Altitude, km	Ozone Hole Lifetime, s	Ozone Hole Size, m
15	2500	3500
20	2500	3000
25	2500	3000
30	4500	6000
35	5000	7000
40	5000	20000

Local effects on Cl₂ and ozone due to SRMs were measured *in-situ* by Ross *et al.*, [1997a,b] and confirmed these findings. These *in-situ* measurements will be discussed in more detail in Section 5. These model simulations of dramatic ozone losses in the first couple of hours after launch have been corroborated by measurements taken after the launch of a different solid rocket (Titan III). The Titan III uses the same oxidizer (ammonium perchlorate) as the Space Shuttle, thus is expected to release HCl into the exhaust plume.

Regional effects (1000 x 1000 km²) associated with rocket effluents were computed (e.g., from the perturbation of Cl_y (Cl, Cl₂, ClO, Cl₂O₂, HCl, HOCl, and ClONO₂)) for a single Space Shuttle launch using a three-dimensional model (Prather *et al.*, [1990b,c]) with a resolution of 8° latitude by 10° longitude. The Cl_y concentration at 40 km, 30°N, 70°W, can increase by a few percent 2 days after the launch, and the corresponding ozone decrease is expected to be less than 1 percent at that height. The subsequent rate at which the chlorine is dispersed depends on season, the summer atmosphere being less dispersive than the winter. After an additional 6 days, the peak chlorine concentrations had fallen by a factor of 4 in the January simulations and a factor of 2 in the July simulations. The Cl_y emitted by the Shuttle became spread over all longitudes in about 30 days and was found to be less than 0.15 percent of background levels.

3.4 Global Scale Effects

3.4.1 Stratosphere/Troposphere Exchange

After about a month, the effects of a given launch are spread over a sufficiently large portion of the atmosphere and diluted to the stage where they contribute less to any ozone reduction than do the remnants of the previous launches. It thus becomes necessary to consider the cumulative global-scale effect of a series of launches. Prather *et al.*, [1994] has suggested that it is highly unlikely that soluble chlorine (as HCl) emitted into the troposphere by perchlorate-fueled solid rocket boosters (e.g. Titan IV, Space Shuttle) will enter into the stratosphere in significant quantities. Numerical simulations using a chemical tracer model using a likely parameterization of wet removal in convective events (75% efficiency), showed that less than 0.5% of the original tropospheric emissions remain in the atmosphere after three months, and less than 0.2% of these original tropospheric emissions were transported across the “tropopause” into the lower stratosphere. Greater than 99.5% of the original emissions are removed by washout, most of which occurs in the first six weeks after launch. Removal occurs primarily nearest the point of launch, with some removal taking place downstream from the launch site. Only emissions above 600 mb transport a noticeable fraction into the tropics and these are also removed by wet convection before entering the stratosphere.

The ability of deep, wet convection to remove soluble species before they enter the stratosphere is supported by these model simulations. Even for small efficiencies of convective removal (as low as 6% removal per event from the convective plume), the tropospheric burden is rapidly reduced, and the amount entering the stratosphere is extremely small, less than 0.2% below 350 mb. This fraction is certainly not known to better than a factor of two, but the upper limit appears robust.

Prather’s [1994] conclusions are strengthened by other independent approaches (e.g., Brady *et al.*, [1997a,b]). Detailed microphysical models (e.g. Tabazadeh *et al.*, [1993]) show that soluble chlorine is efficiently removed in ascending volcanic plumes and does not enter the stratosphere in significant quantities. In spite of the presence of tropospheric HCl (about a part per billion), the stratospheric chlorine budget can be balanced by the chlorine entering the stratosphere as organochlorines (e.g. chlorofluorocarbons) (Zander *et al.*, [1992]). Thus, the HCl present in the lower troposphere must be efficiently removed by wet convection before the air is injected into the stratosphere. Because moist air in the lower stratosphere (about 1% water vapor) must be dehydrated to a few parts per million before it enters the stratosphere, it is difficult to envisage a process that would not remove an equally large fraction of HCl present in solution with water vapor.

3.4.2 Homogeneous Modeling Efforts

The launch of solid rocket motors (SRMs) injects aluminum oxide particles (alumina), hydrogen chloride, carbon monoxide, water vapor, and molecular nitrogen directly into the stratosphere. The global effects on the stratospheric ozone layer from chlorine compounds

emitted by SRMs of the Space Shuttle and Titan IV launch vehicles have been computed previously by Prather *et al.*, [1990a,b]. Specifically, Prather *et al.*, [1990a,b] assessed the steady-state impact of nine Space Shuttles and six Titan IV launches per year on the chlorine loading. The increased stratospheric loading of chlorine from this U.S. launch scenario was computed to be less than 0.25 percent globally of the annual stratospheric chlorine source from halocarbons in the present-day atmosphere. The corresponding changes in chlorine loading and ozone concentration were also calculated. The mixing ratio of Cl_y in the middle to upper stratosphere was computed to increase by a maximum of about 10 pptv (i.e., about 0.3 percent of a 3.3 to 3.5 ppbv background) in the northern middle and high latitudes. Compared to the natural source of chlorine from CH_3Cl (Weisenstein *et al.*, [1991]), this rocket-induced Cl_y enhancement adds about 1.7 percent to a 0.6 ppbv background. The corresponding maximum ozone depletion was calculated to be less than 0.2 percent at 40 km in the winter hemisphere. Maximum column ozone depletion was computed to be much less than 0.1 percent for this scenario (WMO [1991]).

Using the same launch scenario, a computation of the total yearly average global stratospheric ozone depletion was found to be about 0.0065 percent (WMO [1991]). The global effects of Space Shuttle launches have also been computed by Karol *et al.*, [1991]. Scaling the calculations to an equivalent nine Space Shuttle and six Titan IV launches per year Karol *et al.*, [1991] gave a total global ozone depletion of 0.0072 to 0.024 percent.

Pyle *et al.*, [1991] and Jones *et al.*, [1995] studied the global impact on ozone from an Ariane-5 launch rate of ten per year with the use of a two-dimensional model. They performed a 20-year simulation, adding the appropriate amount of chlorine for that scenario until a steady state was established in which the results repeated from one year to the next. Jones *et al.*, [1995] assumed that the alumina would become coated by H_2SO_4 and calculated a 1% increase in the aerosol layer due to the alumina. These computations indicate an effect similar to that reported above for the Prather *et al.*, [1990a,b] work on Shuttle and Titan IV launches (e.g., maximum local ozone depletion is around 0.1 percent near 40 km).

Jackman *et al.*, [1991] used a two-dimensional model computation on the effects of HO_x from emitted H_2 and H_2O for a hypothetical National Aerospace Plane (NASP) on stratospheric ozone. A rate of 40 launches per year results in H_2 and H_2O increases of 0.34 and 0.16 percent, at 35 km altitude and 35°N latitude, respectively. This results in an OH increase of 0.1 percent and a corresponding ozone decrease of 0.006 percent at this location. Total global column ozone impact was calculated to decrease from HO_x chemistry by less than 0.0002 percent.

3.4.3 Heterogeneous Modeling Efforts

One of the major questions remaining from the last major assessment of stratospheric ozone depletion from launch vehicles (WMO [1991]) was the incompleteness found in the models themselves. More specifically, the models were incomplete and, because of their inherent uncertainties regarding heterogeneous chemistry, may have underestimated or possibly

overestimated the ozone depletion expected by rockets. The following section summarizes the recent modeling efforts involving heterogeneous chemistry.

Ko *et al.*, [1999] used the 21 layer GISS/Harvard/UCI Three-Dimensional Chemistry Transport Model (3-D CTM) on the Atmospheric and Environmental Research, Inc. (AER) computer platform to perform a number of simulations to obtain the surface area from accumulation of Al₂O₃ particulates from solid rocket motors, orbital debris, and meteorites. This model was upgraded from the 9 layer Harvard/GISS 3-D CTM for the troposphere, which has been documented and described in detail by Prather *et al.*, [1987, 1990]. Both models have been used to study a variety of problems in the atmosphere, which include CFC simulations (Prather *et al.*, [1987]), the effects of debris from meteors on the Antarctic ozone (Prather *et al.*, [1988]), the dynamical dilution of the Antarctic ozone hole (Prather *et al.*, [1990a]), the Space Shuttle's impact on the stratosphere (Prather *et al.*, [1990b]), the trend and annual cycle in stratospheric CO₂ (Hall *et al.*, [1993]), the seasonal evolution of N₂O, O₃, and CO₂ (Hall *et al.*, [1995]) and trace-tracer correlation in the stratosphere (Avallone *et al.*, [1997]).

Ko *et al.*, [1999] performed two experiments to simulate the distributions of an inert tracer emitted by rocket launches. The source term corresponded to the chlorine emissions from nine annual launches of the Space Shuttle. The source was located above Cape Canaveral, Florida (29°N, 80°W) and its vertical distribution was taken from Prather *et al.*, [1990b]. The input of Cl into the stratosphere was 68 ton for every launch and the total inputs of Cl every year was 68 ton x 9 times/year or 612 ton/year. After a ten year simulation, the tracer distribution reached an annual repeating steady state. The total calculated Cl content in the atmosphere was 1413 ton, which implied that the residence time of Cl from Space Shuttle launches was about 1413[ton] / 612[ton/year] or 2.3 years.

Ko *et al.*, [1999] determined that the initial size distribution of the particulate emitted by SRM was represented by a tri-modal distribution with bulk density of 1.7 gm/cm³. The assumption was made that particles do not interact with each other, so they will evolve independently. Apart from the large-scale transport, particle distributions were affected by sedimentation.

The accumulation of Al₂O₃ particulate in the atmosphere may affect ozone via the heterogeneous reaction ClONO₂ + HCl → HNO₃ + Cl₂ that converts ClONO₂ and HCl, chlorine reservoir species, into the more active form that will deplete ozone in the presence of sunlight. Ko *et al.*, [1999] concluded that because of the very small Al₂O₃ surface areas calculated, ozone depletion on the global scale is very small. The impact on the stratospheric sulfate aerosol layer is likely to be small over most of the stratosphere, but the impact cannot be evaluated with accuracy at this time.

More recently, Jackman *et al.*, [1998] assessed the heterogeneous chemical impact of SRM alumina on stratospheric ozone using the Goddard Space Flight Center two-dimensional photochemistry and transport model. Because alumina is among those substances emitted by solid rocket motors (SRMs), Jackman *et al.*, [1998] used historical launch rates of the Space Shuttle, Titan III, and Titan IV launch vehicles in their time-dependent and steady-state model

calculations to verify the heterogeneous chemistry. The results showed that variations in the temporal ozone depletion correlated with the fluctuation in launch rate frequency. Furthermore, an annually averaged global total ozone (represented with the acronym AAGTO) value was computed for these launch scenarios. The AAGTO so computed was found to decrease by 0.025% by the year 1997, which represented approximately one-third of the annual global total ozone change resulting from SRM-emitted alumina, while the remaining two-thirds resulted from the SRM-emitted hydrogen chloride.

Finally, the increasing influence of the emitted alumina in computed ozone loss is apparent over the 1975-1997 time period. The fractional contribution from the alumina to the total computed ozone loss caused by rocket launches was calculated to increase from less than one-quarter to about one-third over this period. The background upper stratospheric amounts of inorganic chlorine increase over this period from about 1.5 to 3.5 ppbv, thus activation of the chlorine via the reaction $\text{ClONO}_2 + \text{HCl} \rightarrow \text{HNO}_3 + \text{Cl}_2$ on the alumina particles becomes increasingly important.

In short, none of the atmospheric heterogeneous modeling studies, that assumed the present rate of rocket launches, showed a significant global impact on the ozone layer (the calculated impact was predicted to be much smaller than the effect of the solar cycle on ozone).

3.5 Effects of Stratospheric Particulate

Particulate in the form of Al_2O_3 , soot, and ice are released to the atmosphere in chemical rocket launches. Although any chemical rocket launch releases particulates of some form into the atmosphere, most particulate measurements of rocket exhausts are associated with Space Shuttle launches. Measurements have been conducted to obtain samples of the Shuttle-exhausted aluminum oxide particles with the use of aircraft collecting filter samples during descending spiral maneuvers in the exhaust plumes. These measurements show a distribution of particles with significantly more particles below 1 μm than above 1 μm in size (Cofer *et al.*, [1985]).

The first observation of Al_2O_3 particles in the stratosphere was reported by Brownlee *et al.*, [1976]. Zolensky *et al.*, [1989] reported an order of magnitude increase in particles above 0.5 μm , which were mostly aluminum rich between 17 and 19 km from 1976 to 1984. These aluminum-bearing particles are thought to originate from both the Space Shuttle launches and ablating spacecraft material, with the ablating spacecraft material predominating (Zolensky [1989]).

3.5.1 Sedimentation Velocity

Sedimentation is an important process for atmospheric particles, affecting their residence time and vertical distribution. Particles between 0.02 μm and 0.1 μm radius do not settle appreciably in the lower stratosphere, but are influenced by gravitational sedimentation at higher altitudes. Particles greater than 0.1 μm radius are influenced by sedimentation at all altitudes,

and particles greater than 1.0 μm radius are rapidly removed from the stratosphere. At the same altitude, bigger particles have a larger sedimentation velocity because, relatively speaking, the air resistance is smaller for the bigger particles. For particles with the same size, the sedimentation velocity is larger at higher altitude because the thinner air at higher altitude provides less friction for the particles. The sedimentation velocity is almost 20 times larger at 40 km than that at 20 km. Typical magnitudes of the vertical advection velocity from the large-scale circulation are 0.05 km/day at 20 km, and 0.1 km/day at 40 km. Thus sedimentation is important only for particles larger than 0.1 μm (*Ko et al.*, [1999]).

3.5.2 Removal by collision with sulfate aerosol

If alumina particles become coated by H_2SO_4 in the atmosphere, a small increase in the background sulfate particle burden would result, although it would be a minor effect. However, if the alumina particulates remain uncoated, they would have a higher potential for ozone depletion at most stratospheric temperatures, because the rate of the above-mentioned chlorine activation reaction is faster on alumina than on sulfate particulate. Molina *et al.*, [1997] has argued that the alumina particles probably would remain uncoated throughout most of their stratospheric residence time and hence would promote chlorine activation.

Ko et al., [1999] also examined this sulfate aerosol removal process. The size distribution of sulfate particles for background (non-volcanic) conditions was taken from a 2-D model calculation by Weisenstein *et al.*, [1997]. *Ko et al.*, [1999] assumed that Al_2O_3 particles coagulate or collide only with sulfate particles of the same or larger size, ensuring that the Al_2O_3 particulate was coated completely with sulfate, becoming deactivated before being removed. This is discussed in more depth in Section 4.4.

The collision rate tends to be largest for collisions between small and large particles, because small particles have a high thermal velocity and large particles have a large cross-section. Therefore, only the small Al_2O_3 particles are removed efficiently under these assumptions. The collision removal was much slower for particles with 0.13 μm radius than particles with 0.03 μm radius (20 to 30 times slower). The time constant for the 0.13 μm case is much larger than the stratosphere residence time of 800 days. Thus, collision removal should have little effect for 0.13 μm particles (*Ko et al.*, [1999]).

3.5.3 Reaction Probability

Heterogeneous reaction pathways involving water droplets in clouds, fogs, and mists are increasingly recognized as a major mechanism for the chemical transformation of atmospheric trace gases. The relative importance of these aqueous chemistry mechanisms compared to purely gas phase processes depends greatly on the gas/droplet mass transfer rates that may limit the effectiveness of the heterogeneous mechanisms. Gas/liquid mass transfer can be thought of as a convolution of four processes: (1) diffusion of gas molecules to the liquid surface; (2) accommodation of gas molecules on the surfaces; (3) possible chemical conversion to form a

soluble product; and (4) liquid-phase diffusion of dissolved molecules or products away from the liquid surface (*Worsnop [1989]*). Among the most important variables governing the mass transfer rates are the surface mass accommodation or “sticking coefficients” for trace gas molecules on aqueous droplet surfaces (process 2). The sticking coefficient is defined as the probability that a molecule in the gas phase will enter into the liquid upon collision with the liquid surface. In general, it has been shown (*Worsnop et al., [1989]*) that the sticking coefficient may be both an important and a rate limiting parameter if it is in the range from 10^{-2} to 10^{-4} . For larger values, transport by gas phase diffusion will be rate limiting, while for smaller values, heterogeneous processes usually become unimportant when compared to competing gas phase reactions.

The particulate exhausted from launch vehicles may have a large local effect on the stratosphere. The effect of Al_2O_3 aerosols with a mean radius of $0.1 \mu\text{m}$ and a sticking coefficient of 5×10^{-5} was estimated by Karol (*WMO [1991]*). These aerosols produce an additional 30 percent ozone depletion in the immediate 400 to 1500 seconds after emission. Before and after this time period, the additional depletion is mostly less than 5 percent. Because the Al_2O_3 aerosols act as condensation nuclei for sulfate in the stratosphere, it was reasoned that their stratospheric influence after the first 1500 seconds would be like those of other resident aerosols.

Recently, Molina *et al.*, [1997] showed that alumina particles promote the chlorine activation reaction $\text{ClONO}_2 + \text{HCl} \rightarrow \text{HNO}_3 + \text{Cl}_2$ with a reaction probability (γ) of about 0.02 on the particle surfaces. If alumina particles become coated by H_2SO_4 in the atmosphere they would result in a small increase in the background sulfate particle burden, a minor effect. However, if they remain uncoated, the alumina particles would have a higher potential for ozone depletion because the rate of the above-mentioned chlorine activation reaction is faster on alumina than on sulfate particulate at most stratospheric temperatures. Molina *et al.*, [1997] argued that the alumina particles would probably remain uncoated throughout most of their stratospheric residence time and hence promote chlorine activation. These laboratory investigations will be discussed in depth in Section 4.

Because alumina particles are present at all latitudes in all seasons, rather than concentrated in the polar winter like the polar stratospheric clouds, and the reaction probability for chlorine activation is not temperature sensitive, alumina particles offer the potential to impact ozone if they remain uncoated by H_2SO_4 . Jackman *et al.*, [1996a, 1998] assessed the heterogeneous chemical impact of SRM alumina on stratospheric ozone using the Goddard Space Flight Center two-dimensional photochemistry and transport model. Since the launch rate over the past 25 years has been generally smaller than the assumed launch rate of nine Space Shuttle and three Titan IV rockets per year, Jackman *et al.*, [1998] computed the time-dependent ozone changes resulting from the historical launch rate of the Space Shuttle, Titan III, and Titan IV vehicles. The launch rate for 1970-94 was taken from Isakowitz [1995] and for 1995-97 (*Jackman et al., [1998]*). Four time-dependent model simulations were performed for the period 1970-1997: 1) a “base” simulation which did not include any rocket launches; 2) an “alumina perturbed” run which included the historical launch rate with Al_2O_3 emissions only; 3) a “HCl perturbed” run which included the historical launch rate with HCl emissions only; and 4) a “total perturbed” simulation that included the historical launch rate with both HCl and Al_2O_3 emissions. The mass

fraction of emitted alumina in the "alumina perturbed" and "total perturbed" runs were assumed to be 0.12, 0.08, and 0.80 in the small, medium, and large size distributions, respectively (*WMO [1995]*).

Local maximum ozone decreases were computed for the years 1978, 1986, and 1997. The predicted variations in ozone decrease follow directly from the input rocket launch rates. The maximum annually averaged global total ozone predicted decrease of 0.025% occurred in 1997 for the "total perturbed" compared to the "base run." The increasing influence of the emitted alumina in computed ozone loss was apparent over the 1975-1997 time period. The fractional contribution from the alumina to the total computed ozone loss caused by rocket launches increased from less than one-quarter to about one-third over this period. The background upper stratospheric amounts of inorganic chlorine over this period increased from about 1.5 to 3.5 ppbv, thus activation of the chlorine via the reaction $\text{ClONO}_2 + \text{HCl} \rightarrow \text{HNO}_3 + \text{Cl}_2$ on the alumina particles becomes increasingly important.

Aerosols have been implicated in enhancing ozone decrease by chlorine species, even in the absence of polar stratospheric clouds (*Hofmann et al., [1989]*, *Rodriguez et al., [1991]*). *Turco et al., [1982]* has suggested that the Space Shuttle could increase the average ice nuclei concentration in the upper troposphere by a factor of 2. Rough estimates suggest that U.S.-launched rockets increase the global aerosol surface of the unperturbed stratosphere by about 0.1 percent (*Prather et al., [1990b]*; *McDonald et al., [1991]*). However, *Danilin [1993]* and *Denison et al., [1994]* later concluded that ozone in or near the plume was affected in only a minor way when heterogeneous reactions on alumina aerosol were included.

3.6 Stratospheric Plume Diffusion

There are many different parameters that may effect the amount of ozone depletion occurring in the rocket exhaust plume; heterogeneous and homogeneous chemistry being two of the most important. The plume dispersion rate is a vital parameter required for the measurement of the properties of particulate or chemical species in an SRM stratospheric plume. A rapidly expanding plume will quickly lower the particle densities (and chemical concentrations), making real-time detection difficult. The longer these models are allowed to continue the ozone reducing chemical reaction mechanisms included therein, the more ozone will be destroyed.

Until recently, little data were available on plume expansion in the stratosphere (*e.g., Hoshizaki [1975]*, *Pergament et al., [1977]*, *Beiting [1999, 1997]*, *Dao et al., [1997]*). These data will be discussed in more detail in Section 5. The early data showed rates for the first 10 minutes (*i.e.*, 0-600 s). New data (*Beiting [1999]*) measure expansion rates for almost an hour. These expansion rates are generally an order of magnitude higher than those generally attributable to large-scale eddy diffusion. In this section, plume dispersion models are reviewed.

3.6.1 Plume Diffusion Models

An excellent review of this subject was presented in Beiting [1995, 1997b]. A brief review is presented here. Three models of plume dispersion were reviewed. The first is the model of Denison *et al.*, [1994], which is based on the data of Hoshizaki [1975] and is verified for short times (i.e., less than 10 minutes). The second by Watson *et al.*, [1978] is believed to be accurate for times longer than a few hours after launch (> 1 day). The third model is by Ross [1996a] and is designed for times intermediate to these.

3.6.1.1 The Model of Denison *et al.*, [1994]

Denison *et al.*, [1994] used a chemical model and determined the diffusion of the plume by solving the conservation equation in cylindrical coordinates,

$$\delta n / \delta t = K_{yy} \nabla^2 n = (1/r) (\delta / \delta r) r K_{yy} (\delta n / \delta r) \quad (3-22)$$

where n is the number density, r is the radial coordinate, t is the time, and K_{yy} is the diffusion coefficient. Using the plume size measurements of Hoshizaki [1975] taken at an altitude of 18 km, the diffusivity was found to be scale dependent, where

$$K_{yy} = b r , \quad (3-23)$$

and $b = 1.75 \text{ m s}^{-1}$. Under this assumption, the solution of Eq. 2 for a line source is

$$n(r,t) = A t^{-2} \exp(-r / bt) , \quad (3-24)$$

where A is a normalization constant. This solution can be written

$$n(r,t) = n_o (t_o/t)^2 \exp[-1/b(r/t - r_o/t_o)] , \quad (3-25)$$

where n_o is the particle number density at r_o and t_o . Using the relation

$$n(r,t) / n(r=R_i,t) = e^{-2} \quad (3-26)$$

to define a radius, the time dependence of the plume radius was found to be

$$R(t) = R_i + 2 bt , \quad (3-27)$$

where R_i is the initial radius. Assuming $R_i = 5 \text{ m}$, the plume diameters at 1 and 10 minutes are 0.43 and 4.2 km, respectively. This diffusion model was employed also by Kruger [1995] and by Brady *et al.*, [1995a] to calculate the local stratospheric ozone depletion by a solid rocket in their chemical kinetics models.

3.6.1.2 The Diffusion Model of Watson *et al.*, [1978]

Years earlier, Watson *et al.*, [1978] studied the Space Shuttle plume dispersion characteristics of F₂ and N₂O₄ in the stratosphere and mesosphere. Within the stratosphere, plume dispersion is produced by both small- and large-scale eddies that can be parameterized in terms of an overall eddy transport coefficient. Watson *et al.*, [1978] obtained a time scaling of the horizontal diffusion coefficient K_{yy} based on the model results at 100 km. At times less than 10⁵ seconds, this model was found to underestimate the horizontal plume dispersal rate due to an incorrect time evolution of K_{yy}. The vertical dispersal was determined to be two to three orders of magnitude less than this horizontal dispersal rate so the expansion proceeded primarily in two dimensions. Watson *et al.*, [1978] used this model to calculate the plume width and densities at an altitude of 40 km at times of 0 seconds, 1 hour, 5.6 hours, 1 day, 10 days, and 1 month. Because of uncertainties in K_{yy}, the calculations of plume volumes were found to be accurate only to an order of magnitude. An initial expansion rate (0 – 1 h) of 1.4 km/h (0.023 km/min) was calculated, and at longer times a nearly linear expansion rate of 5.2 km/h was found. Brady *et al.*, [1995] used these values shown to scale temporal dependence of the chemical concentrations in the plume and found a time dependence of the concentration given by

$$n(t) = n_o / \{ 1 + [(2 \times 10^{-3}) t]^{2.6} \} \quad (t \text{ in seconds}). \quad (3-28)$$

The initial value of n_o was scaled with local atmospheric pressure.

3.6.1.3 The Model of Ross [1996a]

More recently, Ross [1996a] completed a model of a Titan IV SRM plume in the atmosphere that included a limited chemical reaction set and fluid dynamic mixing in the stratosphere for up to 8 hours after launch. This model assumed cylindrical symmetry in a series of 1-km-thick layers and was built into a three-dimensional model by permitting the layers to move independently according to their altitude-dependent zonal (E-W) and meridional (N-S) wind speeds. This model also parameterized the transport in terms of an eddy diffusion coefficient using a time-dependent value of $K_{yy} \text{ (m}^2\text{s}^{-1}) = 0.01 t \text{ (s)}^{1.3}$, a value assumed to be independent of altitude. This work presented Al₂O₃ number densities at the 1/e² density and calculated an expansion rate of about 3 km/h.

3.6.2 Comparison and Discussion

It is useful to compare the data of the early plume expansion with the dispersion models being employed by the plume chemistry models. Because the data were acquired at different altitudes, this comparison requires some understanding of the altitude scaling of the small-scale eddy diffusion coefficient (*Beiting* [1995]). The large-scale atmospheric eddy diffusion coefficient has received considerably more study for global atmospheric modeling. The scaling of the large vertical eddy diffusion coefficient K_{zz} with altitude between 18 and 40 km varies

from being constant, to increases by a factor of 25 (varying approximately with inverse atmospheric pressure) depending on the model (Beiting [1995]). At 30° north latitude, there is little variation of this parameter in the 20-40 km altitude range. Based on the data presented by Hoshizaki [1975], Denison *et al.*, [1994] found that the small-scale values of K_{yy} at ten minutes are two to three orders of magnitude smaller than those of the large-scale values. Therefore, the applicability of these large-scale altitude variations of K_{yy} and K_{zz} to the small-scale values of K_{yy} is highly questionable and the small-scale altitude variation was unknown until recently measured by Beiting [1999].

Tables 3-7 and 3-8 compare the measured and model values. Given the large variability of climate that can affect plume expansion rates, the agreement among the observed values must be considered remarkable. The models show considerably less agreement among their values. The model of Watson *et al.*, [1978] predicts the smallest value for the 10-minute plume diameter. This is not surprising since the model was designed for long times, and the authors speculated that their model may under-predict the initial diameters. The predictions of the Ross [1996a] model are a factor of two greater than the Watson *et al.*, [1978] model but are still an order of magnitude smaller than the predictions of the model of Denison *et al.*, [1994]. The model of Denison *et al.*, [1994] most closely reproduces the observed diameters, which is not surprising given that its diffusion coefficient is based on the data of Hoshizaki [1975]. The model of Brady *et al.*, 1995 utilizes two dispersion rates, that of Watson *et al.*, [1978] and that of Beiting [1995].

Table 3-7 indicates the expansion rate data that can be used as inputs to the models of stratospheric plume chemistry. Chemical models using the diffusion model of Watson *et al.*, [1978] will predict chemical concentrations that are too large at early times. The dispersion at long times is best approximated by this model, after the eddy diffusion lengths have reached meteorological scales of hundreds of kilometers. This may require a day or more. The model of Denison *et al.*, [1994] should be the most accurate at short times and will result in chemical concentrations that are less than those predicted by Brady *et al.*, [1995] and Ross [1996a]. Because several of the reaction rates have a quadratic dependence on chemical concentration, the chemistry will depend quite severely on this initial expansion rate. Indeed, this dependence has been modeled by Brady *et al.*, [1995], and concluded that the size and persistence of the ozone hole depended on the dispersion rate, peaking for the specific rate chosen for their models. Accordingly, the size and persistence of the predicted local ozone depletion by all of the plume chemistry models critically depend on the initial plume dispersion rate. Since all instruments under consideration for verifying ozone chemistry models of the plume are designed to operate in the first 24 hours, they should use models that employ the early plume dispersion rates. More recently Beiting [1999] measured results of the stratospheric expansion rates of exhaust plumes from nine Space Shuttle and Titan IV vehicles (See Section 5). The expansion rates were found to be constant in time, but increased with increasing altitude (e.g., 4.3 ± 1.0 m/s, 6.8 ± 1.9 m/s, and 8.7 ± 2.5 m/s at 18 km, 24 km, and 30 km, respectively). Beiting reported that attempts to associate the expansion of the exhaust plume with diffusivity were only partially successful. Models that allowed the diffusivity to vary with plume size and altitude were more successful than constant diffusivity models.

Table 3-7. Summary of Plume Expansion Rate & Diffusion Data

SOURCE	DATA	
	Altitude (km)	Expansion Rate (km/hr)
Hoshizaki [1975]	18	18
Strand [1981]	19	9 – 30
Ross [1997b]	18	6.7
Beiting [1999]	18	15.5
Dao [1997]	23	8.5
Beiting [1999]	24	24.5
Beiting [1999]	30	31.3
Beiting [1997]	30	28.8-36.0

Table 3-8. Summary of Plume Expansion Rate & Diffusion Model-Experiment Comparison

SOURCE	DATA	
	Altitude (km)	Expansion Rate (km/hr)
Watson [1978] ^φ	*	1.4
Denison [1994] ^γ	*	25.0
Ross [1996a] ^φ	20	2.9
Ross [1996a] ^φ	30	2.4
Ross [1996a] ^φ	40	4.0
Beiting [1997] ^η	30	36.0

* Model was altitude independent

^φ Based on Model data

^γ Based on Hoshizaki [1975] data at 18 km

^η Based on measurement

There are significant differences between the rate measurements of Hoshizaki [1975], Strand *et al.*, [1981], and Beiting [1999] (large expansion rates) and theories of Dao *et al.*, [1997] and Ross [1996a] (small expansion rates). Some comment is required here. A possible explanation is that the rate is the aggregate expansion of the plume and the small rate is the expansion of a parcel. The LIDAR measurements (Dao *et al.*, [1997]) and WB-57 fly-through measurements (Ross [1996a]) sample only one, or at most a few, parcels and therefore cannot measure the expansion rate of the entire plume. Because the rate calculations of Dao *et al.*,

[1997] and Ross *et al.*, [1996a] were made based on a single parcel or rate, this may be a parcel expansion rate, and would be important for the chemical concentrations in that packet. The aggregate rate would yield the spatial area affected.

3.7 Summary

Rocket launches can have a significant local effect on the stratosphere by reducing ozone substantially (up to 100 percent in the localized plume area) within the expanding exhaust plume. Full recovery of ozone back to ambient levels occurs from 3000 to 6000 seconds after launch, depending on the altitude. Even when such severe reductions take place, the reduction in column ozone is probably less than 10 percent over an area a few kilometers by a few tens of kilometers and is generally much smaller. The local-plume ozone reductions and the regional effects are smaller than can be detected by satellite observations. The size and persistence of the predicted local ozone depletion by all of the plume chemistry models was found to depend on the initial plume dispersion rate chosen. For the short times after the exhaust is released into the stratosphere, the most accurate dispersion rate that should be used is that of Denison *et al.*, [1994], and later confirmed by *in-situ* measurements made by Beiting *et al.*, [1997, 1999]. More discussion on dispersing parcels is presented in Section 5.

In short, none of the global effects of rocket motor and spacecraft operation considered here produces a significant impact on stratospheric ozone. From the global standpoint, material injected into the stratosphere during launch has stratospheric residence lifetimes of a few years or less, which serves to limit the steady state burden. A single motor launch per year is calculated to reduce globally and annually averaged ozone by 0.0006%, with a maximum column loss at the surface of about 0.002%. Therefore, the global impact of rocketry is a third-order or smaller effect compared with other sources of chlorine. If the annual background source from halocarbons is reduced and/or the launch rate increases, the fractional contribution will become larger.

4 LABORATORY MEASUREMENTS OF SRM EMISSION PRODUCTS

4.1 Laboratory Measurements of SRM Emission Products

Validation of computer models is essential to understanding the full ramifications of rocket exhaust on the atmosphere, and this validation is accomplished by laboratory investigations, which is discussed in Section 4, and by *in-situ* measurements of SRM exhaust plumes, which is covered in Section 5.

Section 4.2 introduces the reader to laboratory simulations. Chemical processes and yields are described in Section 4.3. Heterogeneous processes are discussed in depth in Section 4.4. These include rocket exhaust laboratory simulations, chlorine activation reaction dynamics, and reaction probability determinations for ozone depleting chemical reactions. Particulate chemistry is assessed in Section 4.5. This includes reaction mechanisms involving the effects of sulfuric acid vapor and the adsorption of water vapor on the surface of alumina. Section 4.6 describes the aerosol chemistry of aluminum oxide and nitrogen oxide. Finally, a summary of alumina chemistry is covered in Section 4.7.

4.2 Laboratory Simulations

In Section 3, modeling efforts were described concerning the potential impacts on stratospheric ozone due to the launch of vehicles with solid-fuel rocket motors (SRMs). The main concern is that chlorine-containing compounds released by the SRMs may lead to catalytic destruction of ozone in a region surrounding the exhaust plume. The major exhaust gases, and their mole fractions, at the nozzle exit plane of a Titan IV SRM are presented in Table 4-1 and are found in Zittel [1994]. Mole fractions for the exhaust of Space Shuttle SRMs are similar. There is also a large mass of alumina particulate in SRM exhaust, which was discussed in Section 3.6. Both H₂ and CO which are constituents in the hot exhaust, afterburn vigorously upon mixing with ambient air, essentially creating an H₂-CO-O₂ flame. For both Titan IV and the Space Shuttle, this afterburning occurs at all altitudes during boost through the ozone-rich regions of the stratosphere (Zittel [1994], Burke *et al.*, [1998]).

Table 4-1. Major Exhaust Gases and Mole Fractions of a Titan IV SRM

(Reference: Zittel [1994])

Major Exhaust Gases	Mole Fraction
H ₂	0.34
CO	0.27
HCl	0.15
H ₂ O	0.12
N ₂	0.08

Gaseous HCl is inert toward ozone and is slow to photodissociate in the stratosphere, whereas Cl₂ (which rapidly photodissociates), Cl atoms, or ClO may readily contribute to ozone destruction cycles (*Zittel [1994], Burke et al., [1998]*). Model simulations indicate that Cl atoms and Cl₂ should be formed in high abundance from the HCl in the exhaust, with the yield of this "free" chlorine increasing with altitude through the stratosphere (*Zittel [1994]*). Conversions of HCl to free chlorine of approximately 80% have been predicted both for a Titan IV SRM at 40 km (*Zittel [1994]*) and for a smaller SRM at 30 km (*Denison et al., [1994]*). Evaluation of the potential for creation of local ozone-depleted regions following a launch is thus dependent on the accuracy of the product composition predicted by these afterburning models.

Experimental tests of these afterburning models are useful in order to evaluate the accuracy of their predictions. A few previous studies exist that are relevant in terms of the flame composition of interest here. The effects of HCl on H₂-O₂ flames has been investigated in terms of potential flame-inhibition effects (*Blackmore et al., [1964], Butlin et al., [1968], Dixon-Lewis et al., [1976]*), as have other halogen-containing molecules. However, the consumption of HCl and production of other chlorine-containing molecules were not monitored in those studies. Perhaps the most relevant experimental studies in the literature are those of Roesler and co-workers, where the inhibition by HCl of the moist oxidation of CO was examined (*Roesler et al., [1992a,b, 1994]*). In that work, HCl was added to an atmospheric pressure reaction system of CO, O₂, and H₂O at temperatures near 1000 K. The flame composition was monitored as a function of reaction time, and HCl losses on the order of 20% - 40% were measured. These results support the plausibility of HCl conversion via afterburning. However, the fuel composition, pressure, and temperature of the experiments of Roesler *et al., [1994]* are significantly different from the conditions of afterburning.

Burke and Zittel *[1998]* performed laboratory investigations simulating stratospheric afterburning of a SRM plume. They found that under oxygen-rich conditions, a large fraction of the HCl injected into the flame was converted to Cl₂, whereas under fuel-rich conditions, no HCl was lost. Both the loss of HCl and the formation of Cl₂ were quantified via mass spectrometry, with HCl losses up to 40% observed. Over 70% of the chlorine liberated from the loss of HCl are converted to Cl₂. The insensitivity of the emission intensities to the oxygen content of the flame indicated that HCl and other chlorine-containing compounds were undergoing a dynamic inter-conversion in the flame, even under conditions where there was little or no net loss of HCl.

4.3 Chemical Processes and Yields

The experimental results presented in Section 4.1 suggest that the simple description of chlorine chemistry used in the plume afterburning models provides a reasonable representation of the distribution of major chlorine species left in an SRM wake at stratospheric altitudes (*Denison et al., [1994], Lohn et al., [1994], Zittel [1994]*). The models generate free chlorine primarily through the attack on HCl by the OH, O and H radicals, all of which are produced in abundance by the combustion of H₂. These reactions are fast (*Mallard et al., [1994]*) and either exothermic or nearly thermoneutral at the temperatures above 2000 K typically modeled for an afterburning SRM plume at an altitude of 20 km. The predicted concentration of minor chlorine-containing

species (e.g., ClO and ClO₂) may be less certain, requiring more complex reaction paths. However, the impact on ozone loss of the direct production of these species through afterburning is minor.

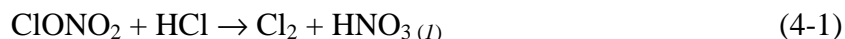
For flame fuel compositions that closely simulated the gaseous components of the exhaust from SRMs, the magnitude of the loss of HCl observed in the laboratory was similar to that predicted by plume afterburning models. The trend predicted by models (i.e., where HCl conversion increases with altitude) was confirmed in the laboratory via experiments at different flame pressures. Quantitative differences between experimental and model results may be due primarily to differences in structure and composition between the laboratory flame and the model plume.

4.4 Rocket Exhaust Heterogeneous Processes

4.4.1 Rocket Exhaust Chemistry

Molina *et al.*, [1999] performed laboratory experiments on chemical processes involving the effects of particles emitted by solid rocket motors (SRMs) on stratospheric ozone. Specifically, emphasis was placed on the efficiency of the catalytic chlorine activation process occurring on the surface of aluminum oxide particles.

In earlier work Molina *et al.*, [1996] had shown that the following reaction is catalyzed by α -alumina surfaces:



This reaction is the most important process leading to the transformation of chlorine reservoir species to free chlorine atoms in the polar stratosphere (*see, e.g., WMO [1995], WMO [1998]*); these atoms efficiently deplete ozone through catalytic cycles that were described in detail in Section 3. This process occurs efficiently on polar stratospheric cloud particles, thus explaining rapid ozone depletion at high latitudes (*Kolb et al., [1995]*). At low latitudes the prevailing aerosols consist of concentrated (70 - 80 % weight) sulfuric acid solutions; the reactant HCl is not soluble in this solutions, and hence the above reaction is not catalyzed by this type of aerosols (*Kolb et al., [1995]*). The importance of solid particles such as those consisting of alumina is that they may facilitate reaction 4-1 at mid latitudes, where the background sulfuric acid aerosols are not effective.

The hypothesis was made that the water adsorbed on the surface of the alumina particles promotes the chlorine activation reaction by providing a layer with high affinity for HCl molecules; to the extent that this hypothesis is correct the detailed properties of the solid surface itself are important only in so far as providing stability for the adsorbed water molecules.

4.4.2 Heterogeneous chlorine activation reaction mechanism

One mechanism that has been suggested in the literature (particularly for ice and for nitric acid trihydrate surfaces (*e.g.*, Peter [1997])) consists of adsorption of HCl molecules on the alumina surface on specific “active” sites, followed by collisions and reaction of the ClONO₂ molecules with the adsorbed HCl. This mechanism predicts that the reaction rate should be proportional to the HCl partial pressure P_{HCl}, the surface concentration of this species being itself proportional to P_{HCl}. Molina *et al.*, [1999] developed a low pressure chemical ionization mass spectrometry (CIMS) method which enabled measurements at much lower P_{HCl} values typical of the lower stratosphere (*i.e.*, 0.5 to 10 x 10⁻⁷ Torr).

Besides chlorine activation, the alumina particles emitted by SRMs have the potential to function as nucleation centers for the formation of polar stratospheric clouds. The more prevalent Type I cloud particles are believed to consist of nitric acid trihydrate (NAT). Meads *et al.*, [1994] investigated the ability of alumina particles to nucleate NAT from supercooled nitric acid solutions, *i.e.*, 3:1, H₂O, HNO₃ (Abbatt *et al.*, [1992a,b], Zhang *et al.*, [1994]); these did not allow nucleation of the supercooled NAT solution. Previously defined in Section 3.4.2, the measured reaction probability, γ , of ClONO₂ + HCl on α -alumina is an order of magnitude less than that on ice and water-rich NAT surfaces. The role of surfaces such as alumina in the activation of chlorine at polar latitudes is expected to be small and their effect limited, even if the reaction probability were to be above 0.1, given their small abundance relative to polar stratospheric clouds.

In short, the background aerosol particles prevalent at low latitudes consist of liquid sulfuric acid solutions with concentrations in the range from about 50 to 70% by weight H₂SO₄. Chlorine activation on these liquid aerosols occurs extremely inefficiently as a consequence of the very small solubility of HCl on these concentrated solutions. Hence, even if alumina particulate represent only a small fraction of the total aerosol loading, they have the potential to affect, at mid-latitudes, the partitioning of chlorine between active and inactive forms.

4.4.3 Measurement of the reaction probability for the ClONO₂ + HCl reaction

The experimental configuration of Molina *et al.*, [1999] was similar to that used previously (*e.g.*, Zhang *et al.*, [1994]), except for the modification to the mass spectrometer apparatus required to operate in the chemical ionization mode. Pseudo first-order rate constants and reaction probabilities (γ) were determined using a non-linear fitting technique (Brown, [1978], Howard [1979]).

As expected, addition of water vapor at pressures in the millitorr range, enough to produce an ice film on the glass tube, yielded reaction probability values which were about an order of magnitude larger, in agreement with earlier measurements (Molina *et al.*, [1996]) and with literature values (DeMore *et al.*, [1994]). In contrast, measurements performed on 'dry surfaces'

(after mild baking and with no water added to carrier gas stream) showed a decrease in γ as successive decay curves were collected. Typically reaction probabilities dropped to half the reported values indicating the accumulation of the reaction product HNO_3 , and the removal of remaining water molecules on the alumina surface. However, the low γ value could be restored to near its original value simply by humidifying the carrier gas stream with small amounts of water (approximately 5% humidity), presumably by replenishing the lost surface water molecules and by driving off the adsorbed HNO_3 .

Molina *et al.*, [1999] concluded that the reaction rate is nearly zero order in HCl for the concentration range covering stratospheric conditions. This result provides a strong indication that the reaction mechanism involves water adsorbed on the alumina surface which solvates HCl, thus explaining the relatively high affinity this molecule has for the surface. Furthermore, the “active sites mechanism” which predicts that the reaction rate should be linearly proportional to the concentration of HCl clearly is not supported by experiment.

4.5 Particulate Chemistry

4.5.1 Adsorption of water vapor on alumina surfaces

Molina *et al.*, [1999] also investigated the uptake of water vapor by two types of α -alumina surfaces: sapphire, and conventional alumina, using essentially the same flowtube technique employed for the reaction probability measurements. George *et al.*, [1996] has suggested that α -alumina would lose its surface hydroxyl groups when heated above 600 K, and that water vapor would not react with the surface to regenerate the hydroxyl groups below that temperature. The implication was that alumina particles in the stratosphere would not adsorb water, because they are formed in the SRMs at relatively high temperatures. Molina *et al.*, [1996] countered that the particles would recover their surface OH groups by reacting with water vapor, but with OH or HO_2 radicals.

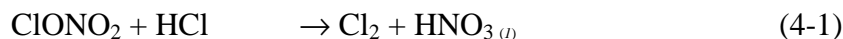
Molina *et al.*, [1999] found that even sapphire, which is an α -alumina form well known for its extremely inert surface, adsorbs monolayer quantities of water after being heated above 600 K. The measurements were carried out over a temperature range from 230 to 300 K and humidity range from about 10 to 80%. Thus, the mechanism Molina *et al.*, [1999] had proposed for the chlorine activation reaction appears to be applicable, the adsorbed water providing the means for reaction 4-1 to take place efficiently. Subsequent work by Elam *et al.*, [1998] determined that OH groups will not be permanently lost as readily as initially envisioned; furthermore, Elam *et al.*, [1998] realized that even dehydroxylated alumina adsorbs water, in agreement with the Molina *et al.*, [1999] laboratory results. In short, α -alumina adsorbs water even after being processed at temperatures well above 900 K, and hence α -alumina particles emitted by SRMs are good catalysts for reaction 4-1.

Molina *et al.*, [1999] revealed differences in the surface activity, and water uptake of sapphire compared to conventional alumina. The uptake by sapphire is reversible, involving only physical adsorption: the water taken up was released by allowing dry carrier gas to flow at or

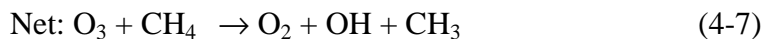
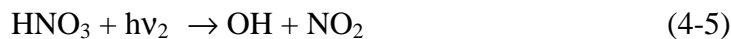
below room temperature. In contrast, the conventional alumina surface chemisorbs some fraction of the water, and at room temperature it only loses upon exposure to dry carrier gas the portion that is physisorbed. Thus, Molina *et al.*, [1999] inferred that alumina particles emitted by SRMs will be catalytically active in the stratosphere, because they will be covered by adsorbed water. Surface imperfections and impurities such as chloride or nitrate groups may modify the extent of chemisorbed water, most likely increasing the amount of physisorbed water, since those groups are hydrophilic. That is, adsorbed water will be surely present, enabling the chlorine activation reaction to take place.

4.5.2 Effect of sulfuric acid vapor on the alumina surface

This effect was first described in Section 3.4.2 and will be described in more depth in this section. Aluminum oxide particulate (Al_2O_3) particulate may impact stratospheric ozone through heterogeneous reactions occurring on the particle surfaces. Reaction 4-1 was re-investigated by



Molina *et al.*, [1999]. A similar reaction to this on polar stratospheric clouds (PSCs) and sulfate aerosol is believed to be responsible for much of the Arctic and Antarctic ozone loss (the “ozone hole”) in springtime. Heterogeneous reaction on Al_2O_3 particles would not be limited to polar regions like the similar reaction on PSCs and, because the reaction rate is not temperature dependent, could occur at all latitudes and seasons, unlike the similar sulfate reaction. The above reaction converts ClONO_2 and HCl , both moderately long-lived chlorine reservoir species, into Cl_2 , a very volatile species that dissociates into atomic Cl rapidly in the presence of sunlight. The chlorine produced may then lead to ozone removal via the following catalytic cycle:



The impact of the Al_2O_3 particulate from SRM on ozone was studied with a 2-D model by Jackman *et al.*, [1998] employing the Molina *et al.*, [1997] rate for $\text{ClONO}_2 + \text{HCl}$ on alumina particles. The calculated ozone impact is extremely small, at most 0.06% ozone depletion in the northern polar region in spring and a global average total ozone change of 0.01% depletion. The

surface area density of Al₂O₃ used by Jackman *et al.*, [1998] is greater than that calculated by Ko *et al.*, [1999] under Case B of his model scenario by factors of 2 to 10. Ko *et al.*, [1999] concluded that ozone depletion on the global scale due to Al₂O₃ emissions by solid rocket motors at the current Shuttle launch rate is less than 0.04% in the northern polar region and about 5×10^{-4} % of the global average.

Alumina particulate from SRMs may affect the background sulfate aerosol layer in two ways. First by collision of Al₂O₃ particles with the background sulfate layer, increasing its mass and surface area, and second by acting as nuclei for H₂SO₄/H₂O condensation, increasing the number of sulfate aerosol particles and decreasing their mean radius.

Ko *et al.*, [1999] obtained an upper limit estimate of the first effect as follows. They assumed that those Al₂O₃ particles that collide with the sulfate particles become coated with sulfate and provide the same surface area for sulfate reactions. Thus, Case A, with no collision removal, and Case B, with collision removal give the difference in surface area. The maximum difference is $4 \times 10^{-4} \mu\text{m}^2/\text{cm}^3$, which is about three orders of magnitude less than the background sulfate aerosol range of 0.1 to 1.0 $\mu\text{m}^2/\text{cm}^3$. Thus, the presence of Al₂O₃ particles will increase the surface area of sulfate by less than 0.1%. This is an upper limit since compensation for decrease in sulfate surface area for the sulfate particles that collided with the Al₂O₃ particles was not made.

Ko *et al.*, [1999] evaluated the second effect by comparing the number of Al₂O₃ particles in the 0.025 – 0.040 μm size bin range (considered to be the only size likely to act as condensation nuclei) with the total number of sulfate particles per unit volume. They concluded that the impact of Al₂O₃ particles as condensation nuclei for sulfate aerosol is probably small at most latitudes and altitudes, but has the potential to increase the particle number density and surface area in localized regions where number density is otherwise small. It should be noted that the efficiency of Al₂O₃ particles to act as condensation nuclei is unknown, so assessing this effect accurately is not possible at this time.

Molina *et al.*, [1999] also investigated the time required for alumina particles in the stratosphere to be coated by sulfuric acid. Theoretically the H₂SO₄ vapor pressure of aqueous sulfuric acid aerosols in the lower stratosphere is extremely low ($< 10^{-3}$ Torr); if equilibrium were to be maintained, only a negligible amount of sulfuric acid vapor would be transferred to the alumina particle surfaces. However, early modeling calculations by Turco *et al.*, [1982] indicate that there is a large supersaturation with respect to H₂SO₄ vapor, and hence the possibility of significant condensation on the particle surface needs to be taken into account. The *in-situ* measurements by Arnold *et al.*, [1981] report H₂SO₄ partial pressures around 10^{-5} Torr between 23 and 27 km altitude; unfortunately, there are no measurements at lower altitudes, which is the region of interest for the chlorine activation processes discussed in this report. Considering the nature of the water layers adsorbed on the alumina surface Molina *et al.*, [1999] estimated that the sticking coefficient would be 0.1 or less, and that laboratory measurements would be needed to establish the actual value. The estimated time required for H₂SO₄ to form a monolayer on the surface of the alumina particles in the lower stratosphere was of the order of 8 months, assuming

an accommodation coefficient of 0.1. Of course, if the actual H₂SO₄ partial pressures at the lower altitudes have values below 10⁻⁵ Torr the required times would increase accordingly.

The ozone depletion potential of SRMs may be higher than that predicted on the basis of chlorine emissions alone, especially at mid-latitudes in the lower stratosphere, where catalytic chlorine activation by background sulfuric acid aerosols is very inefficient. Jackman *et al.*, [1989] carried out detailed stratospheric modeling calculations of ozone depletion caused by SRMs using the reaction probability measurement for reaction (1) on alumina particles ($\gamma = 0.02$). The results of Jackman *et al.*, [1998] indicate that the effect on the annually averaged global total ozone is a decrease of 0.025% by 1997; about one third of this decrease results from the SRM-emitted alumina and the remaining two thirds result from the SRM-emitted hydrogen chloride.

4.6 Aluminum Oxide/Nitrogen Oxide Aerosol Chemistry

4.6.1 Laboratory Studies of Al₂O₃-NO_x Aerosols

Disselkamp [1999] performed laboratory experiments to investigate chemistry in aluminum oxide (γ -Al₂O₃) aerosol samples upon exposure to nitrogen oxide (NO_x) aerosols. The kinetic information obtained in this study may be incorporated into computer models to assess the environmental impact of Al₂O₃ material in the stratosphere. Static aerosol samples were generated in an aerosol chamber and studied by Fourier-transform infrared (FTIR) absorption spectroscopy at stratospheric temperatures ranging from 298 to 183 K. The spectra obtained by FTIR were collected for at least 100 minutes to characterize and monitor the Al₂O₃-NO_x chemistry. Disselkamp [1999] performed stoichiometric analyses of reactant gas depletion and product gas formation and proposed several elementary reactions involving aluminum oxide surface hydroxyl sites with NO_x species.

4.6.2 NO₂/ γ -Al₂O₃ Aerosol Samples

Disselkamp [1999] characterized the reactivity of NO₂ with γ -aluminum oxide aerosols. Table 4-2 lists the experimental conditions, such as chamber temperature, NO₂ concentration, and aluminum oxide concentrations employed in the study. An examination of infrared spectra of Al₂O₃ samples verified that partially dehydroxylated samples have 20% of surface hydroxyl sites removed. An analysis of infrared spectra yielded the amount by which the reactant gas concentration is depleted during the course of an experiment, and the concentration of OH surface sites was computed from the mass of powder placed into the stainless steel cell. Using this data, the ratio of NO₂ molecules depleted to available surface sites available for adsorption was computed for each experiment. The data revealed that only a small uptake of NO₂ occurred during each experiment. Furthermore, the reactivity between surface hydroxyl sites and NO₂ is very small, with increased reactivity at higher sample temperature. A similar experimental approach was used to investigate hydroxylated NO₂/ γ -Al₂O₃ aerosols. An analysis of this experiment is listed as the third column in Table 4-2.

Table 4-2. Analysis of Al₂O₃ Aerosol Samples with NO₂ Reactant Gas

Temperature	268 K	290 K	223 K	223 K
Aerosol	Hydroxylated	dehydroxylated	Hydroxylated	dehydroxylated
Initial NO ₂ concentration ^a	1.2 x 10 ¹⁶	2.3 x 10 ¹⁶	3.5 x 10 ¹⁵	2.1 x 10 ¹⁵
NO ₂ depleted at 120 minutes ^a	2.6 x 10 ¹⁴	1.4 x 10 ¹⁵	8.4 x 10 ¹²	1.8 x 10 ¹³
NO ₂ depleted (%) ^a	2.1	6.4	0.24	0.9
OH Site concentration ^a	2.6 x 10 ¹⁶	2.7 x 10 ¹⁶	2.6 x 10 ¹⁶	2.4 x 10 ¹⁶
Depleted NO ₂ per Total Sites (%)	1.0	5.3	0.032	0.075

^a Concentrations given in units of molecules/cm³

4.6.3 NO/ γ -Al₂O₃ Aerosol Samples at 298 K

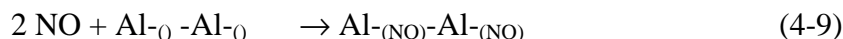
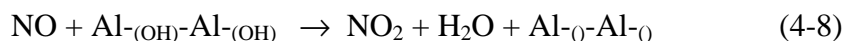
Nitric oxide/ γ -Al₂O₃ aerosol samples exhibit interesting and complex chemistry. The data collected at 298 K revealed a dramatic increase in NO₂ absorption and a decrease in NO absorption. A photometric (i.e., quantitative) analysis confirmed that NO was converted into NO₂ with unity efficiency (*Falcone et al., [1983]*). Similar results were obtained for a hydroxylated aerosol experiment performed at 298 K. An efficient conversion of NO to NO₂ was observed with the chamber wall process converting only 6% of NO to NO₂ over the same time period. Analysis of this experiment is presented in the two left-hand columns of Table 4-3.

Table 4-3. Analysis of Al₂O₃ Aerosol Samples with NO

Temperature	298 K	298 K	183 K	183 K
Aerosol	dehydroxylated	hydroxylated	hydroxylated	dehydroxylated
Initial NO concentration ^a	8.8 x 10 ¹⁶	1.1 x 10 ¹⁷	3.5 x 10 ¹⁵	2.1 x 10 ¹⁵
NO ₂ formed at 100 minutes ^a	1.9 x 10 ¹⁶	3.1 x 10 ¹⁶	8.4 x 10 ¹²	1.8 x 10 ¹³
OH Site concentration ^a	2.6 x 10 ¹⁶	2.6 x 10 ¹⁶	0.24	0.9
[NO] depletion/[NO ₂] formation	2.3	2.1	2.6 x 10 ¹⁶	2.4 x 10 ¹⁶
NO depleted (%) ^a	4.0 x 10 ¹⁶	5.7 x 10 ¹⁶	0.032	0.075

^a Concentrations given in units of molecules/cm³

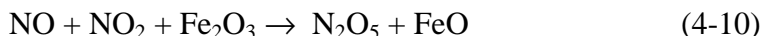
A summary of the time evolution of the dehydroxylated/hydroxylated NO/ γ -Al₂O₃ aerosol experiments at 298 K is presented below. Based on a quantitative analysis of the conversion of NO to NO₂, Disselkamp [*1999*] proposed the following reaction sequence to account for the observed chemistry and data contained in Table 4-3.



Reaction 4-8 describes the reaction of a nitric oxide species with two surface hydroxyl groups to form NO₂ and H₂O. The variability of H₂O absorption arising from purging fluctuations did not enable water formation to be observed. Reaction 4-9 is a subsequent reaction of two nitric oxide species with the bare (dehydroxylated) aluminum oxide surface sites (i.e., represented above as Al-_o). The combined two reactions describe the conversion of 3 NO species into one NO₂, one H₂O, and two surface NO species adsorbed onto γ-Al₂O₃. The first step in examining the viability of reactions 4-8 and 4-9 is identifying the limiting reagent. The concentration of hydroxyl is 2.6 x 10¹⁶ [OH] sites/cm³, and the initial concentration of nitrous oxide is greater than 8 x 10¹⁶ [NO] molecules/cm³. Thus, three NO can reaction with two OH sites, and the limiting reagent is the hydroxyl site concentration. Based on the initial hydroxyl site concentration, 3.9 x 10¹⁶ NO species/cm³ are expected to be depleted in each aerosol experiment, which is close to that observed of 4.0 x 10¹⁶ and 5.7 x 10¹⁶ NO species/cm³ for the dehydroxylated and hydroxylated aerosol experiments, respectively. Furthermore, according to reaction 4-8 and 4-9, the stoichiometric ratio of NO depleted to NO₂ formed is expected to be 3.0. The observed values of 2.1 and 2.3 for the hydroxylated and dehydroxylated experiments are again close to that observed. Disselkamp [1999] concluded that NO undergoes rapid reaction with hydroxyl groups on the surface of γ-Al₂O₃.

4.6.4 NO/γ-Al₂O₃ Aerosol Samples at 183 K

Nitric oxide/γ-Al₂O₃ aerosol experiments at 183 K exhibited more complex chemistry than the corresponding studies at 298 K. A number of observations can be noted from an examination of the variation in absorption intensity over time. First, a 5-fold reduction in concentration of NO and NO₂ took place (final NO and NO₂ concentrations were 14% and 18% of original values, respectively). Second, a 160% increase in N₂O₅ concentration occurred, whereas only a 125% increase in N₂O took place. Although it is difficult to make any definitive statement about these concentration changes inferred from integrated absorption changes, a reaction that accounts for this chemistry is:



Combining reaction 4-10 with reaction 4-8 and 4-9 above suggests that the chamber walls catalyze the conversion of NO to NO₂, and at low temperature, reaction 4-10 results in N₂O₅ formation. The question then arises as to whether γ-Al₂O₃ enhances this chemical conversion of NO to N₂O₅.

The results of a hydroxylated NO/γ-Al₂O₃ aerosol at 183 K are described below. The change in reactant gas concentration is seen to be different than the NO reactant gas-only experiment. The NO, NO₂, and N₂O₅ concentrations decrease to 6%, 10%, and 30% of their original values, whereas the N₂O concentration undergoes a modest increase of 9%. The unexpected result, based on the discussion above of the NO reactant gas data, is the decrease in N₂O₅ concentration. Because the presence of γ-Al₂O₃ will not inhibit wall reaction processes, Disselkamp [1999] proposed that N₂O₅ uptake onto the aluminum oxide surface does occur. A likely reaction sequence for this uptake is surface adsorption, followed by hydrolysis of N₂O₅ to form nitric acid

on the surface of aluminum oxide. Similar results were observed for a dehydroxylated NO/ γ -Al₂O₃ aerosol sample. Again NO, NO₂, and N₂O₅ absorption's decrease over time. However in this dehydroxylated experiment the decrease in NO concentration during the 118 minute reaction time is 57%, much smaller than the decrease to 6% of original concentrations observed for the hydroxylated aerosol. A decrease in the surface water content for the partially dehydroxylated γ -Al₂O₃ aerosol may be the cause of this reduced NO conversion to NO₂/N₂O₅.

4.7 Summary of Al₂O₃/NO_x Chemistry

A significant fraction of the injected alumina surface area will be catalytically active and will remain unaffected in the stratosphere by sulfuric acid vapor. The time required for the alumina particles to be covered by a monolayer of sulfuric acid is of the order of 8 months, assuming an accommodation coefficient of 0.1. Furthermore, coalescence with stratospheric sulfuric acid aerosols will most likely be unimportant for the alumina particles larger than about 0.1 μ m in diameter before they settle out of the stratosphere.

The uptake of NO onto the surface of γ -Al₂O₃ has two potential implications in atmospheric chemistry. First, a decrease in atmospheric NO_x concentrations can enhance the catalytic destruction of ozone by halogen species. In the stratosphere, the hydroxyl site (OH) density is 1.3×10^{15} OH species/cm² (*Peri [1965]*), and each OH site can accommodate one NO species. Thus, the uptake of NO species is 3.9×10^7 NO species/particle. Considering that the ambient NO_x concentration is 10 parts per billion by volume (ppbv), or 2.5×10^{10} molecules/cm³, it would take a particle density of 640 particles/cm³ to deplete all the NO_x species. Therefore, within the wake of rocket exhaust plume, this aluminum oxide chemistry may be important, but not at the aluminum oxide ambient particle concentration of 10 particles/m³.

A second potential atmospheric implication of this chemistry is the uptake of halogen species onto the surface of aluminum oxide particles. For example, a possible reaction that may occur is



The uptake of active halogen species by aluminum oxide to liberate NO would have the effect of increasing the ozone concentration by reducing the contribution of halogen catalyzed ozone destruction. Additional studies would be needed to characterize this halogen chemistry.

5 IN-SITU MEASUREMENTS OF SRM EXHAUST PRODUCTS

5.1 *In-Situ* Measurements of SRM Exhaust Products

In this section, *in-situ* stratospheric measurements are summarized. This section is of extreme importance in the validation of modeling efforts on the impacts of SRM exhaust products on stratospheric ozone. *In-situ* observations are presented in Section 5.2. One of the most extensive measurements on stratospheric ozone (i.e., the Experiment on Rocket Impacts on Stratospheric Ozone, RISO) effects is described in Section 5.3. The RISO objectives, instrumentation, plume measuring techniques, specific ozone and aerosol measurements, and LIDAR (LIght Detection and Ranging) remote sensing are covered here. Section 5.4 presents observations of plume dispersion via electronic imaging of scattered infrared sunlight. Section 5.5 details total ozone mapping spectrometer (TOMS) satellite observations. A new instrument High Resolution Ozone Imager (HIROIG) is described in Section 5.6. A summary of the measurement studies and plume chemistry is included in Section 5.7. Finally a list of references is included in Section 5.8.

5.2 *In-Situ* Observations

A near complete lack of data on the composition of rocket exhaust plumes during the first several hours after launch has prevented even a preliminary evaluation of the completeness of the various models. The first ozone measurement in an SRM plume was reported by Pergament *et al.*, [1997a]. They reported an ozone reduction of 40% during one plume pass at an altitude of 18 km, 13 minutes after a 1975 Titan III launch. The observed loss suggests the presence of an ozone-destroying exhaust component, but the measurement, of uncertain reliability, was never repeated by those investigators, leaving it unclear whether the predictions of substantial ozone loss in solid rocket motor (SRM) plumes are correct. The 1991 WMO Scientific Assessment of Ozone Depletion noted the lack of relevant data and uncertainty over model predictions and recommended additional plume measurements to be made by stratospheric aircraft (WMO [1991]).

A similar situation existed for the particle exhaust of SRMs. Although many measurements of particle size distribution of Space Shuttle exhaust were made in the troposphere (see for example Cofer *et al.*, [1991]) only one *in-situ* measurement was made of the particle size distribution of SRM exhaust in the stratosphere (Strand *et al.*, [1984]). Using the data from Strand *et al.*, [1984] and the measurements of the ambient Al₂O₃ particle size distribution of Zolensky [1989], Beiting [1997b] predicted a tri-modal particle size distribution of SRM exhaust in the stratosphere. This tri-modal character was later verified by the measurements of Ross *et al.*, [1999], but the small size mode differed significantly between the two distributions. The size distribution is important because it not only affects the heterogeneous chemistry as discussed in Section 4.6, but also changes the interpretations of data from optical instruments (see for example Syage *et al.*, [1996]). A discussion of the optical characteristics of the plume in stratosphere and its effects on measurements due to particles and the chemical constituents is

given by Beiting [1997c].

5.3 Rocket Impacts on Stratospheric Ozone (RISO) Experiment

In response to the environmental concerns mentioned above, the Environmental Systems Directorate of The Aerospace Corporation, with support from Thiokol/Cordant and the Launch Programs office of the Air Force Space and Missile System Center, organized the RISO program to obtain new and unique data on the chemistry and dynamics of stratospheric SRM exhaust plumes (Ross [1997b]).

The RISO program was an experimental effort of remote sensing and *in-situ* measurements. The program was not designed to provide a comprehensive picture of the chemistry and dynamics of SRM stratospheric plumes. Rather, the RISO program was designed to provide the Launch Programs office with answers to specific questions regarding the unresolved scientific issues concerning the local effects of SRM exhaust plume deposition in a timely and cost effective manner. The RISO program consisted of three experiments. The first experiment consisted of taking measurements of the solar ultraviolet spectrum and UV-A (i.e., 400 – 320 nanometers, nm) and UV-B (i.e., 320 – 290 nm) fluxes to determine what effect SRM exhaust plumes have on the ultraviolet radiative environment on the ground. Second, an aircraft carried a suite of instruments into exhaust plumes between 17 and 19 kilometers altitude to measure stratospheric plume composition. Third, stratospheric exhaust plumes were illuminated with a three-wavelength LIDAR located at Cape Canaveral to measure the ozone profile through launch plumes and measure plume dispersion rates. The data were used to more fully understand the local response of the stratosphere after medium and heavy launch vehicle passage and validate and improve model prediction. A summary of the RISO experiments is presented (Ross *et al.*, [1997a,b]).

5.3.1 RISO Program Science Objectives

The development of the RISO science objectives was based on the theory that chlorine and alumina in SRM exhaust have the potential to adversely affect ozone concentration in the stratosphere locally. Furthermore any such ozone loss would have the potential to increase the intensity of solar ultraviolet light on the ground near launch sites. The science objectives were limited and focused on the first order unresolved issues falling into three categories (Ross *et al.*, [1997a,b]). First, the theory of transient ozone loss in SRM plumes had to be proven. Second, the various models of the transient effects of SRM exhaust must be evaluated by comparing prediction against measurement. This includes models of cold plume diffusion and hot plume afterburning. Finally, the program had to provide measured quantities for model parameters that were assumed previously (e.g., plume expansion rate and alumina size distribution).

5.3.2 Ultraviolet Network Instrumentation

The goal of the Ultraviolet Network Instrumentation (UNI) plan was to measure the intensity of the ultraviolet solar spectrum as the stratospheric portion of an SRM plume occults the sun. Ultraviolet photometers and spectrographs were located near launch sites to maximize the likelihood that such an occultation would occur. UNI utilized only land-based sites, which severely limited the times of year this scheme could have been used. At Cape Canaveral, stratospheric winds had to blow from east to west to insure that launch vehicle plumes, initially about 10 km east of the coast, were transported over land near the launch site. This requirement limited measurements to daytime Cape Canaveral launches from approximately May to September.

Ross [1997b] described the occurrence of a 10% increase in the intensity of solar ultraviolet radiation or less than a 4% decrease in the ozone column abundance on the ground beneath SRM plumes. This follows from direct observation of the solar spectrum by the UNI experiment and inference based on the character of plume dispersion.

5.3.3 Plume *In-Situ* Measurement

The goal of the Plume *In-Situ* Measurement (PIM) Experiment was to measure the number density of ozone, chlorine, chlorine monoxide, and particulate size distribution in SRM exhaust in the lower stratosphere. The RISO program utilized a NASA WB-57F high altitude research aircraft that was capable of altitudes in excess of 18 km. The four major payloads deployed on the RISO missions were an ultraviolet ozone photometer (University of Houston), a mass spectrometer (Air Force Phillips Laboratory), an aerosol sampling apparatus (University of Missouri-Rolla), and a cosmic dust collector (Ross [1997b]).

The NASA WB-57F aircraft carried this instrumentation into the wakes of two Titan IV rockets on 12 May and 20 December 1996. The Titan IV launch vehicles lifted-off from Vandenberg Air Force Base (120°37' W, 34°48' N) at 13:33 Pacific Standard Time (PST) and 10:04 PST, respectively. In each case, the WB-57F entered the rocket plume wakes approximately 15 minutes after launch at an altitude of 18 km, then traversed the plume every 5 minutes, climbing between plume passes to ensure that the same plume segment was not sampled twice. The WB-57F pilot identified plume segments for each pass and recorded aircraft ingress and egress times on the basis of visual identification of plume boundaries. The duration of the plume passes were highly variable, lasting from 5 to 60 seconds and generally increased with time, reflecting expansion and diffusion of the plume. Plume sampling continued until the plume location could no longer be determined by the pilot or until the flight terminates because of aircraft refueling requirements. Details of the PIM instrumentation and initial results are found in the literature (e.g., Benbrook et al., [1997], Whitefield et al., [1997]).

5.3.4 Ozone *In-Situ* Measurements

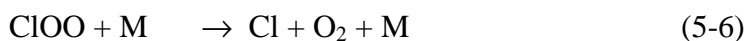
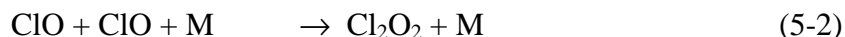
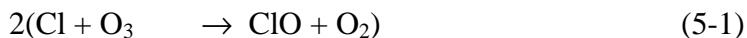
The ozone measurements were made with two ultraviolet-absorption instruments that were carried in the nose compartment of the NASA WB-57F aircraft. Two of the UV instruments had previously made ozone measurements in the stratosphere on various rocket and balloon platforms (*Weinstock et al., [1986], Profitt et al., [1983, 1985]*). Data were recorded in the altitude range between 17.7 and 19.5 km onboard the WB-57F and were sent by telemetry to the ground during several Titan IV missions. Two of the UV instruments had previously made ozone measurements in the stratosphere on various rocket and balloon platforms (*Benbrook et al., [1997]*).

A general course of plume evolution can be drawn from the entire collection of 12 May 1996 plume data from a Titan IV K-22 launch. During the first 15-30 minutes after launch, ozone loss reached several tens of percent in narrow regions a few kilometers across. During the next 30 minutes the plume expanded at a rate of about 0.1 to 0.3 km min⁻¹, and the ozone loss deepened to essentially 100%. Approximately one hour after launch, the plume continued to expand, and although there was some indication of isolated filaments or pockets with significant ozone depletion a few kilometers across, the ozone concentration in the plume had largely recovered back to ambient levels by diffusion and mixing.

The Titan IV data seem to verify models that predict marked temporary ozone depletion in SRM plumes owing to reactive chlorine. However, the data do not provide direct evidence that chlorine is the main agent causing ozone loss. Strong support for a chlorine-based loss mechanism was obtained from evening measurements in a Titan IV plume, which were carried out at stratospheric altitudes during a WB-57F flight on 24 April 1996. Twenty-nine minutes after launch, ozone loss was found to be negligible, despite Cl concentrations reaching about 15% of ambient ozone levels (*Ross et al., [1997c]*). The absence of significant ozone depletion after a night launch indicates that sunlight is required to drive the dominant ozone destruction reactions. This observation excludes exhaust NO or OH from being important ozone-destroying species in the exhaust plume. The presence of NO₂, in contrast, would result in a photocatalytic ozone destruction cycle, but NO₂ has never been considered as a significant SRM exhaust component (*Danilin et al., [1993], Ross et al., [1997c]*). These considerations, in conjunction with the direct observation of significant concentrations of Cl₂, which is converted photolytically into reactive chlorine (Cl) in the plume, strongly implicate chlorine as causing the severe transient ozone losses in the daytime plume wakes (*Burke et al., [1998], Zittel [1994], Denison et al., [1994]*).

Assuming 100% of the exhaust chlorine appeared as Cl₂, instead of the estimated 30%, the greater part of the observed loss could be explained. But plume models do not predict 100% conversion of HCl into Cl₂ at 18 km altitude (*Karol et al., [1992]*). Several possible mechanisms could contribute to ozone removal in the Titan IV exhaust wakes: reaction with exhaust nitrogen radicals, unspecified heterogeneous reactions on the surface of the exhaust alumina, or a fast catalytic cycle involving chlorine (*Burke et al., [1998]*). Models predict only very small NO_x production in the stratosphere, less than 1% exhaust mass fraction for the Titan IV (*Ross et al., [1997a]*), not enough to contribute significantly to the ozone loss.

Solomon [1988] presented a comprehensive review of stratospheric ozone depletion over a decade ago. It was postulated (Molina *et al.*, [1987], Hayman *et al.*, [1986]), that a gas-phase catalytic cycle which could explain the magnitude of the measured ozone destruction in the Antarctic ozone hole involves the ClO dimer. The chemistry may be represented as:



Molina *et al.*, [1987] noted that this pathway must compete with thermal decomposition of Cl_2O_2 , into ClO, which results in no net loss of ozone. The thermal decomposition pathway should proceed relatively under stratospheric conditions relative to the photolytic channel.



Shortly after SRM plume deposition, when ClO and Cl concentrations are predicted at approximately one hundred parts per billion volume, ppbv, the reaction of Cl_2O_2 with Cl will dominate over competing Cl_2O_2 loss mechanisms, including photolysis and thermal decomposition (Martin [1994], Denison *et al.*, [1994], Ross *et al.*, [1996b]). This would occur despite the relatively warm ambient temperature of about 220 K, which promotes thermal decomposition (Molina *et al.*, [1987]). This cycle is expected to be rate-limited by Cl_2 photolysis proceeding at a rate of 0.13 min^{-1} . This rate is fast enough to allow each Cl atom to destroy several ozone molecules during the 30 minute duration of intense ozone removal observed in the Titan IV plumes, and consistent with the estimated ratio of ozone lost to chlorine injected (Kruger [1994]). Additional *in-situ* data on plume composition are needed to confirm this mechanism.

Relevant Titan IV model simulations include those by Ross [1997b] and Brady *et al.*, [1997a,b]. Ross [1997b] and Lohn *et al.*, [1999] have predicted that approximately one hour after launch, ozone essentially is removed completely in a small region about 3-8 kilometers across. These *in-situ* measurements show that the actual ozone removal region after one hour is 6 to 8 kilometers across, suggesting that there is a shortfall in the model calculations, and a need exists to account for some ozone loss mechanism (or possible chlorine source). This compares well with the observed expansion rate of 0.1 to 0.3 km min^{-1} . Finally, Brady *et al.* [1997a,b] predicted an ozone loss on the plume centerline of about 80% and 25% fifteen and fifty-five

minutes after launch, respectively. These ozone measurements show a loss of 35% and about 100% at these times, again suggesting models underestimate the ozone loss. The most likely reason for this discrepancy between model estimates and *in-situ* measurements is the possible choice of diffusion constants used in the models. The effect of diffusion coefficients on model results was described in Section 3.5 and is mentioned again in Section 5.4.

5.3.5 Aerosol *In-Situ* Measurements

Attempts have been made to model the local effects of chlorine and aerosol injection into the stratosphere (*Whitefield et al.*, [1997], *Prather et al.*, [1990], *AIAA* [1991], *Ko et al.*, [1994], *Ross* [1996b]). From an aerosol emission perspective, the Delta rocket has the potential to release not only chlorine, but also aluminum oxide from its nine solid rocket motors, which are firing through the stratosphere generating 70% of the mass flow in the exhaust (only 30% is from the LOX/Kerosene core). This raises the question of the addition into the stratosphere of carbonaceous aerosol from its kerosene oxygen main stage. There is no direct evidence of the existence of such an aerosol (the data only suggest size distribution, not composition); but if it were able to survive afterburning, it could provide additional surface area for heterogeneous reactions. The nature of the aerosols is not well understood and deserves further study, and as a result any interpretation of the aerosols role is at best conjecture.

On the NASA WB-57F aircraft, *Whitefield et al.*, [1997] made measurements during RISO of aerosol emissions in the plumes of two Titan IV launches, K-16 and K-22, both of which took place in the spring of 1996 (*Ross* [1997b]). *Whitefield et al.*, [1997] chose a Tank Sampling and Pressurization System (TSPS) as the primary method for capturing rocket aerosol emissions and measuring their total concentration and their size distributions in the diameter range 10-200 nm (*Howard et al.*, [1996], *Shumann* [1996]). Total relative aerosol concentration and size distributions were measured in the ambient background and in the rocket exhaust plumes for both launches.

Measurements were made of the exhausts of two Titan rockets that utilized a combination of a kerosene/oxygen mainstage and peripheral solid rocket motors. Data were acquired at altitudes between 15 and 21 km within minutes of the launch. This data may be compared with the data from a Shuttle plume taken in the late 1970's using an electric aerosol analyzer by *Strand et al.*, [1981]. *Strand et al.*, [1981] reported similar size distributions for the Shuttle SRMs in the 10-100 nm diameter range and similar total concentrations. Unfortunately, no background distributions were available from that work. The similarity between the shape of the size distributions for background and plume concentrations leads to the speculation that at these altitudes and latitudes, the background aerosol composition is closely linked to the composition of SRM plume emissions. In future planned measurements, it should be a primary objective to gather samples for post flight elemental analysis.

The extended range size distributions acquired during the Delta investigation revealed a bimodal distribution. The peak at smaller aerosol diameters (40-60 nm) was characteristic of the log-normal shaped distributions observed in jet engine exhaust plumes where kerosene and

oxygen were the combusting materials (*Howard [1996]*). There was no evidence of such a peak in the size distributions for the exclusively SRM powered Titans. Comparison of Titan and Delta plume aerosol data with that for ozone for all launches reveal massive reductions in ozone concentration. A correlation between ozone depletion and high aerosol concentration also was observed for the Delta launch (*Whitefield et al., [1997]*).

5.3.6 Plume LIDAR Experiment and Plume's Vertical Extent

The Plume LIDAR Experiment (PLE) was a modification of the Mobile LIDAR Trailer developed at the Air Force Phillips Laboratory, Hanscom AFB. The PLE experiment measured the diffusion and dispersion characteristics of the exhaust plume by observing backscattered light from the plume particulate; very accurate plume dimension and location were determined. A comprehensive description of the apparatus has been given (*Dao et al., [1997]*).

Dao et al., [1997] reported the first LIDAR measurements of the 'cool' exhaust plume of solid rocket motors in the stratosphere. The measurements involved two Titan IV rockets launched from Cape Canaveral, FL on 6 November 1995 and 24 April 1996, Space Shuttle STS-76 launched 22 March 1996, STS-78 on 20 June 1996 and STS-79 on 16 September 1996. The emphasis was on plume physical dimensions, expansion rate, vertical extent, and the wavelength-dependence of its backscattering coefficients. A Mobile LIDAR Trailer (MLT) system, which was a Rayleigh and Differential Absorption LIDAR (DIAL) system with the important addition of computer-controlled scanning mirrors, was used to detect stratospheric ozone. It was designed to measure ozone and particles using the laser wavelengths of 532, 355 and 308 nm. The instrumentation has been described in detail elsewhere (*Dao et al., [1996]*). Representative results are presented below with emphasis on the vertical and horizontal extents of the plumes as well as a preliminary analysis of the dependence of the backscattering signals on laser wavelength.

In the first campaign, MLT measured the exhaust plume of the Titan IV (K-21) rocket, which was launched 6 November 1995. The most striking result of the measurements was on the vertical extent of the plume layers. *Dao et al., [1997]* completed 5 campaigns to measure the ambient exhaust plume of 2 Titan IV and 3 Space Shuttle launches in the stratosphere. Over 700 sets of LIDAR profiles were collected to characterize plumes thickness and expansion rate. The backscattering ratios were analyzed to reveal a weakening in wavelength dependence consistent with an effective particle size that increased with time.

No more than 6 layers were ever observed along a given line of sight though the plume region. The associated total column of plume was small compared to the total thickness of the ozone layer so that even though RISO *in-situ* measurements showed that ozone was largely removed from the plume during approximately the first hour after launch (*Benbrook et al., [1997]*), the total column effect on the ozone layer was found to be very small. Various models describing the stratospheric response to SRM exhaust have assumed plume thickness of at least 1 km; however, these *in-situ* measurements reveal that model predictions need to be reconsidered in light of the much smaller thickness layer that stratospheric exhaust plumes actually form.

Motivated by the observation of extended yet thin layers of plumes in the November campaign (K-21), successive measurements on March 22 (Space Shuttle mission STS-76) and April 24 1996 (K-16) were designed to measure the horizontal extents of plume layers. The horizontal extent of the plume is an important parameter that affects plume dynamics and chemistry. The width was observed to expand with time at a rate of 8.5 km/hr or 0.14 km/min.

5.4 *In-Situ* Video Observations

Beiting *et al.*, [1997b] reports that recent chemical models of solid rocket motor (SRM) exhaust predict that stratospheric ozone levels in the plume are depressed from ambient values by after-burning HCl (Zittel [1994], Denison *et al.*, [1994], Kruger [1994], Brady *et al.*, [1995], Ross [1997b]). Although the size and persistence of the predicted reduced ozone concentrations are a sensitive function of the plume dispersion rate, data measuring this rate are nearly nonexistent (Beiting [1997a]). As mentioned in a previous section, the total database for this parameter prior to these studies consisted of a single plume expansion rate of an unidentified rocket (presumably a Titan III) measured by photographic cameras placed at three ground positions taken more than 20 years ago. These data measured the expansion of the plume at the lower edge of the stratosphere (18 km) for 10 minutes after vehicle passage and were presented in a committee report (Hoshizaki [1975]). The expansion rate reported was about an order of magnitude greater than that used in some of the models of SRM stratospheric plume chemistry.

Because of the deficiency, Beiting [1999] made a comprehensive set of measurements of plume expansion from nine Space Shuttle and Titan IV launch vehicles at altitudes of 18, 24, and 30 km in the stratosphere (see Section 3). These images were used to infer plume motion and expansion at these altitudes representative of the stratosphere. The plume diameters were inferred from electronic images of polarized, near-IR solar radiation scattered from the exhaust particles. The expansion rate was measured for as long as 50 minutes after the vehicle reached altitude. Observations made simultaneously at multiple altitudes showed the expansion rate increased with increasing altitude for six measurements made at Cape Canaveral Air Station (CCAS), but decreased between 24 and 30 km for the one measurement made at Vandenberg Air Force Base (VAFB). The average expansion rates made are presented in Table 5-1. Beiting [1999] found no correlation between the expansion rate and wind speed or wind shear. The expansion rates were found to be constant in time, but increased with increasing altitude for all measurements made at the CCAS. The one measurement made at VAFB showed a higher expansion rate at an altitude of 24 km than at 30 km. There was considerable variability in the magnitude of the expansion rate at a given altitude from launch-to-launch, but this variation did not correlate with wind speed or shear.

Table 5-1. Plume Expansion Measured by Beiting [1999]

Altitude (km)	Plume Diffusion Rate (m/s)	Plume Diffusion Rate (km/min)
18	4.3 ± 1.0	0.26 ± 0.06
24	6.8 ± 1.9	0.41 ± 0.11
30	8.7 ± 2.4	0.52 ± 0.14

The images of the plume presented in this study clearly show a complex morphology in that the plume shears into parcels which can dilute more slowly than the aggregate plume. Beiting [1999] used these data to compare several models for diffusivity and to update a comprehensive particle model of solid rocket motor exhaust in the stratosphere. Expansion rates are required by models to calculate the spatial extent and temporal persistence and thereby constrain the chemistry of local stratospheric ozone depletion caused by solid rocket motor exhaust. Beiting [1999] concluded that models that allowed the diffusivity to vary with plume size were more successful than a constant diffusivity model.

A comparison of the expansion rates as determined by the variety of *in-situ* techniques is presented in Table 5-2.

Table 5-2. Summary of In-situ Expansion or Dispersion Rates

Expansion Rate	Beiting [1999]	Beiting [1999]	Hoshizaki [1975]	Dao <i>et al.</i> , [1997]	Ross <i>et al.</i> , [1997b]
Technique	Video	Video	Photographic	LIDAR	W57F
Altitude	18	30	18	23	18
km/min	0.26	0.52	0.3	0.14	0.1

The expansion rate measured in the W57F fly-through is below that measured by LIDAR and Video. All differences between the models and the *in-situ* measurements may be explained if each plume parcel is expanding at its own rate (Beiting [1999] gives an average). Locating the plume visually up to an hour after launch will bias one toward the most slowly dispersing parcels.

5.5 *In-Situ* Satellite Observations

Since November of 1978, total ozone has been measured on a nearly global basis by the Total Ozone Mapping Spectrometer (TOMS) from a variety of satellite platforms. TOMS measures the earth's ultraviolet albedo at several wavelengths near 300 nm. TOMS provides a cross-wise sweep of 35 positions every 8 seconds. Global coverage is obtained by merging these

scans with those from adjacent orbital tracks. Atmospheric ozone content is determined by comparing the measured directional albedo ratios to computed tables representing inverse solutions of a multiple scattering (Rayleigh) radiative transfer equation (*Klenk et al., [1982]*). These tables depend on total ozone, ozone latitude dependence, solar zenith angle, atmospheric pressure at scattering altitudes, and other climatology conditions (*Syage et al., [1995, 1996]*).

TOMS data analysis assumes that the backscattered radiance is attenuated by ozone absorption and Rayleigh scattering. Methods have been developed to deal with the effect of aerosols on the estimation of total column ozone (*Dave [1978]*, *Torres et al., [1992]*, *Bhartia et al., [1993]*); however, not for the case of an alumina-laden plume. Nor are absorbing species considered other than those that exist in the ambient atmosphere.

The United States Air Force Space and Missile Systems Center (SMC) first assessed ozone depletion in 1988 for Titan Centaur launches, relying heavily on NASA's Environmental Impact Statement for the Space Shuttle, which uses similar solid-fueled rockets. Subsequent data showed problems with the model predictions on which NASA's analyses were based (*McPeters et al., [1991]*, *Syage et al., [1996]*). In 1991, SMC initiated several additional studies to quantify the effect that launches have on stratospheric ozone. These studies concluded that available measurements and models were not adequate for such quantification. The best available data was from NASA's Total Ozone Monitoring Spectrometer (TOMS). However, because TOMS was built to measure global ozone changes, it lacked sufficient resolution to measure ozone loss in a narrow launch corridor. Analysis of ozone data from the Total Ozone Mapping Spectrometer (TOMS) carried on the Nimbus 7 spacecraft, in contrast, failed to provide evidence for rapid local decreases in (ozone after several Space Shuttle launches (*McPeters et al., [1991]*). However, no firm conclusions could be drawn from the TOMS data either with respect to the Space Shuttle or rocket exhaust effects in general. Because the complex aerosol and gas environment of rocket exhaust plumes might have give rise to anomalous scattering and absorption, increased aerosol would compromise the TOMS data (*Stolarski et al., [1992]*, *Ross et al., [1997a]*).

Prather et al., [1990] published a modeling study of the Space Shuttle's impact on the stratosphere that generated a considerable amount of discussion (*Aftergood [1991]*, *McPeters et al., [1991]*). *Prather et al., [1990]* investigated the long-term effects using global atmospheric chemistry and dispersion models, from which they concluded that at current launch rates, solid rocket motor exhaust does not impose a significant global impact on stratospheric chemistry. Furthermore, an attempt was made to examine the transient chemical behavior and local impact. They argued that a local column ozone hole should not occur because the chlorine is released predominantly as HCl, which requires considerable time to be converted to active forms of chlorine. Additionally, the exhaust plume that is passing through the stratosphere is not aligned vertically. Finally, the exhaust gases were found to disperse over a 1000 km range in a day.

Aftergood [1991] challenged these conclusions raising two important points: (1) a U2 flying through the plume of a Titan III observed a 40% reduction in the ambient ozone level (*Pergament et al., 1977b*), although it was noted that this measurement is of uncertain reliability, and (2) chlorine is not necessarily exhausted predominantly as HCl, but may contain

large quantities of Cl due to afterburning chemistry as predicted by an early plume model by Hoshizaki [1975]. More recently Zittel [1994], Denison *et al.*, [1994], Karol *et al.*, [1992] and Lohn *et al.*, [1996] strengthened the evidence for afterburning chemistry using validated plume codes. Burke *et al.*, [1998] has provided experimental verification of these models. The calculations of Denison *et al.* [1994] and Karol *et al.*, [1992] continued the plume exhaust kinetics to longer times and observed significant ozone depletion along the plume centerline. Lohn *et al.*, [1999] and Brady *et al.*, [1996] carried out similar calculations using a comprehensive kinetics model including homogeneous and heterogeneous chemistry and also predicted significant ozone decomposition along the plume centerline. Ross [1996b] calculated three-dimensional chemical profiles using a plume kinetics and dispersion model that also show significant ozone depletion Jackman *et al.* [1996a] recently updated the effects of Shuttle launches on the global ozone balance using a 2D-photochemistry transport model that included heterogeneous chemistry on stratospheric sulfuric acid aerosols. However, the work did not include heterogeneous effects involving aluminum oxide particle exhaust, or the local effect of ozone chemistry in the plume. The local and global effect of catalytic ozone decomposition on alumina has been reported by Hanning-Lee *et al.* [1996].

McPeters *et al.* [1991] rebutted the comment by Aftergood [1991] by citing TOMS results. TOMS has a pixel size resolution of 40x40 km², which would limit the ability to measure precisely a local ozone hole. However, because the ozone measurement precision of TOMS is a few percent, a significant hole of small extent should be observable. For example, McPeters *et al.*, [1991] explained that a 40% column reduction over a 20 x 20 km area would appear as a 10% reduction for a single pixel, which is much greater than the detection limit of the TOMS instrument. The TOMS images of several Shuttle trajectories ranging in time from one hour to one day after passage give no indication of widespread ozone depletion. Furthermore, ozone depletion takes place over such a small area that TOMS is not capable of detecting it, but then the question is whether a decrease so localized can be considered significant on a global scale. Given the non-vertical path of the launch, column-averaged perturbations to ozone cannot be more than tens of kilometers squared. The global-scale long-term decreases predicted by Prather *et al.*, [1991] were too small to be readily detected in TOMS data at all.

To determine if TOMS data could detect localized depletion of ozone from a solid rocket motor, Syage *et al.*, [1996] performed a variety of plume property simulations of TOMS measurements. They observed the typical plume width and calculated ozone depletion is significantly smaller than the TOMS Field of View, the measured change in total ozone understates the true ozone change. The effect of particle attenuation on the TOMS instrument was relatively minor assuming the particle size distribution determined by Beiting [1995]. However, the distortion can increase significantly if the actual particle size distribution has a large component near the wavelength of detected light (namely 0.3 μm) (Syage [1995]). Syage *et al.* [1996] concluded that TOMS could measure local ozone depletion in a rocket plume. However, for a plume in which a 20% column ozone loss extends over several kilometers in radius, TOMS could measure a mere 2% decrease that would register in only one pixel. Choosing a viewing angle aligned along the plume axis may enhance the measured ozone loss. This would maximize the pathlength and overlap with the plume centerline. Syage *et al.*, [1996] reported calculations that showed the potential for enhancement by a factor of three assuming an

aligned plume unperturbed by differential wind velocities. In reality, winds can and will randomize much of the initial alignment.

5.6 High Resolution Ozone Imager

The HIROIG instrument, or High Resolution Ozone Imager, is a state-of-the-art sensor designed to measure ozone depletion by monitoring changes in intensity of backscattered solar ultraviolet (UV) light resulting from rocket launches. The technique employed is similar to that used by other ozone instruments: TOMS (Total Ozone Mapping Spectrometer) and SBUV (Solar Backscatter UV). Solar radiation that is incident on the upper atmosphere is absorbed by the stratospheric ozone layer and Rayleigh-scattered by gas molecules in the air. In the undisturbed stratosphere, the depth to which UV light can penetrate before being completely absorbed by ozone is dependent upon the wavelength of the light. If there is an “ozone hole” at a particular altitude, light that normally penetrates to that altitude is able to reach lower altitudes where the atmospheric density is higher and the light is more strongly scattered, resulting in more intense backscattered light. Light that does not normally penetrate to the holes’ altitude is unaffected. Therefore, the wavelengths at which the backscattered light is intensified are correlated with specific altitudes at which the ozone has been depleted.

More specifically, HIROIG is a UV hyper-spectral imaging spectrograph/polarimeter. It consists of three identical spectrographs; each fitted with a half-wave plate set at a different angle. Combining the signals from the three spectrographs allows the polarization of the incident light to be determined. Each spectrograph simultaneously records 100 spectra divided into 100 wavelength bins in the range 270-370 nm. Spatially, the bin size is equivalent to 1 km at the Earth’s surface when viewed from an altitude of 800 km, giving an effective resolution along the slit of 2 km when the instrument is pointed toward nadir. Thus, the in-track resolution is approximately 2 km.

HIROIG has been utilized in a series of ground-based measurement campaigns and may in the future be deployed to obtain space-based measurements. The first series of ground-based observations were carried out at the Kennedy Space Center, Florida (KSC), in association with the Space Shuttle STS-65 launch. The data from the KSC observations demonstrated HIROIGs ability to detect the evidence of local ozone depletion. A second series of observations on noctilucent clouds were conducted at Søndre Strømfjord, Greenland in July 1995 and demonstrated HIROIGs high sensitivity and usefulness of its polarimetry function (*McKenzie et al., [1998], Hecht et al., [1997]*).

In May 1994, the HIROIG instrument was used to make ground-based observations in conjunction with the launch of the STS-65 Space Shuttle mission between 7-9 July 1994. Observations of the diffuse scattered solar UV spectrum of the sky were made from a site 6.4 km due west of the STS-65 launch pad. Data obtained by the HIROIG instrument in the stratospheric plume of STS-65 indicated that a local decrease in the total ozone column by 2.35% ($\pm 1\sigma$) could account for the observed sudden change in the UV intensity ratio measured (*McKenzie et al., [1998]*). The suggestion that the change in the UV intensity ratio was caused

by stratospheric ozone depletion associated with the STS-65 launch plume was tested with a simple empirical model of plume transport and growth, which included STS-65 event data based on a LIDAR measurement reported in Dao *et al.*, [1997].

Another series of ground-based HIROIG observations were made at Søndre Strømfjord, Greenland on the nights of 30-31 July 1995 and 29-30 July and 4-5 August 1997 (McKenzie *et al.*, [1998], Hecht *et al.*, [1997]). These observations were made on noctilucent clouds (NLCs) which occur only in the arctic summer at altitudes of approximately 85 km and are the highest clouds known. Because they are far above the ozone layer, they are not observable from the ground in the ozone absorption bands, but only in the long-wavelength part of the HIROIG spectral range. They are very faint and, in the UV, can only be seen in scattered sunlight after ground-level sunset, when the Earth and the lower atmosphere are not directly illuminated by the Sun. The analysis of the 1995 observation is complete (Hecht *et al.*, [1997]). The HIROIG instrument was able to determine an upper limit of 0.07 μm on the size of the particles in an NLC (McKenzie *et al.*, [1998]).

In short, HIROIG has been shown to measure the spectrum of solar UV radiation backscattered by the Earth's atmosphere with a spatial resolution of approximately 2 km at nadir. This high spatial resolution is required to monitor launch-vehicle exhaust because regions of ozone depletion caused by such exhaust are expected to be only a few kilometers in size. The deployment of a space-based HIROIG would be a valuable tool for current and future monitoring of launches in distant or restricted locations.

5.7 Summary

Ross *et al.*, [1997a] has reported a general picture of the evolution of ozone concentration in a Titan IV plume wake as follows. During the first thirty minutes after launch, ozone loss reaches several tens of percent in narrow regions a few kilometers across. The following period (i.e., 30-60 min after launch), the plume expands at a rate of about 0.1 km min⁻¹, and the most severe disturbances take place, with ozone losses approaching 100% over regions reaching 8 km across. After an hour, as the plume continues to expand, the relatively large, deeply depleted regions are no longer detected, and ozone concentrations in the plume have returned to ambient levels. This indicates that the ability of plume gases to destroy ozone is spent 60 minutes after launch at the higher altitudes (i.e., 40 km) and less than 60 minutes at lower altitudes (20 km); and ozone-rich air is able to diffuse back into the plume wake to replace the lost ozone. Because ozone production is very slow in the lower stratosphere, ozone is replaced in the plume only in a relative sense. Still the observed behavior of ozone in the plume wake, in conjunction with the distortion of the plume from stratospheric wind shear, implies that the potential for significant changes in the total ozone column or solar ultraviolet exposure near launch sites is extremely limited. Accordingly, the local environmental hazard from transient stratospheric ozone loss after solid-fuelled rocket launches is not significant.

In short, the expansion rate of a rocket exhaust plume measured in the NASA WB-57F fly-through, i.e., 0.1 km/min., (Ross *et al.*, [1997a]) is less than that measured by video camera

(Beiting [1999, 1997]), but similar to that measured by LIDAR (Dao *et al.*, [1997]). All of the differences between models and *in-situ* measurements may be explained if each plume parcel is expanding at its own rate (i.e., Beiting [1999] presented the average expansion rate for three particular altitudes). Locating the plume visually up to an hour after launch will bias one toward observing parcels with the most unique characteristics (i.e., for tracking purposes). Furthermore bias problems were noted in Dao *et al.*, [1997] and Whitefield *et al.*, [1997] for their respective measurements. Taken together, these various techniques provide a better picture of the total morphology of exhaust plume expansion. More *in-situ* measurements should be made to constrain the dispersion rate.

6 PROPELLANTS – CURRENT USAGE AND PROPOSED ALTERNATIVE FUELS

6.1 Propellants

This section will compile and present data on historical fuel use, elimination and reduction efforts to date, and future plans to eliminate and reduce fuels containing Potential Ozone Reducing Substances (PORS), in favor of cleaner burning fuels and alternate propellants to reduce stratospheric ozone depletion. Information on ozone depleting substances, ODS, usage and elimination in the manufacture of large solid motors may be found in other Air Force Handbooks (*SRS Handbook [1995]*). A complete review of the subject on alternative fuels may be found in Lewis *et al.*, [1994].

Section 6.1 introduces the PORS problem. Liquid propellants and their impact on stratospheric ozone are presented in Section 6.2. In Section 6.3, alternate propellants that may reduce the production of PORS are introduced. Section 6.4 identifies chemical species that are relevant to ozone depletion. Identification of chemical species relevant to ozone depletion is presented in here. Section 6.5 identifies alternative propellants that may reduce or eliminate formation of selected PORS. This section includes a discussion on the mitigation of ozone depletion by reducing emissions of chlorine radical (Cl), hydrogen chloride (HCl), alumina (Al₂O₃), water (H₂O), and carbon monoxide (CO₂). Also included is the status of hardware used in these mitigation procedures. Recent investigations by Thiokol describing new propellant combinations are presented in Section 6.6. Section 6.7 includes a review of the propellants to be used in future United States launch activities; these include the portable Sea Launch System and the Evolved Environmental Launch Vehicle (EELV).

6.2 Liquid Propellants

Liquid rocket engine technology based on LOX/LH₂ and LOX/RP-1 is well developed and flight demonstrated (i.e., the F-1) SSME among many examples. This technology is currently not in production in the U.S. for boost systems. All the heavy lift rocket engines currently used in the U.S. are solid propellant based. Launch systems utilizing LOX/LH₂ and LOX/RP-1 are available from other countries, particularly the former USSR or Commonwealth of Independent States, CIS (e.g., Proton, Zenit, the SL-X series, etc.). However, there could be security issues surrounding the use of rocket engines provided to the U.S. by a foreign country (not to mention a former cold war enemy) which may be used to launch classified payloads.

Though not currently in production, it is certainly true that liquid engine technology could be redeveloped, and NASA and the USAF have performed studies on the cost of re-manufacturing the F-1 or creating a new engine for boost to LEO applications. Other NASA programs, with the goal of developing low-cost-to-LEO launch systems, have test stand fired a 40 klbf LOX/LH₂. The LOX/LH₂ engines have I_{sp} greater than 425 seconds and LOX/RP-1 are greater than 280 seconds depending on the design details (*Dressler et al.*, [1993], *Sackheim et al.*, [1994], *Lewis et al.*, [1994]).

6.2.1 Calculations of Ozone Depletion from Conventional Liquid Propellants

The effects of liquid rocket engines on stratospheric ozone were addressed by Lohn *et al.*, [1996]. Specifically, two propellant combinations were addressed: LOX/LH₂ (720 klbf thrust) and LOX/RP-1 (810 klbf thrust). Their analysis of the exhaust plume was divided into two parts: the hot plume and the cold plume. In the hot plume calculation, the plume chemistry and gas dynamics were modeled starting from the combustion chamber where chemical equilibrium was assumed, then followed by a one-dimensional streamtube reacting flow analysis for the flow in nozzle, and finally the finite rate chemistry analysis for the afterburning region downstream of the nozzle exit. In the cold plume regime, the chemistry was dominated by a set of kinetic reactions of ozone-depletion catalytic cycles, photodissociation reactions of byproducts from these catalytic cycles, and diffusion (see Section 3). The specifications for conventional bipropellants are presented in Table 6-1. These specifications include nominal 720 and 810 klbf and 2.4 Mlbf thrust classes of engines.

Table 6-1 Specifications of Liquid Rocket Motor

Liquid Propellant	Liquid H₂/LOX	Liquid H₂/LOX	Liquid RP-1/LOX	Liquid RP-1/LOX
Thrust (lbf)	720 k [#]	2.4 M [*]	2.2 M [*]	2.2 M [*]
O/F Ratio	6.6	6.6	300	1000
Chamber Pressure (psia)	300	1000	7.0	50
Area Ratio	7.0	50	n/a	n/a

k[#] is klbf or THOUSANDS of lbf thrust
M^{*} is Mlbf or MILLIONS of lbf thrust
n/a Data not available

Zittel [1995] used a standard rocket motor nozzle and plume flow-field computer model to estimate the production of nitrogen oxides (NO_x) species by motors of different propellant type at low stratospheric altitudes. He considered two different Titan IV solid-fueled motors, the Titan 3B amine/N₂O₄ fueled first stage, the kerosene/LOX fueled Delta core stage, and a LOX/LH₂ fueled Space Shuttle Main Engine (SSME). Zittel [1995] concluded that the production by afterburning was highly temperature dependent and fell sharply with increasing altitude yielding almost negligible amounts of NO_x (for non-nitrogen containing fuels) at altitudes above 20 km.

6.2.2 Local Stratospheric Impact from Liquid Engines

From a viewpoint of local impact, the effect on stratospheric ozone resulting from bipropellant exhausts is equally unimportant. The cold plume analysis (*Lohn et al., [1996]*) was performed assuming exhaust species deposition at an altitude of 30 km. The low ozone density hole appearing in the ozone concentration profile for early times was caused by a displacement effect rather than by chemical consumption. It took only 50 seconds for diffusion to backfill the plume displacement hole.

The RP-1/LOX system generated considerably less NO_x in the afterburning region and was seen to be qualitatively the same as the LH₂/LOX system. Both RP-1/LOX and LH₂/LOX systems produce approximately 10⁻³ ppb of PORS such as NO_x and HO_x. After about 100 seconds, the diffusion process was essentially completed. Because of the low concentration of nitric oxide, no significant ozone depletion was detected in the plume. In fact, because of the presence of atomic oxygen in the plume, ozone was generated initially through a three-body reaction (i.e., reaction (6-1) below). Instead of depleting ozone, there was a production of the order of 10¹¹ molecules cm⁻¹ s⁻¹ for approximately 0.1 seconds (*Lohn et al., [1996]*).



Similar results were obtained for the 2.4 million lbf thrust rocket systems. The potential ozone reactive species concentration; however, should scale approximately by thrust, because mass flow rate is proportional to thrust. The results corresponding to LH₂/LOX, RP-1/LOX and composite AP/Al are seen to be qualitatively similar to those of the smaller (i.e., 720-810 klbf) thrust engines considered. Little or no ozone depletion was observed for the LH₂/LOX and RP-1/LOX systems. For the solid system; however, the level of local ozone destruction was about a factor of 4 higher than that of the ~700 klbf thrust engine. This factor was consistent with the thrust ratio of the two classes of systems.

6.2.3 NTO Oxidizer Used in Liquid Engines

The remaining liquid engine to discuss is one in which NO is produced directly by use of nitrogen tetroxide, N₂O₄ or NTO, as an oxidizer. In contrast, HCl can decompose to form Cl at lower temperatures as indicated by its lower activation energy. Hence formation of chlorine from HCl by afterburning is an important mechanism for SRMs at stratospheric altitudes.

A hypothetical 2.4 Mlbf class liquid thruster plume was examined by *Lohn et al., [1996]* taking the Titan III cold wake start conditions and turning off the chlorine-related chemistry. The NO/NO₂ concentrations were similar to those emitted from a MMH/NTO thruster (a mole fraction of NO of approximately 10⁻²). The cold wake analysis at 20 km altitude revealed the creation of an ozone hole, which was observed to open, but quickly close after 400-500 seconds. The “depth” of the hole was not as pronounced as for the SRM wake. The ozone levels in the hole were calculated between 25 to 50% of the ambient value, whereas for the case of an SRM, the in-the-hole ozone concentrations were found to be several orders of magnitude less than the

ambient value. Thus, the in-the-hole column density effect of the liquid engine wake was considerably less than the effect caused by an SRM. However, the wake of the liquid engine did consume 50% of the ozone molecules in the ozone hole that it produced.

6.3 Alternate Propellants to Reduce Production of PORS

A number of Ozone Depleting Substances (ODSs) or Chemicals (ODCs) have been part of the manufacture of solid rocket motors and ground activities for decades. The advantages of using these materials include their excellent solvent cleaning properties, rapid “flash off” or drying capacity, non-flammability, relatively low toxicity and high degree of compatibility with a wide range of coating types. The flammability of a substance is an especially important concern in the manufacture of solid rocket motors due to the highly energetic nature of the materials used in these motors. Several ODSs have become “qualified” standard production materials. In space programs, “qualified” is used to denote that a specific process and its associated materials have been analyzed, tested against specific standards of performance, and formally approved by the recognized engineering authority for use in production of a specific solid rocket motor.

Some of the exhaust species produced by these alternate propellants are classified as PORS in the stratosphere. This term was introduced and described in Section 3. The amounts of these species were quantified and found to be acceptably small. The technology status of these propellants and the rocket engines that would utilize them is summarized in the following sections.

6.4 Identification of Chemical Species Relevant to Ozone Depletion

Typical solid propellant rockets produce primarily H_2O , CO_2 , Al_2O_3 , HCl , and other species in lesser amounts. Of these species, oxides of nitrogen (NO_x) and HCl have been identified as PORS. By itself, HCl is a reservoir species and is not a concern in ozone depletion chemistry (*DeMore et al.*, [1990]). Unfortunately, the chemistry of the high temperature, afterburning shear layer at the plume intrinsic core/atmospheric interface converts some of the HCl into Cl_2 or Cl radical which is highly photoreactive.

There are continuing concerns and evolving understanding about the importance of H_2O accumulation at stratospheric altitudes, which can participate in heterogeneous ozone depletion reactions (*DeMore et al.*, [1990]). It is certainly true that the amount of water produced by rockets is small; the majority of the H_2O deposited into the stratosphere from launches will photolyze or react with oxygen atoms to form HO_x species, HO , HO_2 , etc., (*Brady et al.*, [1995], *Johnston* [1992]). But if alternate propellants can be identified which reduce the amount of H_2O produced, such information may be useful in developing environmentally ‘cleaner’ propellants. Furthermore, conventional SRM propellants produce Al_2O_3 in the solid or liquid phase. If heterogeneous ozone depletion chemistry were a concern, then the smaller Al_2O_3 particles in the size distribution as well as condensed liquid Al_2O_3 would both participate in local heterogeneous ozone depletion chemistry. Similar objections have been raised against propellant combinations that produce particulate as part of the exhaust stream or as a consequence of afterburning, such as

carbon or soot; see Section 6 (*Denison et al., [1994], Lewis et al., [1994], Whitefield et al., [1997]*). Carbon dioxide, CO₂ and carbon monoxide, CO, are not of concern as PORS.

Utilization of alternate propellants can reduce or eliminate each of these chemical species, individually or in combination, depending on the specific propellant combination selected. Because all propellants are part of a propulsion system, there is a cost implication whenever any part of the system is modified. However, it is possible to identify a range of alternate propellant combinations with differing impacts on propulsion system hardware. Some of the propellants identified will require relatively minor modifications to their existing propulsion systems. Other propellant combinations are technologically mature, but require existing engine technology that is not currently in production in the U.S. from boost to low Earth orbit (LEO) applications. Finally, there are propellant combinations that have been laboratory or test stand fired but have never been used in operational systems.

The fact that there are several potential propellant combinations available which may be useful for launch systems responsive to reduced PORS production is desirable. It enables the time-phased implementation of different technology solutions with different launch system hardware and cost impacts. This provides flexibility in implementing solutions to the problem of stratospheric ozone depletion. For example, if existing solid propellants can be reformulated to include afterburning suppressant chemicals that reduce or eliminate the conversion of HCl to Cl₂ or Cl radical, this may be an environmentally acceptable solution. If, at some future time, it is necessary to remove HCl entirely, either nitrate/carbonate-based solid propellant may be introduced, or conventional liquids (LOX/LH₂ and LOX/RP-1) may be used in place of solid propellants based on ammonium perchlorate aluminum. If the improved specific impulse (I_{sp}) of the non-perchlorate solids is deemed too low for boost applications, which appears likely (*Lewis et al., [1994]*), or if the concern about heterogeneous ozone depletion due to H₂O mandate its elimination as a plume constituent, advanced fluorine based solid or gelled propellants could be brought on-line, given sufficient development resources and schedule. There are a variety of potential mitigation's to the problem of ozone depletion due to potential ozone reactive species.

6.5 Identification of Alternate Propellants Which Reduce or Eliminate Formation of Selected PORS

Detailed reactive flow calculations (*DeMore et al., [1990]*) on the depletion of stratospheric ozone have identified chemical species that are classified as PORS. Several of these species can be identified as constituents in rocket plume exhausts, either in the primary exhaust stream, such as HCl, or as reaction products of the plume/atmospheric chemistry, such as NO_x and chlorine. One strategy to reduce the amount of PORS produced is to change or modify the exhaust stream composition by using alternate propellants. Propellant combinations can be identified which do not produce selected chemical species or modify the plume chemistry so that certain classes of chemical reactions, such as afterburning, do not take place. *Lewis et al., [1994]* has summarized (see Table 6-2) the ozone depletion effect to be mitigated (e.g., such as Cl₂ production); the method of mitigation (e.g., such as suppression of HCl reaction in the plume/atmosphere shear layer); the hardware implementation (e.g., change the solid propellant formulation by inclusion of

alkali salts); and an indication of the status of hardware technology. Each of the rows of the table is discussed below.

Table 6-2 Summary of Ozone Depletion Mitigation Approaches Utilizing Advanced Propellants

(Reference: Table 2.2-1 in Lewis et al., [1994])

Ozone Depletion Effect Mitigated	Method of Mitigation	Hardware Implementation	Hardware Technology Status
Reduce/Eliminate Cl ₂ Production	Suppress HCl Reaction in Shear Layer	Modify Existing Solid Propellant Formulations to Include Afterburning Suppressants	Modifying Solid Propellant Formulations-Operational Identification of Afterburning Suppressants-Study and Lab/Bench Scale
Remove HCl from Plume Exhaust	Utilize Other Propellants-Solid Propellants Without Chlorine, i.e. Replace AP with Nitrate or Carbonate Based Oxidizers	The Utilization of Alternate Propellants Requires Development of a New Engine System	Solid propellant oxidizers containing no chlorine have been test stand fired, although not at the thrust levels required for boost to LEO applications. There is a significant reduction in the I_{sp} .
	Conventional Liquids LOX/LH ₂ , LOX/RP-1		LOX/LH ₂ and LOX/RP-1 liquid rocket engine technology is flight demonstrated. It is currently not in production in this country for boost to LEO systems. It is in production in other countries in the world.
	Advanced Liquids based on Fluorine Oxidizers-LF ₂ /LH ₂ or LF ₂ /N ₂ H ₄ or Others		Advanced liquid propellants based on fluorine, F ₂ , ClF ₃ , ClF ₅ , FLOX and others, have been test stand fired in both the US and CIS. Turbo-pumped, upper stage engines have been developed and test stand fired in the CIS

Table 6-2 (Continued)
Summary of Ozone Depletion Mitigation Approaches Utilizing Advanced Propellants

(Reference: Table 2.2-1 in Lewis et al., [1994]).

Ozone Depletion Effect Mitigated	Method of Mitigation	Hardware Implementation	Hardware Technology Status
Removal of Al ₂ O ₃ to prevent ozone depletion due to heterogeneous chemical reactions	Advanced Solids Based on Fluorine Oxidizers - NF ₄ BF ₄ / PNF ₂ /B or Other Fuel	The Utilization of Alternate Propellants Requires Development of a New Engine System	Advanced solid propellants based on fluorine oxidizers have been fired as heterogeneous F ₂ gas generators in the US
	Advanced Gels Based on Conventional Oxidizers- i.e. HNO ₃ + LiNO ₃ + SiO ₂ (gel)/ MMH + Al (gel)		There have been considerable development of hybrids and gels, (although not with fluorine based oxidizers) in the US. Hybrids are flight demonstrated, gel propellants have been test stand fired, throttled and pulsed and may have achieved operational status for specific missions. None of these applications are at thrust levels necessary for boost to LEO missions. Gels and hybrids based on fluorine have not been developed
	Advanced Gels Based on Fluorine Oxidizers- i.e. F ₂ (gel)/ N ₂ H ₄ +B (gel)		
	Advanced Hybrids Based on Fluorine Oxidizers-i.e. F ₂ (gel)/ N ₂ H ₄ (liquid)		
	Utilize Other Propellants- Conventional Liquids LOX/LH ₂ , LOX/RP-1		LOX/LH ₂ and LOX/RP-1 liquid rocket engine technology is flight demonstrated. It is currently not in production in this country for boost to LEO systems. It is in production in other countries in the world.
	Advanced Liquids based on Fluorine Oxidizers- LF ₂ /LH ₂ or LF ₂ /N ₂ H ₄		Advanced liquid propellants based on fluorine, F ₂ , ClF ₃ , ClF ₅ , FLOX and others, have been test stand fired in both the US and CIS.
Advanced Solids Based on Fluorine Oxidizers - NF ₄ BF ₄ / PNF ₂ /B	Advanced solid propellants based on fluorine oxidizers have been fired as heterogeneous gas generators in the US		

Table 6-2 (Continued)
Summary of Ozone Depletion Mitigation Approaches Utilizing Advanced Propellants

(Reference: Table 2.2-1 in Lewis et al., [1994]).

Ozone Depletion Effect Mitigated	Method of Mitigation	Hardware Implementation	Hardware Technology Status
Removal of H ₂ O to prevent ozone depletion due to heterogeneous chemical reactions	Advanced Gels Based on Conventional Oxidizers- i.e. HNO ₃ + LiNO ₃ +SiO ₂ (gel)/ MMH+Al (gel)	The Utilization of Alternate Propellants Requires Development of a New Engine System	There have been considerable development of hybrids and gels, (although not with fluorine based oxidizers) in the US. Hybrids are flight demonstrated, gel propellants have certainly been test stand fired and may have achieved operational status for specific missions, although not at boost phase to LEO thrust levels. Gels and hybrids based on fluorine have not been developed.
	Advanced Gels Based on Fluorine Oxidizers- i.e. F ₂ (gel)/ N ₂ H ₄ +B (gel)		
	Advanced Hybrids Based on Fluorine Oxidizers-i.e. F ₂ (gel)/ N ₂ H ₄ (liquid) or Other Fuel.		
	Utilize Other Propellants. Advanced Liquids based on Fluorine Oxidizers- LF ₂ /LH ₂ or LF ₂ /N ₂ H ₄		
Removal of CO ₂ to prevent contribution to greenhouse gas production and global warming	Advanced Solids Based on Fluorine Oxidizers - NF ₄ BF ₄ / PNF ₂ /B or Other Fuel	The Utilization of Alternate Propellants Requires Development of a New Engine System	Advanced liquid propellants based on fluorine, F ₂ , ClF ₃ , ClF ₅ , FLOX and others, have been test stand fired in both the US and CIS.
	Utilize Other Propellants. Advanced Liquids based on Fluorine Oxidizers- LF ₂ /LH ₂ or LF ₂ /N ₂ H ₄		Advanced solid propellants based on fluorine oxidizers have been fired as heterogeneous gas generators in the US
	Advanced Solids Based on Fluorine Oxidizers - NF ₄ BF ₄ / PNF ₂ /B or other fuel		LOX/LH ₂ and LOX/RP-1 liquid rocket engine technology is flight demonstrated. It is currently not in production in this country. It is in production in other countries in the world. Advanced liquid propellants based on fluorine, F ₂ , ClF ₃ , ClF ₅ , FLOX and others, have been test stand fired in both the US and CIS.
			Advanced solid propellants based on fluorine oxidizers have been fired as heterogeneous gas generators in the US

Table 6-2 (Continued)
Summary of Ozone Depletion Mitigation Approaches Utilizing Advanced Propellants

(Reference: Table 2.2-1 in Lewis et al., [1994]).

Ozone Depletion Effect Mitigated	Method of Mitigation	Hardware Implementation	Hardware Technology Status
	Advanced Gels Based on Fluorine Oxidizers- i.e. F ₂ (gel)/ N ₂ H ₄ +B or other fuel (gel) Advanced Hybrids Based on Fluorine Oxidizers-i.e. F ₂ (gel)/ N ₂ H ₄ (liquid)		There have been considerable development of hybrids and gels, (although not with fluorine based oxidizers) in the US. Hybrids are flight demonstrated, gel propellants have been test stand fired and may have achieved operational status for specific missions, although not at boost phase to LEO thrust levels. Gels and hybrids based on fluorine have not been developed.

Table 6-3 Typical Mole Fractions Necessary to Achieve Afterburning Initiation

(Reference: Vanpee et al., [1964])

Afterburning Suppressant Chemical	Mole % Required in Exhaust Products to Halve the Duration of Afterburning
KF	0.048
KCl	0.031
K ₂ SO ₄	0.036
KNO ₃	0.024
LiF	0.410
KBr	0.041

6.5.1 Mitigation of Ozone Depletion by Reducing Cl Production

The first row in Table 6-2 considers existing solid propellant formulations. It has been mentioned that HCl is not by itself a concern, but rather the afterburning of HCl to produce Cl₂ in the plume/atmospheric shear layer is. This suggests that if afterburning in the shear layer could be suppressed, then Cl₂ production would be reduced or perhaps eliminated. Afterburning suppression was investigated by the plume physics community in relation to modifying the signatures of strategic missiles (*Simmons [1982]*). Several compounds have been demonstrated to reduce/suppress afterburning in small lab scale combustors and rocket engines (*Vanpee et al., [1964]*). Alkali salts, such as KF, KCl, K₂SO₄, KNO₃, LiF, LiCl (and others), present in small quantities (typically < 1%, see Table 6-3) in the exhaust stream scavenge H atoms which initiate the afterburning chain reaction, thus quenching one significant component of the afterburning reactions (*i.e., Lewis et al., [1994]*). This suggests that it may be possible to reformulate the

solid propellant by relatively small additions of afterburning suppressant chemicals that would prevent conversion of HCl into Cl₂ or Cl in the shear layer.

By mixing the afterburning suppressant chemicals into the solid propellant, a uniform distribution of the suppressant is achieved. Previous attempts to incorporate alkali salts into liquid rocket engines have not provided uniform distribution of the afterburning suppressant chemicals and were not completely successful (*Simmons [1982]*).

The technology status of solid propellants is operational and the modification of existing solid propellant formulations to obtain better performance is also operational. Potential afterburning suppressant chemicals have been identified in studies and lab/bench scale demonstrations (*Harpole et al., [1990]*, *Skinner et al., [1965]*, *Schott et al., [1958]*, and *Slack et al., [1989]*). There have been no demonstrations of the efficiency of afterburning suppressant chemicals added to AP based solid propellants under flow conditions similar to stratospheric pressure, temperature and ambient air composition.

6.5.2 Mitigation of Ozone Depletion by Removal of HCl

The second row of Table 6-2 lists removal of HCl as the next most severe implementation of alternate propellants in mitigating ozone depletion. By removing HCl as an exhaust stream effluent, the effects of Cl radical on ozone depletion are eliminated. Implementing this step has more severe launch system hardware ramifications than reformulating the solid propellant to include afterburning suppressants. A new rocket engine will have to be developed or re-manufactured and the engine will have to be integrated into the launch system. Several potential alternate propellants have been identified; solid propellants that do not contain chlorine, conventional liquid propellants such as LOX/LH₂ or LOX/RP-1, liquid propellants based on fluorine based oxidizers, solid propellants based on fluorine, and gelled and hybrid propellants based on conventional acid oxidizers or fluorine. The hardware technology status of these approaches is discussed in Section 6.3.5.

The use of conventional liquid propellants is attractive in that concerns about HCl effects on ozone are eliminated. The engineering of rocket engines utilizing conventional liquid propellants is well understood and these engines have a history of operational success. These types of propellants produce CO₂, CO, H₂ and H₂O as combustion products. It is possible that thermal NO_x is formed as a consequence of afterburning in LOX/RP-1 systems. *Lewis et al., [1994]* concluded that this has a small effect on ozone depletion. There are continuing concerns and evolving understanding about the importance of H₂O condensation forming sites for heterogeneous ozone depletion chemistry in the plume. However, should it be case that HCl must be removed from the propellants, launch systems based on conventional liquid propellants are a credible alternative. Even if it is the case that conventional liquids are ultimately unsatisfactory due to heterogeneous ozone depletion due to H₂O, launch systems based on conventional liquids are the only demonstrated technology available in the near term (i.e., < 5 years) which could conceivably replace conventional AP based solid propellants. While LOX/rubber hybrids are also potentially credible, they do not have the operational history that

conventional liquid systems do. The same concern could be raised regarding gel propellants that are based on nitric acid oxidizers. All of these carbon/hydrogen/nitrogen/oxygen systems produce some amount of NO_x that has been identified as a PORs. The NO_x can be produced either in the engine or in reactions in the atmospheric shear layer.

6.5.3 Mitigation of Ozone Depletion by Removal of Al₂O₃ and H₂O

The next two rows of Table 6-2 will be discussed together. These ozone depletion mitigation techniques are the next most severe and involve removing either or both H₂O and Al₂O₃ from the rocket exhaust effluent stream. The concern about H₂O is that upon condensation, water forms sites for heterogeneous ozone depleting reactions. The same concern can be raised about Al₂O₃. Because Al₂O₃ particles are generated as a distribution of sizes in the rocket engine combustion chamber, the smaller particles in the distribution can serve as sites for heterogeneous ozone depletion chemistry. Likewise, liquid Al₂O₃ can condense in rocket plumes and form sites for heterogeneous ozone depletion reactions.

Conventional liquid propellants are potential launch system implementations that eliminate Al₂O₃ only. If it is necessary to eliminate both Al₂O₃ and H₂O then advanced oxidizers will be required. Fluorine is prominent as a high performance oxidizer that forms combustion products such as HF which are not PORs. HF is stable, with a strong H to F bond and has a low photolytic cross section. On the other hand, there are severe materials compatibility issues when using fluorine, and fluorine is highly toxic. It is not likely that liquid fluorine would be considered as a credible oxidizer in a launch system. There are solid propellants available using fluorine oxidizers that may be attractive. Oxidizers that are fluorine-based (e.g., NF₄BF₄) have been identified and fired as F₂ heterogeneous gas generators, and fluorine based rubbers (e.g., PNF₂) have been known for decades. While much technology work has been done on the elements of a solid propellant motor using fluorine based oxidizers, considerable development is still required to field a boost-to-LEO fluorine based propulsion system (*Lewis et al., [1994]*).

6.5.4 Mitigation of Ozone Depletion by Removal of CO₂

While CO₂ is not an ODS, there is continuing discussion in the scientific community about the importance of greenhouse gases on global warming, so mitigation of greenhouse gases by removal of CO₂ is considered. If it is concluded that CO₂ content in the plume should be minimized, and that HCl must be removed and heterogeneous ozone depletion reactions are not a concern (so H₂O as an effluent species is acceptable), then conventional LOX/LH₂ propellants are adequate. It is possible that thermal NO_x can be created from LOX/LH₂ combustion in the afterburning shear layer (See Section 3). *Lewis et al., [1994]* concluded that this had a small effect on ozone depletion. As mentioned previously, this type of technology is mature, although currently is not in production in the U. S. at the necessary boost phase thrust levels.

If HCl, H₂O, and CO₂ all must be removed from the exhaust stream, the oxidizers based on fluorine must be considered. As mentioned above advanced launch systems based on liquid

fluorine are unlikely for safety related reasons, but solid, gelled and even hybrid systems using fluorine oxidizers are acceptable alternatives for reducing ozone depletion.

6.5.5 Hardware Technology Status

Afterburning suppressants have been demonstrated in lab/bench scale tests studies as well as in studies (*Simmons [1982]*, *Vanpee et al., [1964]*, *Chou et al., [1991]*, and *Lewis et al., [1989]*). *Lewis et al., [1994]* cited demonstrations on small liquid engines using salt rods placed in the combustion chamber (*Simmons [1982]*), and presented data on a number of lab tests tabulating the efficiency of compounds as to their ability to inhibit after-burning initiation (*Vanpee et al., [1964]*). Furthermore, afterburning shutdown by ox/fuel (i.e., O/F) variation was demonstrated by eliminating the formation of H atoms (*Chou et al., [1991]*). *Lewis et al., [1989]* presented calculations on several advanced propellant concepts, such as $\text{LF}_2/\text{N}_2\text{H}_4$ and gelled ClF_5 with gelled N_2H_4 metals, which do not afterburn, if the O/F ratio is equal to 1 and the nozzle exit plane temperature is sufficiently low. All lab/bench and test stand demonstrations have been at much lower thrust levels than those required of boost to LEO systems.

Of all the approaches listed in the Table 6-2, reformulated conventional solid propellants with afterburning suppressants will have the least overall impact at the launch system level, supposing that suitable afterburning suppressants can be identified. Should a conventional solid propellant with suppressants be fielded successfully, and the new propellant placed in a new booster engine, the change is transparent to the user infrastructure, if there is no substantial degradation of the I_{sp} . Given that the mass fractions of afterburning suppressants would very likely be small, a few mass percent typically, the effect on I_{sp} should be minimal.

Solid propellant oxidizers containing no chlorine have been contractor developed under USAF sponsorship and test stand fired (at AFRPL/AFAL, now the Phillips Lab, Edwards AFB). These firings were successful, although not at the thrust levels required for boost to LEO applications. There is a significant reduction in the I_{sp} in replacing perchlorate oxidizers with nitrate/carbonate formulations. While it is credible that such formulations could be scaled to booster-sized thrust levels, these boosters would be of different sizes than the solids of today because of the reduced I_{sp} . In any event this would be a major engine development effort. The HCl would be removed from the plume exhaust. However, H_2O and Al_2O_3 would remain with any attendant environmental concerns related to those species.

Advanced liquid propellants based using fluorine-based oxidizers, such as F_2 , ClF_3 , ClF_5 , FLOX, ClOF_3 and others, have been test stand fired in both the U.S. and the Commonwealth of Independent States, CIS. Even the RL-10 has been fired with FLOX/ CH_4 and F_2/H_2 (*Brown [1993]*). Through the late 1960s and early 1970s test stand firings using these advanced oxidizers were not uncommon. The attraction of fluorine based oxidizers has always high performance, with specific impulse values in the range of 370 to 400+ seconds depending on the engine configuration; chamber pressure, ox/fuel selection, O/F ratio and expansion ratio. This propellant technology fell out of favor in the U.S., given the stringent materials compatibility, and safety and handling requirements associated with fluorine. CIS has continued to develop

20 klbf turbo-pumped upper stage engines utilizing LF_2 and NH_3 fuel. 'Energomash' was the engine developer. The engine I_{sp} was about 400 seconds. This design was ultimately test stand fired but never incorporated into operational systems. The use of fluorine as a flow medium for high power HF/DF chemical lasers provided the motivation to continue to develop materials compatibility and handling technology in the U.S. However, the handling procedures necessary for the safe utilization of liquid fluorine based oxidizers probably preclude them from use in boost to LEO systems. However, utilization of fluorine in some other form, such solid or gelled F_2 , may be attractive, since both solid and gels are in wide use today, and the safety and handling procedures are well understood. It is a fact that gels have such attractive handling characteristics that they have been classified as insensitive propellants.

The combustion products in the plume exhaust of fluorine based oxidizers contain HF and H_2 for LF_2 oxidizer and N_2H_4 , NH_3 or LH_2 (or slush H_2) fuel. Given that a goal of moving to alternate propellants is to remove HCl from the exhaust stream ClF_3 and ClF_5 and other chlorine containing oxidizers would be not be acceptable (*DeMore et al., [1990]*). At this time, HF is not identified as an ODC, because it is stable molecule in the atmosphere and does not actively participate in ozone depletion chemistry. Its bond strength is high and photolytic cross section small. Because it may be desirable to reduce the amount of HF and/or F_2 injected into the atmosphere operation at low O/F ratio may be necessary. While this does decrease the I_{sp} to around 300 seconds at O/F of about 1, the amount of HF is reduced by about 50%. Low O/F operation raises the question of afterburning the H_2 into H_2O , and if this can be prevented.

Advanced solid propellants based on fluorine oxidizers have been fired as heterogeneous F_2 gas generators in the U.S. To be a credible solid propellant it is necessary to identify an oxidizer, fuel, and binder. There are several oxidizers available, the most attractive being NF_4BF_4 . Fluorine-based rubbers, such as PNF_2 , are well known. Given that an oxidizer and binder are available a heterogeneous solid propellant utilizing a metal fuel is a natural development. These elements were incorporated into a solid propellant gas generator using NF_4BF_4 with Al fuel, which was used to generate F_2 , on the MADS (Modular Array Demonstration Program), a U.S. Army laser development program. While it is true that no rocket engines of any substantial thrust have been developed using solid fluorine based oxidizers, there is sufficient previous technology development to suggest that it could be done. Thermochemical calculations based on estimated enthalpy of formation for NF_4BF_4 yield I_{sp} estimates 300 seconds with an exhaust stream containing no particulate or condensed phase material.

Hybrids and gels have undergone considerable development, (although not with fluorine based oxidizers) in the U.S. Hybrids are flight demonstrated. The HASP drones used liquid acid oxidizer with fiberglass fuel, and AMROC in Camarillo, CA has developed LOX oxidizer/rubber fuel launch vehicles that have been test stand fired but, as yet, never launched. Gelled propellants also have a long development history. Gelled rocket engines have been test stand fired at the 15 klbf thrust range, throttled by factors of 10 in chamber pressure and pulsed to 4-6 msec. Gelled engine designs are part of U.S. Army missiles currently under development (*Anon [1994]*) and gel engines have been developed for USAF sponsored ejection seat programs. There has been considerable technology development and test stand firings, but none has occurred at thrust levels sufficiently high for boost to LEO applications. Gels based on fluorine based

oxidizers have not been developed. The same observation can be made for hybrid systems, but the case for liquid fuel with solid fluorine based oxidizers is stronger. The fluorine oxidizer, NF_4BF_4 and fluorine based rubber binder, PNF_2 are demonstrated. The elements of a potentially successful hybrid exist but have never been integrated into a propulsion system.

Rocket engine performance is always a consideration in the design of boost to LEO systems. Liquids generally offer higher I_{sp} values over a wide range of O/F ratios. This is desirable, since it has been demonstrated in lab scale tests that rocket engine operation under fuel rich conditions reduces flame temperatures and H atom concentrations. These features enable afterburning shutdown under simulated stratospheric altitude conditions, (about 25 km). Depending on the alternate propellant type considered, there may be either an I_{sp} performance decrease or increase. The conventional liquid, LOX/RP-1 at O/F=1.6 with an I_{sp} =320 seconds shows a slight performance decrease relative to the solid propellant. Though not shown on the chart, solid propellants with nitrate or carbonate oxidizers have generally lower I_{sp} values. Propellants utilizing cryogenic oxidizers such as LOX/LH₂ or LF₂/N₂H₄ at O/F~1 have I_{sp} values greater than 370 seconds. Finally, LOX/LH₂ engines are well known and have high I_{sp} , but low density implying large propellant volumes.

6.6 Development and Scale-Up of a Reduced HCl Propellant

Although previous modeling, laboratory, and *in-situ* studies (refer to Sections 3, 4, and 5, respectively) have concluded that rocket exhaust plumes have very little environmental impact, the possibility remains that some of the exhaust species from current space launch and ICBM boosters will be regulated in the future. The two major environmental issues which have been raised are the impact of acidic species, in particular HCl, on the local environment around the launch or test site, and the impact of chlorine containing species on the stratospheric ozone layer. Thiokol introduced the Reduced HCl Program, which was designed to investigate the properties of both low HCl and non-chlorine propellants. This section will describe their efforts.

A new family of Class 1.3, reduced HCl solid propellants for booster applications has been developed by Thiokol and demonstrated in a full scale mix and an 800 lbf BATES motor (*Bennett et al., [1998]*). It was determined that, as a minimum requirement, the propellant must be Class 1.3, the principal requirement of which is that the propellant be less than 70 cards in an NOL large gap test (*Bennett et al., [1998]*). The majority of this Thiokol propellant study was based on a nitrocellulose binder (TEPAL), while a second based on a PGN binder was carried along as a backup. TEPAL is an acronym for Thiokol Environmental Plastisol Propellant containing Aluminum. Its binder system consists of pelletized nitrocellulose (PNC), swelled by a plasticizer. Unlike a conventional chemically cured propellant, in which a relatively low molecular weight pre-polymer is chemically cross-linked to provide the required mechanical properties, TEPAL utilizes a physical cure in which the already high molecular weight PNC molecules become entangled and associated through hydrogen bonding. This technology has the advantage of omitting the bulk of the curative, and hence the bulk of the moisture concerns. Nitrocellulose has often been used for propellants in the past, but in those cases, the propellant

was generally made within the case, with plasticizer levels such that the propellants are rather hard and exhibit low performance and/or high detonability.

Initially this program planned two major propellant approaches to reducing the HCl content of the rocket exhaust plumes. The original primary approach was to use sodium nitrate and ammonium perchlorate (AP) as co-oxidizers. The sodium ions produced during the combustion of the sodium nitrate acted as chlorine scavengers, preventing the formation of HCl. The major drawback of this approach was the low specific impulse (I_{sp}) inherent with sodium nitrate oxidized propellants. A number of materials were considered for evaluation on this program. The ingredients evaluated and their function as used in a solid propellant are given in Table 6-4.

Thiokol selected these ingredients on the basis of performance potential, past experience, availability, chlorine content, and cost. Sodium nitrate and potassium perchlorate were eliminated on the basis of poor performance, and, in the case of KP, chlorine content. HMX and other nitramines were eliminated on the basis of high detonability. Inert polymers were eliminated because of low impulse and low density. BTTN was determined to be too detonable in these formulations, and CDN decreased mechanical properties with no measurable improvement in hazards. PGN was eventually eliminated because of poor mechanical properties and cure problems. BuNENA was not used in the full-scale mix for the reason discussed below, but continues to be a promising material in metallized systems (*Bennett et al., [1998]*).

The theoretical performance calculations of Bennett *et al., [1998]* revealed that TEPAL propellants were capable of specific impulse values in excess of 264 lbf-sec/lbm, which was about 2 seconds higher than Space Shuttle propellant, while still remaining Class 1.3. These values were obtained by using BuNENA as a plasticizer (see Table 6-4), about 40 percent ammonium nitrate oxidizer, and 22 - 24 percent aluminum fuel. Unfortunately, the maximum theoretical performance values could not be achieved in a practical sense because ammonium nitrate (AN) combusts aluminum rather poorly. For comparison, an alternate fuel (e.g., magnesium) needed to be incorporated into the formulation. However, so long as there was sufficient oxygen present to fully combust the metal, the use of aluminum was preferred over the use of magnesium. While BuNENA did provide the TEPAL propellant with the greatest I_{sp} in a Class 1.3 formulation, the plasticizer eventually selected for the full-scale mix was TEGDN (Table 6-4). This selection was made on the basis that TEGDN had better mechanical properties, a higher burn rate capability, a greater density, a lower cost and better availability, and more consistent properties.

Finally, Bennett *et al., [1998]* determined that the target burn rate for the full scale mix was 0.40 ips at 1000 psi, which was roughly equivalent to the burn rate of the Castor 120 propellant. Ammonium nitrate propellants typically have burn rates well below that value, particularly in low energy binders. Additionally, AN propellants have little margin to be tailored in a ballistic sense and have rather high burn rate pressure exponents. Two different supplemental oxidizers/ballistic additives were investigated: KDN and AP. KDN had the advantage of being energetic, dense, and chlorine free. Not only does it act as a ballistic additive, but also it stabilizes the unwanted AN phase transition which normally occurs at slightly elevated

temperatures. Its major disadvantages for this Thiokol study were its immaturity, cost, and availability.

Table 6-4. Ingredients Considered for Use in Reduced HCl Propellants

(Reference: Bennett *et al.*, [1998])

Material	Use
Ammonium Nitrate (AN)	Non-Chlorine Oxidizer
Sodium Nitrate	Non-Chlorine Oxidizer
Ammonium Perchlorate (AP)	Chlorine Containing Oxidizer
Potassium Perchlorate (KP)	Chlorine Containing Oxidizer
Cyclotetramethylene tetranitramine (HMX)	Energetic Nitramine Additive
Hexanitrohexaazaisowurtzitane (CL-20)	Energetic Nitramine Oxidizer
Potassium Dinitramide (KDN)	Energetic AN Stabilizer/Ballistic Modifier
Nitrocellulose (NC)	Energetic Polymer
Polyglycidyl Nitrate (PGN)	Energetic Polymer
Polyethylene Glycol (PEG), other polyethers	Inert Polymer
Glycidyl Azide Polymer (GAP)	Energetic Polymer
Hydroxy Terminated Polybutadiene (HTPB)	Inert Polymer
Cyclodextrin Nitrate (CDN)	Energetic Additive
Butanetriol Tinitrate (BTTN)	Energetic Nitrate Ester Plasticizer
n-butyl-2-nitrateethyl-nitramine (BuNENA)	Energetic Nitrate Ester/Nitramine Plasticizer
Triethyleneglycol Dinitrate (TEGDN)	Energetic Nitrate Ester Plasticizer
Triacetin	Inert Plasticizer
Isophorone Diisocyanate (IPDI)	Curative
Desmodur N-100	Curative
Aluminum	Fuel
Magnesium	Fuel
Methylnitroaniline (MNA)	Nitrate Ester Stabilizer
2-Nitrodiphenylaniline (2-NDPA)	Nitrate Ester Stabilizer

Although it would be necessary to conduct further studies to identify the source of the mechanical property inconsistencies observed during its development, TEPAL propellant has been demonstrated to be a feasible approach to reducing the HCl output of a solid rocket motor. When optimized, Bennett *et al.*, [1998] reported the mechanical properties of TEPAL propellant as excellent, with high stress and strain capabilities over a wide range of temperatures and rates. The ballistic properties were shown to be consistent and capable of matching those of typical Castor 120 propellant. The propellant could be processed in a production scale mixer with adequate working life. Several Class 1.3 formulations have been demonstrated. One of these formulations was selected (i.e., TEGDN) and successfully demonstrated in the full-scale mixer and in an 800 lbf BATES motor static test. In short, the propellant performance was in the range expected for this type of test vehicle.

6.7 Liquid Versus Solid Fuel Comparisons

The nominal 720 klb and 810 klb class engines were analyzed for the LH₂/LOX and RP-1/LOX systems, respectively (Lewis et al., [1994]). The total mass flow rate from the solid rocket exhaust was observed as a function of downstream location of the plume. The presence of an afterburning region where CO is converted into CO₂, H₂ into H₂O, and more importantly HCl into Cl₂ or Cl radical, was found. This region extended about 3000 feet (i.e., ~ 0.9 km) downstream beyond which no significant chemical reaction occurred. From a local ozone depletion standpoint, the formation of Cl₂ from HCl in this region was significant because Cl₂ photodissociates into Cl readily in the presence of sunlight, which in turn can contribute to the depletion of local ozone through the Cl catalytic cycle. The concentration of nitric oxide remained fixed to the level in the combustion chamber and no additional NO was formed in the afterburning region where the temperature was relatively low. In addition, OH was consumed completely in reactions involving H₂ or CO.

The centerline concentrations of the exhaust species as a function of downstream locations for the LH₂ /LOX system were analyzed. Because of the fuel-rich condition, H₂ appeared as a combustion product in the exhaust and provided the necessary fuel to sustain chemical reactions in the afterburning region. The level of NO formed in the afterburning region was extremely low, about 1 ppb; and upon dilution with entrainment of ambient air, the level dropped to 10⁻³ ppb.

In addition, the centerline species concentration profiles for the RP-1/LOX system revealed a low production of NO in the afterburning region. In fact, the level of NO was almost one order of magnitude lower than that of the LH₂ /LOX system. Again because of the fuel-rich conditions, CO appeared as an exhaust product that was oxidized quickly into CO₂. Table 6-5 summarizes the production of PORS for the rocket system under consideration.

Table 6-5 Comparison of PORS Production from Liquid and Solid Engines (in kg s⁻¹)

(Reference: Lewis et al., [1994])

PORS	Solid	LH ₂ /LOX	RP-1/LOX
HCl	200	0.0	0.0
Cl _y	750	0.0	0.0
NO _x	7.0	10 ⁻⁶	10 ⁻⁶
HO _x	1	10 ⁻³	10 ⁻³
H ₂ O	800	757	380

For comparison purposes, Table 6-5 present effluent calculations for the bipropellant systems considered and for the emissions from a SRM launch vehicle. It is evident that the solid rocket system produces more potential ozone reactive species than either liquid bipropellant

system. Aside from greenhouse gas considerations, the RP-1/LOX system is more benign than the LH₂/LOX system. Finally, it should be noted that RP-1/LOX systems tend to burn on the rich side. Generally, motors do not burn as cleanly as nozzle model codes implicitly assume (i.e., clean-burning fuels in the sense that fuel and oxidizer are assumed to be mixed completely in the combustion chamber and brought to thermodynamic equilibrium before nozzle expansion), and the effects of incomplete combustion may be significant (*Zittel [1995]*). This RP-1/LOX system also has the potential for formation of carbon soot in the exhaust, which may provide active sites for heterogeneous ozone conversion. None of the models thus far have been able to characterize this potential soot formation (*Lewis et al., [1994]*).

Brady *et al.*, [1997] used a chemical kinetics model to estimate the impact of a variety of launch vehicles; a Titan IV and IIIB, a Delta core, and an SSME (See Table 6-6). Brady *et al.*, [1997] concluded that there is not a significant difference between the LOX vehicles, and they destroyed the least amount of stratospheric ozone. Solid propellants were analyzed too and those not containing chlorine were found to destroy between 3 and 20 times as much ozone depending on the dispersion rate used. The largest ozone impact is from solid rocket motors when the effects of chlorine are included; these destroy between 3 and 200 times as much ozone as the T3B, depending on the dispersion and time-scale used. The T3B, which contains the NTO oxidizer discussed in Section 6.2.3, was found to destroy the most ozone if only NO_x destruction mechanisms were considered.

Table 6-6 Launch Vehicles Modeled in Brady *et al.*, [1997]

Vehicle	Thrust (klbf)	Fuel	Oxidizer
Titan IV (SRB or SRM)	~ 1,600	PBAN, HTPB	NH ₄ ClO ₄ (68%) Al (16-19%)
Titan IIIB (T3B)	520	A-50	NTO
Delta (Core)	270	RP-1	LOX
Space Shuttle Main Engine (SSME)	520	LH ₂	LOX

Because of the predominance of Cl_y deposition, and to a lesser extent because of the production of NO, the impact on local ozone reduction was significant for the solid propellant system. The presence of a local ozone hole easily could be seen and it lasted for as much as 2000 seconds; about 60% of the depletion occurred in a hole with a radius of approximately 1000 meters (*Lohn et al., [1996]*). As much as 10²¹ molecules of ozone potentially could be lost. Judging from the liquid system calculations, diffusion accounted for only 50 seconds of the time. Therefore, a significant amount of ozone must have been consumed. Considering 100 launches per year of any ammonium perchlorate (AP) based solid rockets, traveling through approximately 25 km distance of the stratosphere, this translates into an approximately 0.00001 % loss of the total ozone concentration (*Lohn et al., [1996]*).

In short, the liquid bipropellant system exhibited no deleterious effect on the environment. However, current analyses have not included the potentially harmful effect due to large deposition of H₂O vapor or droplets into the basically dry stratosphere. The ozone depletion potential may be identified from two sources: namely, heterogeneous reaction on droplet surfaces in the form of polar stratospheric clouds commonly found in Antarctica; or homogenous reactions according to the OH catalytic cycle, particularly in the upper stratosphere where the abundance of O₂(¹Δ) can convert H₂O into OH radicals.

6.8 Future U.S. Launch Vehicle Programs and Propellant Usage

The United States Government has pushed for the development of the next generation of launch vehicles in an effort to make space access more affordable, while increasing reliability and operability, and minimizing the effects on the environment. Three of these next generation launch programs are the Sea Launch Limited Partnership (SLLP), the Evolved Expendable Launch Vehicle (EELV), and the Reusable Launch Vehicle Programs (i.e., X-33 and VenturestarTM). These programs were designed to replace the more costly and aging Titan, Atlas, and Delta programs.

6.8.1 Sea Launch Limited Partnership (SLLP)

The Sea Launch Limited Partnership or SLLP is an international commercial venture formed with the objective of launching commercial satellites. The partnership members consist of Boeing Commercial Space Company of the United States; RSC Energia of Russia; KB Yuzhnoye of the Ukraine; and Kvaerner Maritime of Norway.

SLLP proposes to conduct commercial space launch operations from a mobile, floating platform in international waters in the east-central equatorial Pacific Ocean. It would provide a commercial alternative to launching satellites from Federal installations within the continental United States. The proposed Sea Launch activities would make available infrastructure for placing telecommunications, scientific, and research payloads in equatorial low earth orbit (LEO), geosynchronous earth orbit (GEO), geosynchronous transfer orbit (GTO) or medium earth orbit (MEO). The Russian built Zenit-3SL expendable launch vehicle (LV) is fueled by LOX/RP-1 and would be the only launch vehicle used at the Sea Launch facilities (*FEAFSLP [1999]*).

SLLP conducted its first demonstration payload launch in March 1999. Two satellites are scheduled for launch during its first year of operation; six launches are proposed for each subsequent year (*FEAFSLP [1999]*). The lifetime of the Sea Launch system would be limited by the useful life of the launching platform or LP, which is estimated to be twenty years. The high-speed movement of the Zenit-3SL rocket and the re-entry of the stages after their use may impact stratospheric ozone. This will be discussed in the next section.

6.8.1.1 Sea Launch Atmospheric Emissions

Downrange from the launch location, the mass and energy of the rocket's emissions into the atmosphere are functions of velocity and rate of combustion. Atmospheric effects caused by the flight of the Sea Launch rocket would arise from two factors: the combustion of onboard fuel stocks (Table 6-7) with the associated emissions of gases and particulate matter (Tables 6-8 through 6-10), and the physical passage of the LV through the atmosphere. Consumption and emissions quantities listed in Tables 6-8 through 6-10 are based on normal trajectory without payload weight and fuels. Altitude ranges have been rounded to the nearest kilometer.

Table 6-7 Sea Launch Zenit-3SL Fuel Profile*

(Reference: FEAFSLP [1999])

Fuel Type	Stage 1	Stage 2	Upper Stage (Block DM-SL)
LOX	235,331 kg	58,703 kg	10,543 kg
Kerosene	89,773 kg	22,950 kg	4,325 kg
N ₂ O ₄ /MMH	n/a	n/a	95 kg

* Does not include payload fuels

Table 6-8 Zenit-3SL Kerosene-LOX

(Reference: FEAFSLP [1999])

Altitude Range (km)	Propellant Consumed (kg)	Emission Products (kg)			
		CO	CO ₂	H ₂	H ₂ O
0.0 – 2.0	61,714	17,033	26,907	432	17,342
2.0 – 10.0	69,100	19,072	30,128	484	19,417
10.0 - 51.0	158,831	43,837	69,250	1,112	44,632
51.0 – 292	124,697	33,987	55,508	991	34,226
Total	414,342	113,929	181,793	3,019	115,616

The Zenit rocket emissions released in the stratosphere would consist of Stage-1 fuel combustion byproducts. In general, rocket exhaust components that may play a role in ozone destruction are chlorine compounds, nitrogen compounds, and hydrogen compounds. As shown in Tables 6-8 through 6-10, there would be no chlorine or chlorine compounds released during Stage-1 burn.

Table 6-9 Solid Fuel Separation Rockets (end of first stage)*(Reference: FEAFLP [1999])*

Altitude Range (km)	Propellant Consumed (kg)	Emission Products (kg)					
		CO	CO ₂	H ₂	H ₂ O	N ₂	Pb
0.0 – 2.0	0	0	0	0	0	0	0
2.0 – 10.0	0	0	0	0	0	0	0
10.0 - 51.0	0	0	0	0	0	0	0
51.0 – 292	105	40.5	14.8	21.5	12.3	15.8	0.1
Total	105	40.5	14.8	21.5	12.3	15.8	0.1

Table 6-10 Upper Stage Attitude Control/Ullage Motors (places payload in correct orbit)*(Reference: FEAFLP [1999])*

Altitude Range (km)	Propellant Consumed (kg)	Emission Products (kg)				
		CO	CO ₂	H ₂	H ₂ O	N ₂
0.0 – 2.0	0	0	0	0	0	0
2.0 – 10.0	0	0	0	0	0	0
10.0 - 51.0	0	0	0	0	0	0
51.0 – 292	57	2.0	5.5	2.8	26.2	20.5
Total	57	2.0	5.5	2.8	26.2	20.5

Due to nitrogen compounds in the exhaust trail of liquid propellant rockets like the Zenit-3SL, models predict a substantial, temporary reduction of ozone. However, recovery to near background levels occurs within a few hours. Again, satellite observations by the Nimbus 7 Total Ozone Mapping Spectrometer have shown no detectable reduction of ozone over the area around Kennedy Space Center several hours to one day after a Space Shuttle launch (*Syage et al., [1996]*). Models and measurements of other space systems comparable to Sea Launch indicate these impacts are temporary, and the atmosphere is capable of replacing by migration or regeneration the destroyed ozone within a few hours (*AIAA [1991]*, *Harwood et. al., [1991]*, *Brady et al., [1997]*, *Lohn [1994]*). The bulk of the atmospheric effects are due to mixing of the rocket exhaust constituents with the ambient air (*McDonald et al., [1995]*). *Tishin et al., [1995]* reported that the actual volume where ozone depletion (to a level less than or equal to 90% of background) occurs for a typical Russian rocket, similar to the Zenit-3SL rocket, is a cylinder with an estimated radius of approximately 360 m along the rocket trajectory in the stratosphere (*FEAFLP [1999]*).

Table 6-11 Ozone Destruction by Chemical Compounds

(Reference: *FEAFSLP [1999]*)

Chemical Compound	Ozone Destruction Contribution	Portion Attributable to ALL Rockets
Nitrogen Oxides	32 %	0.0005 %
Hydrogen/Hydroxyl	26 %	0.0012 %
Oxygen	23 %	< 0.00005 %
Chlorine	19 %	0.032 %

Table 6-11 (derived from *McDonald et al., [1995]*) shows the relative impact on ozone destruction due to the principal classes of ozone destroyers. Specifically, the portion of the impact attributable to rocket launches is less than 0.034%. From these data, it can be seen that in relative terms, chlorine releases constitute the greatest impact of rocket emissions worldwide. Since the Zenit-3SL vehicle would not be releasing chlorine or chlorine compounds, it is concluded that the Sea Launch program would have no significant impact on the global ozone layer (*FEAFSLP [1999]*). This is consistent with conclusions reached by Russian scientists (*Tishin et al., [1995]*).

6.8.2 Evolved Expendable Launch Vehicle (EELV)

The EELV launch system is designed to satisfy the U.S. governments planned launch requirements while reducing the expected costs of those launches by at least 25 percent (*EELV [1998, 1999]*). Two versions of the EELV are currently under development. In October 1998, the United States Air Force (USAF) awarded a contract to Lockheed Martin Corporation to complete development of its EELV, named Atlas V, and approved nine launches. Simultaneously, the USAF awarded the Boeing Company a development contract for their version of the EELV, the Delta IV launch vehicle for nineteen missions between 2002 and 2006.

In 1998, a Final Environmental Impact Statement, Evolved Expendable Launch Vehicle Program (*EELV [1998]*) was prepared to evaluate the impacts associated with the development and operation of the Evolved Expendable Launch Vehicle (EELV) systems. That action included replacing the Atlas IIA, Delta II, and Titan IVB launch vehicles in the National Executable Mission Model. The primary requirement of the EELV program is to provide the capability for lifting medium (2,500 to 17,000 pounds) and heavy (13,500 to 41,000 pounds) satellites into a variety of different orbits through the year 2020. The EELV program provides the capability to launch unmanned National Security, National Aeronautics and Space Administration (NASA), and commercial payloads into orbit. Subsequent to the publication of the FEIS (*EELV [1998]*), both EELV program launch vehicle contractors have proposed in the 1999 draft Supplemental Environmental Impact Statement, SEIS (*EELV [1999]*), the use of solid-propellant strap-on rocket motors as an economical way to bridge the gap between their respective medium-lift vehicles (MLVs) and heavy-lift vehicles (HLVs).

The Proposed Action of the SEIS (*EELV [1999]*) is to allow use of launch vehicles with up to five strap-on SRMs. Lockheed Martin proposes adding up to five strap-on SRMs to the current Atlas V MLV, while Boeing proposes a Delta IV MLV with two or four SRMs that are larger than those proposed in the 1998 FEIS. Both Atlas V and Delta IV systems with added SRMs would be designed so that all configurations could be launched from both Cape Canaveral AS in Brevard County, Florida, and Vandenberg AFB in Santa Barbara County, California. The Proposed Action would provide an intermediate-lift launch capability between the EELV medium- and heavy-lift variants that should increase the market capture of space launches by EELV vehicles, and could potentially address government mission requirements.

Both selected companies are streamlining procedures and processes while embracing the Department of Defense’s goals of more insight versus oversight and allowing use of commercial-based business practices where prudent and cost effective. The impact of these two EELV programs on stratospheric ozone will be discussed in the following section.

6.8.2.1 Individual EELV Atmospheric Emissions

A detailed analysis of the emissions from these vehicles may be found in *EELV [1998]* and *EELV [1999]*. A brief review is presented below. For the purpose of the emissions analyses, the assumption was made that the vehicle configurations representing the upper bound to atmospheric emissions are the Atlas V with five SRMs attached and the Delta IV with four GEM 60 SRMs attached. Illustrated in Table 6-12 are the flight travel times through the layers of the atmosphere for the LEO and GTO trajectories for the Delta IV M+ (5,4) and Atlas V 551/552 vehicles.

Table 6-12. Flight Trajectory Times for Atlas V 551/552 with Five SRMs and for Delta IV M+ (5,4)

[Table Compiled from Reference EELV [1999]]

Atmospheric Layer Designation	Layer Elevation (feet)	Atlas V 551/552 With Five SRMs		Delta IV M+ (5,4)	
		CCAS Trajectory (GTO) (seconds)	VAFB Trajectory (LEO) (seconds)	CCAS Trajectory (GTO) (seconds)	VAFB Trajectory (LEO) (seconds)
Lower Atmosphere	0 to 3,000	14.5	14.2	14.5	13.4
Free Troposphere	3,000 to 49,000	84.6	85.2	88.0	86.2
Stratosphere	49,000 to 164,000	113.4	113.5	129.2	126.2

GTO = Geosynchronous Transfer Orbit

LEO = Low-Earth Orbit

CCAS = Cape Canaveral Air Station, Florida

VAFB = Vandenberg Air Force Base, California

The amount of particulate, NO_x, and Cl_x emitted into specific altitude regions are shown in Table 6-13. At approximately 125,000 feet in altitude, the solid motors would burn out in both EELV platforms and later would be jettisoned from the vehicle. Therefore, the solid motors would not burn all the way through the stratosphere.

Table 6-13. Summary of Atlas V and Delta IV Flight Emissions into the Upper Atmospheric Layers (tons per launch).

{Table Compiled from Reference EELV [1999]}

Lift Vehicle/Atmospheric Layer	Particulate^a	NO_x^b	Cl_x^c
Atlas V 300/400			
Free Troposphere	0.0	0.61	0.0
Stratosphere	0.0	0.0035	0.0
Atlas V 551/552			
Free Troposphere	41	0.75	21
Stratosphere	30	0.028	15
Atlas V Heavy			
Free Troposphere	0.0	1.8	0.0
Stratosphere	0.0	0.010	0.0
Delta IV M			
Free Troposphere	0.0	0.28	0.0
Stratosphere	0.0	0.0035	0.0
Delta IV M+ (5,4)			
Free Troposphere	26	0.49	13
Stratosphere	12	0.014	16
Delta IV H			
Free Troposphere	0.0	0.83	0.0
Stratosphere	0.0	0.010	0.0

^a Particulate represents the total of Al₂O₃ + AlO_xH_yCl_z

^b NO_x represents the total of NO and a small amount of NO₂.

^c Cl_x represents the total of HCl, Cl₂, Cl, and ClO.

H = Heavy-lift vehicle

M = Medium-lift vehicle

M+ = MLV with solid rocket motors

Table 6-14 shows a comparison of the stratospheric emissions of particulate (as alumina) and Cl_x compounds between different U.S. lift vehicles. Cl_x is defined as the total of the HCl, ClO, Cl₂, and Cl species. NO_x emissions were not included in Table 6-14 because NO_x emissions tend to be much smaller than the particulate and chlorine emissions. The Atlas V 551/552 lift vehicle deposits fewer particulate and chlorine compounds into the stratosphere than

the Titan IV or the Space Shuttle, but more than the smaller vehicles in Table 6-14. The quantities of emissions deposited in the stratosphere depend on the altitude reached before the SRM burns out.

Table 6-14. Vehicle Deposition Rates in the Stratosphere for Atlas V 551/552 and Delta IV M+ (5,4) Compared to Other U.S. Lift Vehicles Using SRMs

{Table Compiled from Reference EELV [1999]}

Lift Vehicle	Tons per Launch	
	Particulate ^a	Cl _x ^b
Space Shuttle ^c	112	79
Titan IV w/ SRMs ^c	93	55
Proposed Atlas V 551/552	30	15
Proposed Delta IV M+ (5,4)	12	6
No-Action Delta IV M+	2	0.9
Atlas II AS ^c	3	5
Delta II ^c	12	8

^aParticulate represents the total of Al₂O₃ + AlO_xH_yCl_z

^bCl_x represents the total of HCl, Cl₂, Cl, and ClO.

^cBrady *et al.*, [1994]

M+ = Medium-lift vehicle with solid rocket motors

In order to compare local stratospheric impacts, the size and duration of a potential ozone hole in the wake of an Atlas V 551/552 and a Delta IV M+ (5,4) lift vehicle was estimated based on the work of Brady and Martin [1995] and Brady *et al.*, [1997]. Table 6-15 shows these values compared to similar estimates for other U.S. lift vehicles. These estimated values are for an altitude of 20 kilometers.

Table 6-15. Ozone Depletion Time and Hole Size at an Altitude of 20 Kilometers for Atlas V 551/552 and Delta IV M+ (5,4), Compared to Other U.S. Lift Vehicles with Solid Rocket Motors.

{Table Compiled from Reference EELV [1999]}

Lift Vehicle	Chlorine Release Rate	Hole Diameter	Hole Duration
	(tons/km)	(km)	(minutes)
Space Shuttle	4.3	5	97
Titan IV	2.0	4	25
Proposed Atlas V 551/552	0.65	2	3.6
Proposed Delta IV M+ (5,4)	0.36	3	1.3
No-Action Delta IV M+	0.42	2	1.0
Atlas II AS	0.10	0.8	0.1
Delta II	0.30	1	0.9

Source: Brady *et al.* [1994], Brady and Martin [1995], and Brady *et al.*, [1997].

M = Medium-lift vehicle with solid rocket motors.

For the proposed EELV lift vehicles, the estimated ozone hole would last a few minutes and would have a limited size. Because the flight trajectory is not vertical, and because wind shears occur, the ground-level UV increase from loss of stratospheric ozone would be less than would be the case if the ozone depletion occurred in a uniform vertical column.

6.8.2.2 Combined EELV Atmospheric Emissions

The total EELV program emission rates under the proposed Action were estimated for each year using the launch rates provided by each contractor, and the peak annual launch emissions for the free troposphere and the stratosphere from each launch site and from the two combined are shown in Table 6-16.

Table 6-16. Peak Annual combined EELV Launch Emissions into the Upper Atmosphere

Proposed Action (in tons).

{Reference: EELV [1999]}

	Particulate^a	NO_x^b	Cl_x^c
<i>Vandenberg AFB (all values for year 2008)</i>			
Free Troposphere	200	6.0	100
Stratosphere	130	0.14	64
<i>Cape Canaveral AS</i>			
Free Troposphere	700 ^d	14 ^e	350 ^d
Stratosphere	440 ^d	0.42 ^e	220 ^d
<i>Cape Canaveral AS + Vandenberg AFB (all values for year 2008)</i>			
Free Troposphere	870	18	440
Stratosphere	550	0.54	270

^aParticulate represents the total of Al₂O₃ + AlO_xH_yCl_z

^bNO_x represents the total of NO and a small amount of NO₂.

^cCl_x represents the total of HCl, Cl₂, Cl, and ClO.

^dPeak annual emissions in year 2004.

^ePeak annual emissions in year 2015.

The release of lift vehicle emissions into the stratosphere from both EELV platforms of the Proposed Action could result in combined local and global impacts (*EELV [1999]*). In terms of local effects, the passage of a lift vehicle through the stratosphere will cause a temporary, local decrease in the amount of ozone, a so-called local “hole” in the ozone layer. This reduction in stratospheric ozone along the flight path of the lift vehicle may cause a corresponding temporary, local increase in the amount of biologically damaging ultraviolet light that reaches the ground.

These local holes only exist for a matter of minutes to hours. Because launches at the two ranges are always separated by at least a few days, combined impacts in the sense of these local holes combining or reinforcing one another cannot occur (*EELV [1999]*). However, there is the potential for a secondary combined impact from the repeated local reduction of the stratospheric ozone concentration. Thus, the peak annual combined EELV program emissions of the Proposed Action into the stratosphere (given individually for VAFB and CCAS in Table 6-16) are presented to quantify the maximum annual potential for this kind of local impact. As noted in Table 6-16, the year in which the most pollutants would be emitted locally into both the free troposphere and the stratosphere at Vandenberg AFB from launches under the Proposed Action is expected to be 2008 (*EELV [1999]*). Similarly, the year in which the most pollutants would be emitted locally into both the free troposphere at Cape Canaveral AS from launches under the Proposed Action is expected to be 2004 for particulates and Cl_x, and 2015 for NO_x (*EELV [1999]*).

Based on the calculations of Jackman *et al.*, [1998], cumulative global impacts to the stratosphere from EELV launch activities were considered by Boeing and Lockheed Martin (*EELV [1999]*). Using the values of Jackman *et al.*, [1998] for both EELV platforms, the total annual chlorine and Al₂O₃ loading would be 1,941 tons per year, which results in an annual global ozone depletion of 1.7×10^{-3} percent per ton released and a peak depletion of 6.18×10^{-2} percent per ton. Assuming that the Proposed Action would deposit 820 tons (see Table 6-16) of CCAS and VAFB emissions of chlorine and Al₂O₃ in the stratosphere every year, the estimated global average ozone reduction would be approximately 0.014 percent per year. The worldwide contribution of ODS from lift vehicles using SRMs would depend on the launch rates of U.S. and foreign vehicles.

In the 1998 FEIS (*EELV [1999]*), it was assumed for estimation purposes that all CCAS launches will be GTO missions and that all VAFB launches would be LEO missions. The Atlas V lift vehicles use a common core booster that burns RP-1 and LO₂, which results in emissions of mainly CO₂ and H₂O, with small quantities of NO_x and CO. No SRM strap-ons are used with the No-Action Atlas V variants. Because the quantity of NO_x emitted is small, and the other compounds do not affect stratospheric ozone depletion, the impact of the No-Action Atlas V to stratospheric ozone would be negligible. The No-Action Delta IV lift vehicles use an LH₂/LO₂ core booster. The Delta IV M+ variant considered in the 1998 FEIS uses up to four SRMs (GEM-46) (*EELV [1999]*). As a result, this variant emits alumina particulate, NO_x, and chlorine substances into the upper atmosphere. However, these motors are approximately 40 percent smaller than those used in the Proposed Action. The quantities of aluminum oxide and chlorine released from the No-Action Delta IV M+ vehicle are compared to emissions from the Proposed Action and other vehicles in Table 6-14. The local ozone depletion from the No-Action Delta IV M+ is compared to the Proposed Action vehicles in Table 6-15. Under the No-Action Alternative, the Delta IV M and Delta IV H variants would have negligible NO_x emissions and therefore, negligible effect on stratospheric ozone.

Table 6-17 summarizes the peak annual upper atmospheric emissions from the No-Action Alternative. Because there are fewer launches and smaller SRMs in the No-Action Alternative,

the total amount of chlorine and Al₂O₃ deposition to the stratosphere will be less than for the Proposed Action. Furthermore, only the Boeing Delta IV M+ vehicle would use SRMs.

**Table 6-17. No-Action Peak Annual Launch Emissions into the Upper Atmosphere
(tons per year)**

{Reference: EELV [1999]}

	Particulate ^a	NO _x ^b	Cl _x ^c
<i>Vandenberg AFB (all values for year 2008)</i>			
Free Troposphere	56	6.5	28
Stratosphere	5.3	0.050	2.6
<i>Cape Canaveral AS</i>			
Free Troposphere	110 ^d	14 ^e	56 ^d
Stratosphere	11 ^d	0.10 ^e	5.3 ^d
<i>Cape Canaveral AS + Vandenberg AFB (all values for year 2008)</i>			
Free Troposphere	170	17	84
Stratosphere	16	0.14	8.0

^aParticulate represents the total of Al₂O₃ + AlO_xH_yCl_z

^bNO_x represents the total of NO and a small amount of NO₂.

^cCl_x represents the total of HCl, Cl₂, Cl, and ClO.

^dPeak annual emissions in year 2004.

^ePeak annual emissions in year 2015.

To summarize, the increased use of SRMs from the Proposed Action (*EELV [1999]*) would generate increased emissions of aluminum oxide, nitrogen oxides, and chlorine compounds into the stratosphere that could affect stratospheric ozone. Temporary local ozone losses would occur more frequently and over larger areas than under the No-Action Alternative. Cumulative global impacts to stratospheric ozone over the lifetime of the EELV program would depend on the future rate of EELV program commercial launches with SRMs. The yearly EELV contribution to the total annual global ozone decrease has been estimated to be less than 0.1 percent of existing conditions (*EELV [1999]*).

The Air Force is addressing the impacts of these proposals in the 1999 SEIS because of the potential that these variants could carry Air Force and other government payloads in the future.

6.8.3 Reusable Launch Vehicles (RLVs): the Experimental X-33 and Venturestar™

Following the National Space Transportation Policy announced in 1994, NASA initiated the RLV program and solicited proposals for the single-stage-to-orbit (SSTO) X-33 experimental demonstrator. The Experimental or X-33 program was initiated to develop a proof-of-concept prototype for integrated RLV technologies, paving the way for full-scale development of a reusable launch vehicle that would be contracted for government and commercial use. The X-33 is targeted to reach high hypersonic speeds and demonstrate SSTO and autonomous operations capabilities. NASA hopes the program will lead to the development of RLVs that will reduce the cost of space launches to at most one quarter of today's prices (*RLV [1998]*).

Lockheed Martin's design relies on a lifting body rather than wings. The X-33 will measure about 20 meters in length, with a dry mass of about 28,350-kg. The X-33 vehicle is sometimes referred to as Venturestar™, but in this context, Venturestar™ refers to Lockheed Martin's intended full-scale operational RLV design. The Venturestar™ vehicle will be similar in design to the X-33, but twice the size and about eight times the launch mass (*RLV [1998]*). The X-33 and the Venturestar™ will be powered by linear aerospike engines under development by Rocketdyne that do not use conventional cone-shaped exhaust nozzles, but allow the exhaust flow to adjust to changes in atmospheric pressure.

Development of the Venturestar™ vehicle is underway in parallel with the X-33, but Lockheed Martin has not yet made a firm decision to proceed with Venturestar™ construction. Complete development of an operational Venturestar™ will require significant funds, and Lockheed Martin is examining whether the market will support a return on investment that will make the vehicle feasible. More importantly, it also means the U.S. will stay competitive with the space transportation services of Europe, China, and Russia. The Venturestar™ is scheduled for its first launch in 2004 (*RLV [1998]*, *EELV [1998]*).

6.8.3.1 Emissions from the X-33 and Venturestar™ Launch Vehicles

Venturestar™ launch vehicles would produce no emissions into the stratosphere of any effective PORS, and would therefore not cause any degradation of the stratospheric ozone layer. Because of the lack of nitrogen in the fuels utilized for X-33 vehicles and the rapid decrease in the efficiency of after-burning to produce NO, negligible amounts of NO_x are deposited into the stratosphere. The annual perturbation of the stratosphere CO budget due to X-33 vehicles is less than 1 part in 15,000. If all fuel is converted to water, the resulting annual perturbation is less than 1 part in 1,000. Such perturbations, by either chemical, would fail to substantially alter the stratospheric chemistry or its heat budget (*EELV [1998]*, *RLV [1998]*).

7 CONCLUSIONS & RECOMMENDATIONS

7.1 Conclusions & Recommendation

Rocket launches have the potential to affect the atmosphere both in an immediate, episodic manner, and in a long-term, cumulative manner. When the stratosphere is affected immediately after launch, the perturbation occurs along or near the flight trajectory. Emissions from some types of launch vehicles significantly perturb the atmosphere along the launch trajectory at a range of a kilometer or less from the rocket passage. Ozone concentration is temporarily reduced, an aerosol plume may be produced, and combustion products such as chlorinated compounds, alumina, NO_x, and reactive radicals can temporarily change the normal chemistry along the vehicle path. This final section presents the conclusions (Section 8.2) and recommendations for future studies (Section 8.3). The references include here may be found at the end of the previous sections.

Potential long-term effects include a global reduction in stratospheric ozone, an increase in the chlorine loading of the stratosphere, and an increase in the particulate burden. As we have shown, it is the immediate or local destruction of ozone that is the primary consequences – global implications appear to be extremely minor.

7.2 Conclusions

7.2.1 Modeling, *In-situ*, and Laboratory Investigations

In compliance with the National Environmental Policy Act (NEPA) of 1969 and Executive Order 12114, Environmental Effects Abroad of Major Federal Actions, the National Aeronautics and Space Administration and the Department of the Air Force have been actively engaged in studies to determine the effects of launch vehicles on air quality. Under these policies, it is essential to understand qualitatively and quantitatively the effects of rocket launches on the environment. This report was provided to SMC to document the current knowledge of the environmental impact on stratospheric ozone depletion of solid-fuel rocket launches for the purpose of establishing potential constraints on launch activities. Included was a comprehensive review of modeling efforts, both the local stratospheric ozone impact of rocket exhaust from launch vehicles, as well as global and long-term effects. Additionally, detailed laboratory studies concerning the heterogeneous effects of SRM exhaust particulate, including aluminum oxide, were described. The limited data that does exist on *in-situ* sampling of exhaust plumes was presented to validate the modeling efforts, as well as to provide the first glimpse into the chemistry that occurs in the plumes. Furthermore, a variety of fuels and propellants were assessed to provide less harmful alternatives for future launch vehicle manufacturing. Finally the effects of deorbiting space and meteorite debris on stratospheric ozone were summarized.

Rocket launches can have a significant local effect on the stratosphere by reducing ozone substantially within the expanding exhaust plume up to 2 hours after launch. An ozone hole is

observed within this plume and found to increase in size during this period. Ozone concentrations recover to background levels as time passes and ozone back-fills into the hole by diffusion processes. The time for this hole to refill to ambient ozone levels was 3000 seconds at 15-20 km and 6000 seconds at 40 km based on measurement (*Ross [1997]*) and modeling (*Lohn [1999]*) studies. It was long thought that hydrogen chloride, a relatively inactive form of chlorine, was the only SRM chlorine containing emission species. Calculations and laboratory experiments have shown that chlorine is also present as Cl₂ or Cl radical. This is significant, because, while hydrogen chloride primarily adds to the global chlorine burden and, hence the global ozone depletion, the extremely active Cl (Cl₂ photolyzes rapidly to Cl) can participate in immediate, local destruction of ozone.

The process of ozone destruction is controlled by the rate at which plume species diffuse into the ambient atmosphere and by the reaction of ozone with chlorine (with ClO as a product) and the subsequent reproduction of chlorine by photoreactions, and reactions associated with chlorine chemistry. It is this cyclic regeneration of Cl that has caused the generation of an ozone hole. These model simulations of dramatic ozone losses in the first couple of hours after launch have been corroborated by measurements taken after the launch of a variety of SRM vehicles (namely Titan III, Titan IV, and Space Shuttle).

In-situ results clearly have suggested that these SRM launch vehicles produce transient ozone loss following launch. A comparison of *in-situ* data to recent modeling efforts has confirmed that the models only slightly underestimate both the size and the duration of the region of ozone removal in the wake of large and medium launch vehicles (*Beiting [1999]*). However, even when such reductions occurred, the reduction in column ozone was found to exist over an area a few kilometers by a few tens of kilometers and was generally much smaller. The local-plume ozone reductions decrease to near zero over the course of a day and the plume has spread to over 100 kilometers. These regional effects were smaller than could be detected by TOMS satellite observations (*Syage et al., [1996]*).

Laboratory investigations by Disselkamp [*1999*] assessed the uptake of NO and NO₂ onto the surface of Al₂O₃. These reactions have two potential implications in atmospheric chemistry. First, a decrease in atmospheric NO_x concentrations could enhance the catalytic destruction of ozone by halogen species. Considering that the ambient stratospheric NO_x concentration was approximately 2.5x10¹⁰ molecules/cm³, it would take a Al₂O₃ particle density of 640 particles/cm³ to deplete all the NO_x species. Therefore, within the wake of rocket exhaust plume, this aluminum oxide chemistry may be important, but not at the aluminum oxide ambient particle concentration of 10 particles/m³. A second potential atmospheric implication of this chemistry was to consider the uptake of halogen species onto the surface of aluminum oxide particles. The uptake of active halogen species by aluminum oxide to liberate NO would have the effect of increasing the ozone concentration by reducing the contribution of halogen catalyzed ozone destruction. Additional studies would be needed to characterize this halogen chemistry.

The reaction probability, γ , was measured by Molina [*1999*] for the reaction of ClONO₂ with HCl on alumina surfaces. The result was $\gamma = 0.02$ under conditions similar to those which would

be encountered at mid-latitudes in the lower stratosphere; it was in very good agreement with other published measurements on alumina and on glass surfaces conducted with larger reactant concentrations. The reaction was found to be nearly zero order in HCl, and the mechanism was not dependent on the detailed nature of the refractory oxide surface itself; it was dependent on the presence of absorbed water layers. Furthermore, it was determined that a significant fraction of the injected alumina surface area would be catalytically active and would remain unaffected in the stratosphere by sulfuric acid vapor. The time required for the alumina particulate to be covered by a monolayer of sulfuric acid was estimated at 8 months, assuming an accommodation coefficient of 0.1. Finally, coalescence with stratospheric sulfuric acid aerosols would most likely be unimportant for the alumina particles larger than about 0.1 μm in diameter before they settle out of the stratosphere. These results were confirmed by 3-D model calculations of Ko *et al.*, [1999].

Jackman *et al.*, [1998] carried out detailed stratospheric modeling calculations of ozone depletion caused by SRMs using the reaction probability measurement of Molina [1999] on alumina particles. Their result indicate that the effect on the annually averaged global total ozone is a decrease of 0.025% by the year 1997; about one-third of this decrease results from the SRM-emitted alumina and the remaining two-thirds results from the SRM-emitted hydrogen chloride. These results were confirmed independently by the modeling efforts of both Lohn *et al.*, [1999] and Ko *et al.*, [1999].

7.2.2 Alternative Propellants

A methodology for the systematic removal of Potential Ozone Reactive Species or PORS from rocket plume exhaust streams using alternate propellants was presented. The impacts from launch vehicles range from a minimum of a reformulated conventional solid propellant containing ammonium perchlorate, but with afterburning suppressant chemicals added, to a completely reformulated solid propellant that incorporated nitrate/carbonate oxidizers, to new engines based on fluorine oxidizers or redeveloped engines burning conventional liquid propellants. Reformulated solids with afterburning suppressants could be implemented as a direct response to Cl_2 production; conventional liquid engines utilizing LOX/LH₂ and/or LOX/RP-1 could be implemented to remove HCl; and fluorine systems (solids and/or gels) could be implemented to eliminate H₂O and CO₂ (Lewis *et al.*, [1994]).

Although modeling and *in-situ* studies have concluded that rocket exhaust plumes have very little environmental impact, the possibility remains that some of the exhaust species from current space launch and SRM boosters will be regulated in the future. The effects of liquid rocket engines (e.g., LH₂/LOX, RP-1/LOX, etc.) on stratospheric ozone were addressed (Brady *et al.*, [1997]). The loss of ozone was found to “exhibit no deleterious effect on the environment” which translates into extremely small ozone losses (Lewis *et al.*, [1994]). The sole mechanism considered was destruction by NO and NO₂ produced by afterburning. The lack of ozone destruction was a result of the lack of NO/NO_x in the plume. Afterburning temperatures must be in excess of 2000 K in order to produce appreciable NO/NO_x, but for liquid systems, such a high temperature is not reached by afterburning in the stratosphere. The local ozone hole that was created persisted for only tens of minutes and was driven by chemical reactions and turbulent

diffusion. The plume-induced species diffused and ultimately reached concentrations equivalent to the corresponding background levels or, as in the case of chlorine, react to form a stable compound or reservoir species that prevented the SRM-borne chlorine atoms from further destruction of ozone. The effects of wind shear can complicate this process. For example, the physical process of large-scale vertical wind shear can act to stretch the plume and to slow the radial growth. This effect could serve to hold the ozone-attacking species concentration to high levels for a longer period of time and allow, by diffusion of ambient ozone to the distorted plume, cause additional loss of ozone.

Based on the scenario of 10 Titan launches per year the analysis results presented indicated that global stratospheric ozone was perturbed only slightly, probably within the range of seasonal variations. In earlier times after the launch, the level of ozone column density loss is about 0.25% over an area of 20 km² after 2 hours, and after 9 hours, the plume size had increased and the influenced area is increased to about 70 km² at approximately 0.1%. From a global steady state standpoint, the effect is larger in the Polar regions and relatively small in other areas. In the northern Polar region, the loss peaks at about 0.06% while the rest of the globe has a loss of about 0.01%. Because of the assumption of complete ozone loss within the stabilized plume, the “line of sight” ozone depletion calculated here represents a conservative or worst-case assessment. Consideration of plume diffusion would increase the area of the surface plume footprint, but would probably not increase the ozone loss. Therefore, the global impact of rocketry is considered a third-order or smaller effect compared with other sources of chlorine. If the annual background source from halocarbons were reduced and/or the launch rate increased, the fractional contribution of rocketry would become larger (*Lohn et al., [1994]*).

The status of fluorine based oxidizer rocket engine technology was reviewed briefly (*Lewis et al., [1994]*). While liquid fluorine rocket engines have been developed and tested, it is unlikely such engines would be flown in boost to LEO applications. This conclusion stems from safety considerations, including toxicity, storage, and handling, which significantly reduce the viability of using these liquid propellant alternatives. Should fluorine oxidizer launch systems be developed, they will most likely be as solid or gelled systems. There is sufficient technology available that suggests that solid propellants based on fluorine oxidizers could be produced at thrust levels supporting boost applications. Gelled propellant technology applied to fluorine oxidizers has not been demonstrated. Hybrid engine technology based on a liquid fuel (i.e., LH₂, slush H₂, liquid N₂H₄ with solid fluorine based oxidizer) is credible but has not been developed.

Rocket engine technology utilizing conventional liquids as alternate propellants such as LOX/LH₂ and/or LOX/RP-1 is well developed, but this technology is not in current use in the United States for heavy lift boost applications. NASA engine development programs (e.g., EELV) focusing low cost boost to LEO engines provide directly applicable technology solutions to ozone depletion mitigation. Conventional liquid propellant systems represent the best near term solution to the PORS problem, if reformulated solid propellants are unacceptable.

Finally, given that afterburning suppression to prevent Cl₂ formation may be an acceptable near term solution to PORS production, a series of lab/bench/test stand tests were identified (Thiokol Corporation and Alliant Corporation). These tests have demonstrated that afterburning

suppressant chemicals can be used as additives to supplement existing solid propellant formulations. At the laboratory or bench scale, potential suppressant chemical additives were tested in either simulated plume/atmosphere shear layers or bombs to quantify afterburning suppression efficiency. Optical diagnostics could be used to probe the exhaust plume for HCl to Cl₂ conversion. When potential afterburning chemicals were identified, candidate propellants with suppressants were formulated and test stand fired while probing the plume for HCl and other chlorine reactions (*Bennett et al., [1994]*).

7.2.3 Deorbiting Debris

Finally, a discussion of the impact on stratospheric ozone from deorbiting debris was presented. Consideration of the individual studies assessed in this document leads to the conclusion that the physical and chemical phenomena associated with deorbiting debris and meteoroids do not have a significant impact on global stratospheric ozone. The reasons are twofold: slow reaction rate and low particle density. However, it was noted that large deposition of particles in the stratosphere due to volcanic eruptions could have a significant impact on the local ozone column density. The effect of meteoroids on the stratospheric ozone layer also was investigated. The meteoroid population for micron to millimeter size objects was found to be comparable to the orbital debris flux. To the extent that they are comparable, it may be concluded that meteoroids pose little or no threat to global stratospheric ozone.

An area of further scientific investigation is the assumption made by *Ko et al., [1999]* using 30 tons/year as the meteor source, and 10 tons/year for the orbital debris source. These numbers are quite small, when compared with the rocket source of 1000 tons/year, and may have overlooked the possibility that deorbiting debris may form soot in the trailing plume. The chemical rate constants of soot generated from deorbiting debris or LOX/RP-1 and kerosene fuels are either unknown or poorly understood. These chemical reactions also should be investigated.

7.3 Recommendations

During the last decade the space community has witnessed an explosion of space activities in the military as well as the commercial arena. Particularly in the telecommunication area the demand for new space vehicles has increased by several hundred percent. Further investigations may be examined from two points of view. The first point of view is the launch vehicle effects. Launch vehicles have caused localized ozone depletion that lasted for approximately 6000 seconds at high stratospheric altitudes before returning to ambient levels. Global depletion was shown to be minimal. Nevertheless from an environmental and scientific viewpoint, there is much to be understood. Equipped with the knowledge of the various ozone depletion mechanisms, the author's propose the following tasks in order to assess the impact on stratospheric ozone as a result of expanding space activities.

First, model assessment should be made on the effect on stratospheric ozone resulting from planned or unplanned destruction of SRM, as well as liquid launch vehicles. The impact on ozone caused by combustion/explosion of solid propellant could be similarly characterized (i.e., assessment of HCl production and its subsequent fate in terms of dissociation into chlorine). The liquid bipropellant systems (LH₂/LOX and RP-1/LOX) exhibited no deleterious effect on the environment. However, current analyses have not included the potentially harmful effect due to large deposition of H₂O vapor or droplets into the basically dry stratosphere. The ozone depletion potential may be identified from two sources: namely, heterogeneous reaction on droplet surfaces in the form of polar stratospheric clouds commonly found in Antarctica; or homogenous reactions according to the OH catalytic cycle, particularly in the upper stratosphere where the abundance of O₂(¹Δ) can convert H₂O into H, OH, and HO₂ radicals. It is well known that ozone can be consumed through the HO_x mechanism as described in reactions (8-1) and (8-2):



These reactions have been reviewed (*Denison et al., [1994], Lohn et al., [1994], Brady et al., [1997]*), but need to be reexamined, especially if the commercial component increases, and the conversion from SRM to liquid launch engines is made.

In order to assess the effects of emissions from alternative propellants, their chemistry and dynamics must be modeled. This may comprise upgrading the current models. For example, liquid hydrocarbon fuels such as RP-1 produces soot in the exhaust. This soot production has never been adequately modeled. Nor have the potential heterogeneous chemistry effects of soot been analyzed.

Second, model assessment should be made on the transport of exhaust gases produced by spacecraft functions such as fuel dumps, station keeping, pointing, and drag makeup. As a result of increased space activities large amount of effluents released in high altitude will diffuse and potentially be transported downward through the thermosphere and mesosphere into the stratosphere. These effluents upon arriving in the upper stratosphere may undergo catalytic cycles (e.g., the NO_x and HO_x cycles) to deplete ozone.

Furthermore, statistical evaluation of the crosswind gradient effects on both local and global ozone depletion should be conducted. This task would use computational fluid dynamics to quantify the column dynamics and “pinching” effects under a set of typical stratospheric wind profiles. The anchored cold wake model would be used to calculate column and “pinched off” volume ozone depletion, and the outputs of the local depletion analysis would be used to upgrade global impact estimates.

Future *in-situ* measurement campaigns, similar to RISO, should be conducted to focus on the chemistry that occurs within plume layers at higher altitudes, in particular, to measure ClO

and other ozone depleting species, as well as determining the particle size distribution of alumina, water and soot. These measurements would further validate the existing model inputs as to heterogeneous reaction kinetics. Future campaigns should use multiple sites to discover the three-dimensional shape of the plume, to determine the stratification of the plume into distinct layers, and to aid in the identification of plume break-up and dispersion. Measurements should be conducted in different seasons to validate transport within the stratosphere.

This report recommends space-based monitoring be conducted as well. There are two principal reasons why space-based instrumentation is needed to measure ozone depletion by launch vehicles. First, space-based UV-backscatter instruments can measure the altitude profile of ozone loss as well as providing the three-dimensional image of ozone depletion in the launch corridor. The vertical information allows for a better understanding of the specific mechanism by which ozone loss is occurring and provides the extent to which vertical transport of air parcels is involved. Second, an instrument deployed in a polar orbit would be able to monitor launches occurring from any location on Earth. Thus, it could determine effects on the stratospheric ozone layer from both U.S. and international launches, which use a wide variety of propellants. This is critical for assessing the environmental impacts of current propellants of launch vehicles as well as for the development of alternative propellants that will not cause ozone depletion, especially in regions of the world where *in-situ* measurements would be impossible to attain.

One instrument that appears capable of satisfying these requirements is the proposed High Resolution Ozone Imager (HIROIG). HIROIG is a state-of-the-art sensor designed to measure ozone depletion ozone by monitoring changes in intensity of backscattered solar ultraviolet (UV) light resulting from rocket launches. In the undisturbed stratosphere, the depth to which UV light can penetrate before being completely absorbed by ozone is dependent upon the wavelength of the light. If there is an “ozone hole” at a particular altitude, light that normally penetrates to that altitude is able to reach lower altitudes where the atmospheric density is higher and the light is more strongly scattered, resulting in more intense backscattered light. Light that does not normally penetrate to the holes’ altitude is unaffected. Therefore, the wavelengths at which the backscattered light is intensified are correlated with specific altitudes at which the ozone has been depleted.

By observing different intensities of solar UV light at many different wavelengths, HIROIG is able to determine the stratospheric ozone concentration at altitudes up to 50 km in 7-km intervals. HIROIG utilizes a state-of-the-art charge coupled device (CCD) detector to achieve it’s uniquely high spatial resolution of 2 km x 2 km, which is necessary to measure ozone depletion in the narrow launch corridor. The resulting three-dimensional data obtained from HIROIG will provide a detailed profile of ozone loss in the atmosphere due to launch vehicles, even if the loss occurs in a localized region.

When operational, HIROIG would be mounted on a satellite in a polar orbit about 800 km above the earth and would provide a full altitude profile of the ozone loss. It would monitor the area of the atmosphere affected by a rocket’s exhaust (i.e., the launch corridor) within one to three hours after the launch, during which the concentration of ozone is predicted to reach its lowest level. HIROIG would be capable of imaging a 2-km x 2-km spatial resolution, which is

1000 times greater than NASA's Total Ozone Monitoring Spectrometer (TOMS) or any other existing instrument. The data obtained would be used for verification of three-dimensional computational models of ozone depletion in the launch corridor. HIROIG is expected to observe between one-fourth and one-third of the launches that occur without the cooperative launch scheduling required by balloon-based or aircraft measurements. Finally, HIROIG could certainly be used in more general studies of the Earth's ozone layer and other areas of environmental concern. Following its launch, a continuous record of global observations would become available. Perturbations to stratospheric sulfur dioxide and ozone from natural phenomena, such as volcanic eruptions in remote regions, would be recorded, as well as those caused by high-altitude aircraft, would be readily observed.

COMPLETE LIST OF REFERENCES

- Abbatt, J. P. D. and M. J. Molina, *Geophys. Res. Lett.*, 19, 461, 1992a.
- Abbatt, J. P. D. and M. J. Molina, "Heterogeneous Interactions of ClONO₂ and HCl on Nitric Acid Trihydrate at 202K," *J. Phys. Chem.*, 96, 7674, 1992b.
- Aftergood, S., Comment on "The Space Shuttle's impact on the stratosphere," by Michael J. Prather, *et al.*, *J. Geophys. Res.*, 96, 17377, 1991.
- AIAA (American Institute of Aeronautics and Astronautics), International Reference Guide to Space Launch Systems, 2nd Edition, Steven J. Isakowitz, Washington, D.C., 1994.
- AIAA (American Institute of Aeronautics and Astronautics), Atmospheric effects of chemical rocket propulsion, *Report of AIAA Workshop*, Washington, D.C., October 1, 1991.
- Anon., "TRW 'Smart' Propulsion Systems Will Power 'Smart' Army Missiles," TRW Infolink April 25, 1994; Also "TACAWS Minimum Smoke Gel Propulsion System Hazards Program," Contract Sales Number 54470, Contract DAA HO 1-90-3-0900, 1994.
- Arnold, F., R. Fabian, and W. Joos, "Measurements of height variation of sulfuric acid vapor concentrations in the stratosphere," *Geophys. Res. Lett.*, 8, 293-296, 1981.
- Avallone, L.M., and M. J. Prather, "Tracer-Tracer Correlations: Three-dimensional model simulations and comparisons to observations," *J. Geophys. Res.*, 102, 19233-19346, 1997.
- Bauer, E., "Introduction and Overview: The stratosphere in its application to CIAP," in CIAP Monograph 1, The National Stratosphere of 1974, *DOT-TST-75-51*, Department of Transportation, Washington, D.C., 1975.
- Beiting, E.J., "Measurements of Stratospheric Plume Dispersion by Imagery of Solid Rocket Motor Exhaust," *J. Geophys. Res.*, 1999 (*submitted*).
- Beiting, E. J., and R. A. Klingberg, "K-2 Titan IV Stratospheric Plume Dispersion," Aerospace Technical Report No. *TR-97(1306)-1*, 1997a.
- Beiting, E.J., "Solid Rocket Motor Exhaust Model for Alumina Particles in the Stratosphere," *Journal of Spacecraft and Rockets*, 34, 303-310, 1997b.
- Beiting, E.J., "Predicted Optical Characteristics of Solid Rocket Motor Exhaust in the Stratosphere," *Journal of Spacecraft and Rockets*, 34, 311-317, 1997c.
- Beiting, E. J., "Characteristics of Alumina Particles from Solid Rocket Motor Exhaust in the Stratosphere," The Aerospace Report Corporation, *TR-95(5231)-8*, 1995.

- Benbrook, J. R., and W. R. Sheldon, “*In-Situ Dual Beam UV Absorption Measurement of Ozone in SRM Plumes*,” *AIAA-97-0528*, 6-10 January 1997.
- Benbrook, J., *Project RISO Workshop*, The Aerospace Corp., Los Angeles, California, 11 June 1996
- Bennett, R. R., R. B. Cragun, J. D. Shuler, and L. L. Biegert, “Development and Scale-Up of a Reduced HCl Propellant,” Thiokol Corporation, presented at *1998 JANNAF Propellant Development and Characterization and Safety and Environmental Protection Subcommittee Meeting*, NASA Johnson Space Center, Houston TX, 21-23 April 1998.
- Bennett, R.R., and J. C. Hinshaw, “The effects of chemical propulsion on the stratospheric ozone,” Internal report, Thiokol Corporation, Brigham City, Utah, 1991.
- Benson, S. W., *Thermochemical Kinetics, Methods for the Estimation of Thermochemical Data and Rate Parameters*, Second edition, John Wiley & Sons Inc., 1976.
- Bhartia, P. K., J. Herman, R. D. McPeters, and O. Torres, “Effect of Mount Pinatubo aerosols on total ozone measurements from backscatter ultraviolet (BUV) experiments,” *J. Geophys. Res.*, 98, 18547-18554, 1993.
- Blackmore, D. R., G. O'Donnell, and R. F. Simmons, *Tenth Symposium (International) on Combustion*, The Combustion Institute, Pittsburgh, p. 303, 1964.
- Bojkov, R. D., L Bishop, W. J. Hill, G. C. Reinsel, G. C. Tiao, “A Statistical Trend Analysis of Revised Dobson Total Ozone Data Over the Northern Hemisphere,” *J. Geophys. Res.* 95, 9785, 1990.
- Brady, B. B., L. R. Martin, and V. I. Lang, “Effects of Launch Vehicle Emissions in the Stratosphere,” *J. Spacecraft and Rockets*, 34, 774-779, 1997a.
- Brady, B. B., L. R. Martin, and V. I. Lang, “Effects of Launch Vehicle Emissions in the Stratosphere,” *AIAA-97-0531*, 1997b.
- Brady, B. B., and L. R. Martin, “Modeling solid rocket booster exhaust plumes in the stratosphere with SURFACE CHEMKIN,” The Aerospace Corporation, *TR-95(5231)-9*, 1996.
- Brady B. B., and L. R. Martin, “Modeling Solid Rocket Booster Exhaust Plumes in the Stratosphere with SURFACE CHEMKIN,” Aerospace Report No. *TR-95(5231)-16*, 17 October, 1995a.

- Brady B. B., L. R. Martin, "Use of SURFACE CHEMKIN to Model Multiphase Atmospheric Chemistry: Application to Nitrogen Tetroxide Spills," *Atmospheric Environment*, 29, 715-25, 1995b.
- Brady B. B., L. R. Martin, "Modeling Multiphase Chemistry with SURFACE CHEMKIN," Aerospace Report No. *ATR-96(1410)-2*, 1995c.
- Brady B. B., E. W. Fournier, L. R. Martin, and R. B. Cohen, "Stratospheric Ozone Reactive Chemicals Generated by Space Launches Worldwide," Aerospace Report No. *TR-94(4231)-6*, 23 June 1994.
- Brasseur, G. B., and S. Solomon, "Aeronomy of the Middle Atmosphere," D. Reidel Publishing Co., Dordrecht, Holland, 1984.
- Brown, J. R., "The RL-10 Program-35 Years of Lessons", Paper Presented at "Lessons Learned In Liquid Propulsion" AIAA Joint Propulsion Conference, Monterey, CA, Sponsored by the *AIAA Liquid Propulsion Technical Committee*, AIAA, Washington, D.C., 20024-2518, June 26-27, 1993.
- Brown, R. L., "Tubular flow reactors with first order kinetics," *J. Res. Nat. Bur. Stand.*, 83, 1-8, 1978.
- Brownlee, D. E., G. V. Ferry, and D. Tomandl, "Stratospheric aluminum oxide," *Science*, 191, 1270-1271, 1976.
- Burke, M. L., and P. F. Zittel, "Laboratory Generation of Free Chlorine from HCl under Stratospheric Afterburning Conditions," *Combustion and Flame*, 112, 210-220, 1998.
- Burke, M. L., and P. F. Zittel, "Laboratory generation of free chlorine from HCl under stratospheric afterburning conditions," The Aerospace Corporation, *TR-96(1306)-3*, 1996.
- Butlin, R. N., and R. F. Simmons, *Combustion & Flame*, 12, 447, 1968
- Chapman, S., "A Theory of Upper Atmospheric Ozone," *Q. J. R. Meteorol. Soc.*, 3, 103-125, 1930.
- Chou, M. S. et al., "Evaluation of Plume Signature Modification by Use of Subscale Tests and Modeling," *19th JANNAF Exhaust Plume Technology Subcommittee Meeting*, U.S. Army Missile Command, Redstone arsenal, AL, 13-16 May 1991, CPIA, the Johns Hopkins University, Columbia, Md., Publication 568, May, 1991
- Cocchiaro, J. E. (editor), "Environmental Impacts of Launch Vehicles – A Bibliography," *Report No. LS98-11*, Chemical Propulsion Information Agency (CPIA), The Johns Hopkins University, Columbia, MD, August 1998.

- Cofer, W. R. III, G. C. Purgold, E. L. Winstead, and R. A. Edahl, "Space Shuttle Exhausted Aluminum Oxide," *J. Geophys. Res.*, *96*, 17,371-17,376, 1991.
- Cofer, W. R. III, R. J. Bendura, D. I. Sebacher, G. L. Pellett, G. L. Gregory, and G. L. Maddrea, Jr., "Airborne measurements of Space Shuttle exhaust constituents," *AIAA.*, *23*, 283-287, 1985.
- Coltrin M. E., R. J. Kee, and F. M. Rupley, "SURFACE CHEMKIN (Version 4.0): A FORTRAN Package for Analyzing Heterogeneous Chemical Kinetics at a Solid-Surface - Gas-Phase Interface," *Sandia Report SAND90-8003B.UC-401*, p91, 1991.
- Cour-Palais, B. G., ed.: "Proceedings of the Space Shuttle Environmental Assessment Workshop on Tropospheric Effects," *NASA TM X-58199*, Feb. 1977.
- Crutzen, P. J., and F. Arnold, "Nitric Acid Cloud Formation in the Cold Antarctic Stratosphere: A Major Cause for the Springtime 'Ozone Hole'," *Nature*, *324*, 651, 1986.
- Danilin, M. Y., "Local Stratospheric effects of solid-fueled rocket emissions," *Ann. Geophysicae*, *11*, 828-836, 1993.
- Dao, P. D., J. A. Gelbwachs, R. Farley, R. Garner, P. Soletsky, and G. Davidson, "LIDAR Stratospheric SRM Exhaust Plume Measurement," *AIAA 35th Aerospace Sciences Meeting 97-0526*, 6-10 January 1997.
- Dao, P., R. Farley, P. Soletsky, R. Garner, Gilbert Davidson, and J. A. Gelbwachs, "Scanning LIDAR for Monitoring the Impacts of Solid Rocket Motor Exhaust Plumes upon the Stratosphere," *Optical Engineering*, 1996.
- Dave, J. V., "Effect of aerosols on the estimation of total ozone in an atmospheric column from the measurements of its ultraviolet radiance," *J. Atmos. Sci.*, *35*, 899-911, 1978.
- DeMore, W. B., D. M. Golden, R. F. Hampson, C. J. Howard, C. E. Kolb, M. J. Kurylo, M. J. Molina, A. R. Ravishankara, and S. P. Sander, "Chemical Kinetics and Photochemical Data for Use in Stratospheric Modeling, Evaluation Number 11," *JPL Publ. 94-26*, 1994.
- DeMore, W. B., D. M. Golden, R. F. Hampson, C. J. Howard, M. J. Kurylo, M. J. Molina, A. R. Ravishankara, and S. P. Sander, "Chemical Kinetics and Photochemical Data for Use in Stratospheric Modeling, Evaluation Number 9," *JPL Publ. 90-1*, Jet Propulsion Laboratory, 1 January, 1990.
- Denison, M. R., J. L. Lamb, W. D. Bjorndahl, E. Y. Wong, P. D. Lohn, "Solid Rocket Exhaust in the Stratosphere: Plume Diffusion and Chemical Reactions," *Journal of Spacecraft & Rockets*, *31*, 435-442, May 1994.

Department of Air Force (AF), “*Environmental Assessment for Complementary Expendable Launch Vehicles*,” June 1996.

Department of the Air Force (AF), “*Environmental Assessment Lockheed Launch Vehicles. Vandenberg Air Force Base, CA.*,” February 1994.

Department of the Air Force (AF), “*Draft Programmatic Environmental Assessment Medium Launch Vehicle III Program*,” June 1991.

Department of the Air Force (AF), “*Environmental Assessment Titan IV/Solid Rocket Motor Upgrade Program. Cape Canaveral Air Force Station, FL, Vandenberg Air Force Base, CA.*,” February 1990.

Department of Transportation (DOT), “*Environmental Impact Statement for Commercial Reentry Vehicles*,” Washington, D.C., May 1992.

Disselkamp, R., “Laboratory Studies of Al₂O₃-NO_x Aerosols,” Report submitted to TRW, Redondo Beach, California, August 1999.

Dixon-Lewis, G., and R. J. Simpson, *Sixteenth Symposium (International) on Combustion*, The Combustion Institute, Pittsburgh, p. 1111, 1976.

Dobson, G. M. B., *Annals of the International Geophysical Year V, Part I*, (Pergamon, New York, pp. 46-89, 1957.

Dressler, G. A., F. J. Stoddard, K. R. Favitt, and M. D. Klem, “Test Results from a Simple, Low Cost Pressure-Fed Liquid Hydrogen/Liquid Oxygen Rocket Combustor,” Paper Presented at *1993 JANNAF Propulsion Meeting and JANNAF Combustion Subcommittee Meeting*, Monterey, CA, 15-17 November 1993.

EELV, “*Draft Supplemental Environmental Impact Statement (DSEIS) of the Evolved Expendable Launch Vehicle (EELV) Program*,” U. S. Air Force, November 1999.

EELV, “*Final Environmental Impact Statement (FEIS) of the Evolved Expendable Launch Vehicle (EELV) Program*,” U. S. Air Force, April 1998.

EIS, “*Environmental Impact Statement for the Space Shuttle Program*,” NASA Headquarters, Washington, D.C., July 1977.

Elam, J.W., C. E. Nelson, M. A. Cameron, M. A. Tolbert and S. M. George, “Adsorption of H₂O on single crystal α -Al₂O₃ (001) surfaces modeling rocket exhaust particles,” submitted for publication to *J. Phys. Chem.*, 1998.

Falcone, P. K., R. K. Hanson, C. H. Kruger, *J. Quant. Spectrosc. Rad. Trans.*, 29, 205, 1983

Farman, J. C., B. G. Gardiner, J. D. Shanklin, "Large Losses of Total Ozone in Antarctica Reveal Seasonal ClO_x/NO_x Interaction," *Nature*, 315, 207, 1985.

FEAFSLP, "Final Environmental Assessment For the SEA LAUNCH Project," Prepared for the U.S. Department of Transportation Federal Aviation Administration, Office of the Associate Administrator for Commercial Space Transportation, Washington, D.C. by ICF Kaiser Consulting Group, February 10, 1999.

Flatoday; Reference to <http://www.flatoday.com/space/today/index.htm>, 1999.

George, S. M., M. A. Tolbert, M. A. Cameron, and C. E. Nelson, "Hydroxylation and dehydroxylation of aluminum oxide surfaces," paper presented at the symposium on *The Impact of Rockets on the Stratosphere*, Redondo Beach, California, May 1996.

Gershenson, Y., S. Zvenigorodsky, and V. Rosenshtein, *Adv. in Chemistry (Uspehi Hymii)*, 59, 1601-1626, 1990.

Hall, T. M., and M. J. Prather, "Seasonal evolution of N₂O, O₃, and CO₂: Three-dimensional simulations of stratospheric correlations," *J. Geophys. Res.*, 100, 16,699-16,720, 1995.

Hall, T. M., and M. J. Prather, "Simulations of the trend and annual cycle in stratospheric CO₂," *J. Geophys. Res.*, 98, 10,573-10,581, 1993.

Hanning-Lee, M. A., B. B. Brady, L. R. Martin, and J. A. Syage, "Ozone decomposition on alumina: Implications for solid rocket motor exhaust," *Geophys. Res. Lett.*, 23, 1961-1964, 1996.

Harpole, G. M. and M. S. Chou, "Surveillance Phenomenology," TRW IR&D Project, Project Number 90351000, Report Date: 31 March 1990.

Harwood, R. S., and C. H. Jackman, I.L. Karol, and L. X. Qiu, "Predicted Rocket and Shuttle Effects on Stratospheric Ozone, in *Scientific Assessment of Ozone Depletion: 1991*," National Aeronautics and Space Administration (NASA), Washington, D.C., 1991.

Hayman, G. D., J. M. Davies, and R. A. Cox, "Kinetics of the reaction ClO and ClO to products and its potential relevance to Antarctic Ozone," *Geophys. Res. Lett.*, 13, 1347, 1986.

Hea-Harvard, Reference to <http://hea-www.harvard.edu/~jcm/space/log/launch.htm>, 1999.

Hecht, J. H., J. P. Thayer, D. J. Gutierrez, and D. L. McKenzie, "Multi-instrument Zenith Observations of Noctilucent Clouds over Greenland on July 30/31, 1995," *J. Geophys. Res.*, 102, 1959-1970, 1997.

Hofmann, D. J., and S. Solomon, "Ozone destruction through heterogeneous chemistry following the eruption of El Chichon," *J. Geophys. Res.*, 94, 5029-5041, 1989.

- Howard, R. P., L. C. Wormhoudt and P. D. Whitefield, "Experimental Characterization of Gas Turbine Emissions at Simulated Flight Altitude conditions," *AEDC-TR-96-3*, September 1996.
- Howard, C. L., "Kinetic measurements using flow tubes," *J. Phys. Chem.*, 83(1), 3-9, 1979.
- Hoshizaki, H. (chairman), Aircraft wake microscale phenomena, Chap. 2, pp. 60-73, in *The Stratosphere Perturbed by Propulsion Effluents, CIAP Monogr. 3*, Climatic Impact Assessment Program, U.S. Dept. of Transportation, Washington, D.C., 1975.
- Isakowitz, S. J., *International Reference Guide to Space Launch Systems*, 2nd Edition, updated by Jeff Samela, published by AIAA, Washington, D.C., 1995.
- Jackman, C. H., D. B. Considine, and E. L. Fleming, "A Global modeling study of solid rocket aluminum oxide emission effects on stratospheric ozone," *Geophys. Res. Lett.*, 25, 907-910, 1998.
- Jackman, C. H., D. B. Considine, and E. L. Fleming, "The Space Shuttle's Impact on the Stratosphere: An Update," *J. Geophys. Res.*, 101, 12523-12529, 1996a.
- Jackman, C. H., et al., "Past, present and future modeled ozone trends with comparisons to observed trends," *J. Geophys. Res.*, 101, 28753-28767, 1996b.
- Jackman, C. H., A. R. Douglass, and K. F. Bmeske, "A simulation of the effects of the National Aerospace Plane testing on the stratosphere using a two-dimensional model," Code 916. NASAJGSFC, Greenbelt, MD 20771, preprint of a report given to the U.S. Air Force, 1991.
- Johnston, H. S., "Atmospheric Ozone," *Annual Review of Physical Chemistry*, 43, 1-32, 1992.
- Johnston H., "Depletion of stratospheric ozone due to the catalytic effect of NO_x, emitted from a proposed fleet of supersonic transports," *Science*, 173, 517, 1971.
- Jones Technologies, Inc., Mangi Environmental Group, Inc., "*Programmatic Environmental Impact Statement Commercial Expendable Launch Vehicle Program*," April 1996.
- Jones A. E., S. Bekki, and J. A. Pyle, "On the atmospheric impact of launching the Ariane 5 rocket," *J. Geophys. Res.*, 100, 16,651-16,660, 1995.
- Karol I. L., Y. E. Ozolin, and E. V. Rozanov, "Effect of Space Rocket Launches on Ozone," *Ann. Geophysicae*, 10, 810-814, 1992.
- Karol, I. L., Y. E. Ozolin, and E. V. Rozanov, "Effect of Space Rocket Launches on Ozone and Other Atmospheric Gases," Paper presented at the *European Geophysical Association Conference*, Wiesbaden, 1991.

- Kasten, F., "Falling speed of aerosol particles," *J. Appl. Met.*, 7, 944-947, 1968.
- Kee, R. J., F. M. Rupley, and J. A. Miller, "The CHEMKIN Thermodynamic Data Base," Sandia Report SAND87-8215B, UC-4, p155, 1991a.
- Kee, R. J., F. M. Rupley, and J. A. Miller, "CHEMKIN-II: A FORTRAN Chemical Kinetics Package for the Analysis of Gas-Phase Chemical Kinetics," Sandia Report SAND89-8009, UC-401, p 127, 1991b.
- Kerr, J. B. and C. T. McElroy, "Evidence for large Upward Trends of Ultraviolet-B Radiation Linked to Ozone Depletion," *Science*, 262, 1032-1034, 1993.
- Keyser, L. F., NASA Technical Memorandum 33-782, 1976.
- Klenk, K. F., P. K. Bhartia, A. J. Fleig, V. G. Kaveeshwar, R. D. McPeters, and P. M. Smith, "Total ozone determination from the backscattered ultraviolet (BUV) experiment," *J. Appl. Meteorol.*, 21, 1672-1684, 1982.
- Klimovskii, A. O., A.V. Bavin, V. S. Tkalich, and A. A Lisachenko, *React. Kinet. Catal. Lett.*, 23, 95-8, 1983.
- Ko, M., R.-L. Shia, D. Weisenstein, J. Rodriguez and N.-D. Sze, "Global Stratospheric Impact of Solid Rocket Motor Launchers," Report submitted to TRW, Redondo Beach, California, August 1999.
- Ko, M, K., N. D. Sze, and M. J. Prather, "Better protection for the ozone layer," *Nature*, 367, 505-509, 1994.
- Kolb, C. E., D. R. Worsnop, M. S. Zahniser, P. Davidovits, C. F. Keyser, M. T. Leu, M. J. Molina, D. R. Hanson, A. R. Ravishankara, L. R. Williams, and M. A. Tolbert, "Laboratory studies of atmospheric heterogeneous chemistry," In *Current Problems and Progress in Atmospheric Chemistry*, edited by J.R. Barker, in *Advances in Physical Chemistry Series*, Volume 3, 771-875, World Scientific Publishing, 1995.
- Kruger, B. C., "Ozone depletion in the plume of a solid-fuel rocket," *Ann. Geophysicae*, 12, 409-416, 1994.
- Kruger, B. C., M. M. Hirschberg, and P. Fabian, "Effect of solid-fueled rocket exhausts on the stratospheric ozone layer," *Ber. Bunsenges. Phys. Chem.*, 96, 268-272, 1992.
- Lewis, D. H., J. E. Trost, E. Wong, W. D. English, "Utilization of Alternate Propellants to Reduce Stratospheric Ozone Depletion," Prepared by TRW for Space and Missile Systems Center, 31 May 1994.

- Lewis, D. H., et al., "IR Boost Phase Countermeasures," Study for USAF/Ballistic Missiles Office under Advanced Small Missile System (ASMA) SE/TA Contract, 1987.
- Louis, J. F., "Two-Dimensional Transport Model of the Atmosphere," Thesis, University of Colorado, Boulder, Colorado, 1974.
- Lohn, P. D., and E. Y. Wong, "Rocket exhaust impact on stratospheric ozone," Prepared by TRW for Space and Missile Systems Center, El Segundo, California, June 1999.
- Lohn, P. D., E. Y. Wong, D. D. Spencer, R. M., L. T. Molina, and M. J. Molina, P. S. Connell, J. J. Walton, J. E. Penner and C. O'Connor, "The Effects of Rocket Exhaust on Stratospheric Ozone: Chemistry and Diffusion," Prepared by TRW for Space and Missile Systems Center, August 1996
- Lohn, P. D., E. Y. Wong, M. J. Molina, M. R. Denison, J. J. Lamb, "The Impact of Deorbiting Space Debris on Stratospheric Ozone," Prepared by TRW for Space and Missile Systems Center, May 31, 1994.
- Mallard, W. G., F. Westley, J. T. Herron, R. F. Hampson, and D. H. Frizzell, "NIST Chemical Kinetics Database; Version 6.0," NIST, Gaithersburg, MD, 1994.
- Mankin, W. G., and M. T. Coffey, "Latitudinal Distributions and Temporal Changes of Stratospheric HCl and HF," *J. Geophys. Res.*, 88, 10,776-10,884, 1983.
- Martin L. R., "A Survey of the Potential Effects of Increasing UV-B Radiation on the Biosphere," Aerospace Technical Report No. *TR-98(1306)-6*, 30 September 1998.
- Martin L. R., "Possible Effect of the Chlorine Oxide Dimer on Transient Ozone Loss in Rocket Plumes," Aerospace Report No. *ATR-94(4231)-1*, 15 March 1994.
- Martin, L. R., and M. N. Ross, Aerospace Technical Report *ATR-93(3231)-2*, 1993.
- McDonald, Allan and Robert Bennett, "*Environmental Impacts from Launching Chemical Rockets*," Advisory Group for Aerospace Research and Development (AGARD) Conference Proceedings no 559, Canadian Communication Group, Hull, Quebec, Canada, 1995.
- McDonald, A. J., R. R. Bennett, J. C. Hinshaw, and M. W. Barnes, "Chemical propulsion and the environment," *Aerospace America*, 32-36, May 1991.
- McKenzie, D. L., K. B. Crawford, D. J. Gutierrez, J. H. Hecht, N. Katz, D. J. Mabry, and W. J. Skinner, "High-Resolution Ozone Imager (HIROIG) Final Report," Aerospace Technical Report *ATR-98(1306)-2*, 1998
- McPeters, R., M. Prather, and S. Doiron, "Reply to 'Comment on 'the Space Shuttle's impact on the stratosphere,'" *J. Geophys. Res.*, 96, 17379-17381, 1991.

- Meads, R., Darryl D. Spencer, and Mario J. Molina, "The Stratospheric Chemistry of Aluminum Oxide Particles," Report to TRW, June 1994.
- Molina, M. J., "Stratospheric Effects of Rocket Exhaust: Heterogeneous Processes," Report submitted to TRW, Redondo Beach, California, August 1999.
- Molina, M. J., L. T. Molina, R. Zhang, R. F. Meads, and D. D. Spencer, "The reaction of ClONO₂ with HCl on aluminum oxide," *Geophys. Res. Lett.*, *24*, 1619-1622, 1997.
- Molina, M. J., D. D. Spencer, L. T. Molina, and R. F. Meads, "Chlorine Activation on Alumina and Glass Surfaces," paper presented at the symposium on *The Impact of Rockets on the Stratosphere*, Redondo Beach, California, May 1996.
- Molina, L. T., and M. J. Molina, "Production of Cl₂O₂ from Self-Reaction of the ClO Radical," *J. Phys. Chem.*, *91*, 433-436, 1987.
- Molina, M. J. and F. S. Rowland, "Stratospheric sink for chlorofluoromethanes: chlorine atom-catalyzed destruction of ozone," *Nature*, *249*, 810, 1974.
- NSWC Indian Head Division, "Combustion Products of Solid Rocket Motors," August 1996.
- Pergament, H. S., R. I. Gomberg, and I. G. Poppoff, "*Proceedings of the Space Shuttle Environmental Assessment Workshop on Stratospheric Effects*," *NASA Tech. Memo X-58198*, NASA, Houston, TX, 1977a.
- Pergament H. S., R. I. Gomberg, and I. G. Poppoff, "NO_x Deposition in the Stratosphere from the Space Shuttle Rocket Motors," Appendix G to Proceedings of the Space Shuttle Environmental Assessment Workshop on Stratospheric Effects, JSC11633, *NASA TM X-58198*, January 1997b.
- Peri, J. B., "Infrared and Gravimetric Study of Surface Hydration of γ -Alumina," *J. Phys. Chem.*, *69*, 211, 1965.
- Peter, T., "Microphysics and heterogeneous chemistry of polar stratospheric clouds," *Ann. Rev. Phys. Chem.*, *48*, 785-822, 1997.
- Potter, A.E., "Environmental effects of the Space Shuttle," *J. Environ. Sci.*, *21*, 15-21, 1978.
- Potter, A. E., ed., "Proceedings of the Space Shuttle Environmental Assessment Workshop on Stratospheric Effects," *NASA TM X-58198*, Jan. 1977.
- Prather, M. J., "The Impact of Tropospheric Rocket Exhaust on Stratospheric Ozone," Prepared by TRW for Space and Missile Systems Center, May 1994.

- Prather, M. J., M. M. Garcia, R. Suozzo, and D. Rind, "Global impact of the Antarctic ozone hole: Dynamical dilution with a 3-D chemical transport model," *J. Geophys. Res.*, *95*, 3449-3471, 1990a.
- Prather, M. J., M. M. Garcia, A. R. Douglass, C. H. Jackman, M. K. W. Ko, and N.-D. Sze, "The Space Shuttle's impact on the stratosphere," *J. Geophys. Res.*, *95*, 18583-18590, 1990b.
- Prather, M. J., M. M. Garcia, A. R. Douglass, C. H. Jackman, M. K. W. Ko, and N.-D. Sze, "An assessment of the impact on stratospheric chemistry and ozone caused by the launch of the Space Shuttle and Titan IV," in Present State of Knowledge of the Upper Atmosphere 1990: An Assessment Report, NASA Reference Publication 1242, 111-122, 1990c.
- Prather, M. J., and R. T. Watson, "Stratospheric Ozone Depletion and Future Levels of Atmospheric Chlorine and Bromine," *Nature*, *344*, 729-734, 1990d.
- Prather, M. J., and J. M. Rodriguez, "Antarctic ozone: Meteoric control of HNO₃," *Geophys. Res. Lett.*, *15*, 1-4, 1988.
- Prather, M. J., M. McElroy, S. Wofsy, G. Russell, and D. Rind, "Chemistry of the global troposphere: Fluorocarbons as tracers of air motions," *J. Geophys. Res.*, *92*, 6579-6613, 1987.
- Prather, M.J., "Numerical advection by conservation of second-order moments," *J. Geophys. Res.* *91*, 6671-6681, 1986.
- Proffitt, M. H., "Ozone measurement from a balloon payload using a new fast-response UV-absorption photometer," 470-474, in: Zerefos, C. S. and Ghazi, A. (eds), *Atmospheric Ozone*, D. Reidel Pub. Co, Dordrecht, Holland, 1985.
- Proffitt, M. H., and R. J. McLaughlin, "Fast-response dual-beam UV-absorption photometer for use on stratospheric balloons," *Rev. Sci. Instrum.*, *54*, 1719-1728, 1983.
- Pyle, J. A., and A. E. Jones, "An investigation of the impact of the Ariane-5 launches on stratospheric ozone," Prepared for the European Space Agency, 1991.
- RLV, "*Reusable Launch Vehicle Programs and Concepts*," Associate Administrator for Commercial Space Transportation, Federal Aviation Administration, January 1998.
- Rodriguez, J. M., M. K. W. Ko, and N.-D. Sze, "Role of heterogeneous conversion of N₂O on sulphate aerosols in global ozone losses," *Nature*, *352*, 134-137, 1991.
- Roesler, J. F., R. A. Yetter, and F. L. Dryer, "Kinetic Interactions of CO, NO_x, and HCl Emissions in Photo-combustion Gases," *Combustion & Flame*, *100*, 495-504, 1995.

- Roesler, J. F., R. A. Yetter, and F. L. Dryer, "The Inhibition of the CO/H₂O/O₂ Reaction by Trace Quantities of HCl," *Combust. Sci. and Tech.*, 82, 87-100, 1992a.
- Roesler, J. F., R. A. Yetter, and F. L. Dryer, "Detailed Kinetic Modeling of Moist CO Oxidation Inhibited by Trace Quantities of HCl," *Combust. Sci. and Tech.*, 85, 11-22, 1992b.
- Ross, M. N., P. D. Whitefield, D. E. Hagen, and A. R. Hopkins, "In-situ Measurement of the Aerosol Size Distribution in Stratospheric Solid Rocket Motor Exhaust Plumes," *Geophys. Res. Lett.*, in press, 1999.
- Ross, M. N., J. O. Ballenthin, R. B. Gosselin, R. F. Meads, P. F. Zittel, J. R. Benbrook, and W. R. Sheldon, "In-situ measurement of Cl₂ and O₃ in a stratospheric solid rocket motor exhaust plume," *Geophys. Res. Lett.*, 24, 1755-1758, 1997a.
- Ross, M. R., J. R. Benbrook, W. R. Sheldon, P. F. Zittel, & D. L. McKenzie, "Observation of stratospheric ozone depletion in rocket exhaust plumes," *Nature*, 390, 62-64, 1997b.
- Ross, M. N., "Rocket Impacts on Stratospheric Ozone," AIAA-97-0525, 6-10 January 1997c.
- Ross M. N., "Local Impact of Large Solid Rocket Motor Exhaust on Stratospheric Ozone and Surface Ultraviolet Flux," *J. Spacecraft and Rockets*, 33, 435, 1996a.
- Ross, M. R., J. R. Benbrook, W. R. Sheldon, P. F. Zittel & D. L. McKenzie, "Local effects of solid rocket motor exhaust on stratospheric ozone," *J. Spacecraft Rockets*, 33, 144-153, 1996b.
- Ross, M. N., "Potential impact of solid rocket exhaust on stratospheric ozone," The Aerospace Corporation, TOR-92(2565)-2, 1992.
- Rowland, F. S., "President's Lecture: The need for Scientific Communication with the Public," *Science*, 260, 1571-6, 1993.
- Rowland, F. S., "Stratospheric Ozone Depletion," *Annual Review of Physical Chemistry*, 42, 731-768, 1991.
- Rowland, F. S., and M. J. Molina, "Chlorofluoromethanes in the Environment," *Rev. Geophys. Space Phys.*, 13, 1-35, 1975.
- Sackheim, R. L., F. J. Stoddard, and J. A. Hardgrove, "Propulsion Advancements to Lower the Cost of Satellite Based Communications Systems," *AIAA Paper 94-0930*, 1994.
- Schott, G. L, and J. L. Kinsey, "Kinetic Studies of Hydroxyl Radicals in Shock Waves II. Induction Times in the Hydrogen-Oxygen Reaction," *J. Chem. Phys.*, 29, 1177, November 1958.

- Shumann, U., Editor, "Pollution from Aircraft Emissions in the North Atlantic Flight Corridor (POLINAT)," Final Report to the Commission of European Communities, October 1996.
- Simmons, F. S. "A Handbook for Infrared Emission from Missile Plumes-Volume I: Low Altitudes", *TOR-0083(3753-08)-1*, Vol:1, Aerospace Corp., El Segundo, Ca., 1 October 1982, SECRET.
- Skinner, G. B., and G. H. Ringrose, "Ignition Delays of a Hydrogen–Oxygen–Argon Mixture at Relatively Low Temperature," *J. Chemical Physics*, 42, 2190, March 15, 1965.
- Slack, M., J. W. Cox, A. Grillo, R. Ryan, and O. Smith, "Potassium Kinetics in Heavily Seeded Atmospheric Pressure Laminar Methane Flames," *Combustion and Flame*, 77, 311–320, 1989.
- Solomon, S., "The Mystery of the Antarctic Ozone Hole," *Rev. Geophys.*, 26, 131, 1988.
- Solomon, S., R. R. Garcia, F. S. Rowland, D. J. Wuebbles, "On the Depletion of Antarctic Ozone," *Nature*, 321, 755, 1986.
- SRS Handbook, "*Eliminating Use of Ozone Depleting Substances in Solid Rocket Motor Manufacturing*," from the Handbook of Solid Rocket Motor Manufacturing within the United States, Prepared by SRS Technologies for Space and Missile Systems Center, 5 February 1995.
- Stolarski, R., R. Bojkov, L. Bishop, C. Zerefos, J. Staehelin, J. Zawodny, "Measured Trends in Stratospheric Ozone," *Science*, 256, 342-349, 1992.
- Stolarski, R. S., P. Bloomfield, R. D. McPeters, J. R. Herman, *Geophys. Res. Lett.*, 18, 1015, 1991.
- Strand, L. D., J. M. Bowyer, G. Varsi, E. G. Laue and R. Gauldin, "Characterization of Particulates in the Exhaust Plume of Large Solid-Propellant Rockets," *J. Spacecraft Rockets*, 18(4), 297-305, 1984.
- Syage, J. A., and M. N. Ross, "An assessment of the total ozone mapping spectrometer for measuring ozone levels in a solid rocket plume," *Geophys. Res. Lett.*, 23, 3227-3230, 1996.
- Syage, J. A., "Can the total ozone mapping spectrometer (TOMS) measure ozone depletion in rocket plumes," The Aerospace Corporation, *TR-95(5231)-4* [AFSMC Report SMC-TR-95-31], 1995.
- Tabazadeh, A. and R.P. Turco. "Stratospheric chlorine injection by volcanic eruptions: HCl scavenging and implications for ozone," *Science*, 260, 1082-1086, 1993.

- Tishin, Anatoli and Eric Alenandrov, “*The Impact of Space Rocket Launches on the Earth Ozone Layer*”; Advisory Group for Aerospace Research and Development (AGARD); Conference Proceedings no. 559, Canadian Communication Group, Hull, Quebec, Canada, 1995.
- Torres, O., Z. Ahmed, and J. R. Herman, “Optical effects of polar stratospheric clouds on the retrieval of TOMS total ozone,” *J. Geophys. Res.*, *95*, 13015-13024, 1992.
- TRW Space Log, Volume 31, TRW Space & Electronics Group, One Space Park, Redondo Beach, CA 90278, 1996.
- Turco, R. P., O. B. Toon, R. C. Whitten, and R. J. Cicerone, “Space Shuttle ice nuclei,” *Nature*, *298*, 830-832, 1982.
- Turco, R. P., O. B. Toon, J. B. Pollack, R. C. Whitten, J. G. Poppoff, and P. Hamill, “Stratospheric aerosol modification by supersonic transport and Space Shuttle operations - climate implications,” *J. Appl. Meteor.*, *19*, 78-89, 1980.
- Vanpee, M., R. H. Tromans, and D. Burgess, “Inhibition of Afterburning by Metal Compounds,” in *Heterogeneous Combustion, Progress in Aeronautics and Astronautics*, Volume 15. Edited by H. G. Wolfhard, I. Glassman and L. Green, Jr., Academic Press, 1964.
- Versar, Inc., “*Final Environmental Assessment Vandenberg Air Force Base Atlas II Program*,” August 1991.
- Warneck, P., “*Chemistry of the Natural Atmosphere*,” International Geophysics Series, Volume 41, Academic Press, Inc., San Diego, CA., 1988.
- Watson, R. T., P. E. Smokler, and W. B. DeMore, “An assessment of an F₂ or N₂O₄ atmospheric injection from an aborted Space Shuttle mission,” NASA JPL Publication 77-81, 1978.
- Weisenstein, D. K., G. K. Yue, M. K. W. Ko, N.-D. Sze, J. M. Rodriguez, and C. J. Scott, “A two-dimensional model of sulfur species and aerosols,” *J. Geophys. Res.*, *102*, 13,019-13,035, 1997.
- Weisenstein, D., M. K. W. Ko, and N.-D. Sze, “The chlorine budget of the present-day atmosphere: A modeling study,” *J. Geophys. Res.*, *97*, 2547-2559, 1992.
- Weinstock, E. M., C. M. Schiller, and J. G. Anderson, “*In-situ* stratospheric ozone measurements by long path UV absorption: developments and interpretation,” *J. Geophys. Res.*, *94*, 5237-5248, 1986.
- Whitefield, P. D., D. E. Hagan, A. R. Hopkins, and M. N. Ross, “Rocket Impact on Stratospheric Ozone: Submicron Aerosol Measurement,” *AIAA-97-0529*, 6-10 January 1997.
- Worsnop, D. R., M. S. Zahniser, C. E. Kolb, J. A. Gardner, L. R. Watson, J. M. Van Doren, J. T.

- Jayne, and P. Davidovits, *J. Phys. Chem.*, *93*, 1157-72, 1989.
- WMO, World Meteorological Organization, “*Scientific Assessment of Ozone Depletion: 1998*,” Rep. No. 44, Global Ozone Research and Monitoring Project, Geneva, Switzerland, 1998.
- WMO, World Meteorological Organization, “*Scientific Assessment of Ozone Depletion: 1994*,” Rep. 37, Global Ozone Research and Monitoring Project, Geneva, Switzerland, 1995.
- WMO, World Meteorological Organization, “*Scientific Assessment of Ozone Depletion: 1991*,” Ch. 10, Rep. No. 25, Global Ozone Research and Monitoring Project, Geneva, Switzerland, 1991.
- WMO, World Meteorological Organization, “*Report of the International Ozone Trends Panel: 1988*,” Rep. 18, Geneva, Switzerland, 1988.
- WMO, World Meteorological Organization, “*Atmospheric Ozone: Assessment of Our Understanding of the Processes Controlling Its Present Distribution and Change: 1985*,” Rep. No. 16, Global Ozone Research and Monitoring Project, Geneva, Switzerland, 1985.
- X-33, National Aeronautics and Space Administration (NASA), “*Final X-33 Programmatic Environmental Assessment: Vehicle and Technology Demonstration Concept*,” NASA Marshall Space Flight Center, Environmental Engineering and Management Office, AL, June 1996.
- Zander, R., M. R. Gunson, C. B. Farmer, C. P. Rinsland, F. W. Irion, and E. Mahieu, “The 1985 chlorine and fluorine inventories in the stratosphere based on ATMOS observations at 30 North Latitude,” *J. Atm. Chem.*, *15*, 171-186, 1992.
- Zhang, R., J. T. Jayne and M. J. Molina, “Heterogeneous interactions of ClONO₂ and HCl with sulphuric acid tetrahydrate: Implications for the stratosphere,” *J. Phys. Chem.*, *98*, 867-874, 1994.
- Zittel, P. F., “Computer Model Calculations of NO_x Production in Rocket Motors and Plumes,” Aerospace Technical Report *TOR-96(1306)-1*, 1995.
- Zittel, P. F. “Computer Model Predictions of the Local Effects of Large, Solid-Fuel Rocket Motors on Stratospheric Ozone,” Aerospace Technical Report *TR-94(4231)-9* [AFSMC Report *SMC-TR-94-36*], The Aerospace Corporation, September 1994.
- Zittel, P. F., “Local effects of large, solid rocket motors on stratospheric ozone,” Aerospace Technical Report *ATR-92(9558)-2*, 1992.
- Zolensky, M. E., D. S. McKay, and L. A. Kaczor, “A tenfold increase in the abundance of large solid particles in the stratosphere, as measured over the period 1976-1984,” *J. Geophys. Res.*, *94*, 1047-1056, 1989.

APPENDIX A

List Of Acronyms & Abbreviations

A-50	Aerazine-50 fuel (50% N ₂ H ₄ and 50% UDMH)
AER	Atmospheric and Environmental Research, Inc.
AF	Air Force
AFB	Air Force Base
AFSPC	Air Force Space Command
AIAA	American Institute of Aeronautics and Astronautics, Inc.
AKM	Apogee Kick Motor
Al	Aluminum
Alumina	Particulate generated from Aluminum and Aluminum Oxide
AN	Ammonium Nitrate
AP	Ammonium Perchlorate
APE	Auxiliary Propulsion Engines
AR40, etc.	Ariane-40, etc.
AS	Air Station
AST	Office of the Associate Administrator for Commercial Space Transportation (Formerly known as Office of Commercial Space Transportation)
AXAF	Air Force Environmental Management Division
BCSC	Boeing Commercial Space Company
BTTN	Butanetriol Trinitrate
BuNENA	n-butyl-2-nitratoethyl-nitramine
BUV	Backscatter Ultraviolet Spectrometer
CALT	China Academy of Launch Vehicle Technology
CCAS	Cape Canaveral Air Station, Florida
CCN	Cloud Condensation Nuclei
CDN	Cyclodextrin Nitrate
CFC	Chlorofluorocarbon
CFR	Code of Federal Regulations
CGWIC	China Great Wall Industry Corporation
CIMS	Chemical Ionization Mass Spectrometer
CIS	Commonwealth of Independent States (Formerly USSR)
CLTC	China Satellite Launch
CNES	Centre National d'Etudes Spatiales (French Space Agency)
COMSTAC	Commercial Space Transportation Advisory Council
CSLA	Commercial Space Launch Act
CTM	Chemistry Transport Model
CUS	Cryogenic Upper Stage
CZ	Chang Zheng (China Launch Vehicle)

APPENDIX A
List Of Acronyms & Abbreviations (Continued)

1-D	One Dimensional Computational Model
2-D	Two Dimensional Computational Model
3-D	Three Dimensional Computational Model
DIAL	Differential Absorption LIDAR
DOD	Department of Defense
DOT	Department of Transportation
DU	Dobson Unit
EELV	Evolved Expendable Launch Vehicle
EEZ	Exclusive economic zone
EIS	Environmental Impact Statement
EOS	Earth Observing System
EPA	Environmental Protection Agency
ESA	European Space Agency
ET	External Tank
EUS	Energia Upper Stage
FAA	Federal Aviation Administration
FB	Feng Bao (Storm Booster)
FEIS	Final Environmental Impact Statement
FLOX	Fluorine Liquid Oxygen Oxidizer
FOV	Field of View
FTIR	Fourier Transform Infrared Absorption Spectroscopy
γ	Reaction Probability
GAP	Glycidyl Azide Polymer
GEO	Geosynchronous Earth Orbit
GHE	Gaseous Helium
GMT	Greenwich Mean Time
GN2	Gaseous Nitrogen
GTO	Geosynchronous Transfer Orbit
GWP	Global Warming Potential
H18	Cryogenic Stage (18 metric tons propellant)
H155	Cryogenic Stage (155 metric tons propellant)
h	Planck's Constant
HCFC	Hydrochlorofluorocarbon
HFC	Hydrofluorocarbon

APPENDIX A
List Of Acronyms & Abbreviations (Continued)

HLV	Heavy Launch Vehicle
HMX	Cyclotetramethylene tetranitramine
HTPB	Hydroxy Terminated Polybutadiene, Polymeric binders and catalysts
hPa	hectoPascal
HSCT	High Speed Civil Transports
ICBM	Intercontinental Ballistic Missile
IPDI	Isophorone Diisocyanate
IR	Infrared
IRBM	Intermediate Range Ballistic Missile
IRFNA	Inhibited Red Fuming Nitric Acid
I_{sp}	Specific Impulse
JSLC	Jiuquan Satellite Launch Center (China)
K	Degrees Kelvin
KDN	Potassium Dinitramide
kg	Kilogram
km	Kilometer
KP	Potassium Perchlorate
L9	Storable Stage (9 metric tons propellant)
L140	Liquid Stage (140 metric tons propellant)
L	Liters (Volume Measurement)
LAAFB	Los Angeles Air Force Base
LDEF	Long Duration Exposure Facility
LEL	Lower Explosion Limit
LEO	Low Earth Orbit
LH ₂	Liquid Hydrogen Fuel
LIDAR	LIght Detection and Ranging
LIMS	Limb Infrared Monitor of the Stratosphere
LLV	Lockheed Launch Vehicle
LM	Long March (China LV)
LOX	Liquid Oxygen Fuel
LP	Launch Platform
LRB	Liquid Rocket Booster
LV	Launch Vehicle

APPENDIX A
List Of Acronyms & Abbreviations (Continued)

μm	Micron, Micrometer (10 ⁻⁶ m)
m	Meter
mb	Millibar
MADS	Modular Array Demonstration Program
MEO	Medium Earth Orbit
MLT	Mobile LIDAR System
MLV	Medium launch vehicle
MMH	Monomethyl Hydrazine
MNA	Methylnitroaniline
n/a	Not Applicable or Data Not Available
N ₂ H ₄	Anhydrous Hydrazine
N ₂ O ₄	Nitrogen Tetroxide
NASA	National Aeronautics and Space Administration
NAT	Nitric Acid Trihydrate
NASP	National Aerospace Plane
NBS	National Bureau of Standards (now NIST)
2-NDPA	2-Nitrodiphenylaniline
NC	Nitrocellulose
NEPA	National Environmental Policy Act of 1969
NFPA	National Fire Protection Association
NIST	National Institute of Standards and Technology (formerly NBS) (US)
nm	Nanometer (10 ⁻⁹ m)
NMHCs	Non-methane hydrocarbons
NMM	National Executable Mission Model
NOAA	National Oceanic and Atmospheric Administration
NO _x	Oxides of Nitrogen
NTO	Nitrogen Tetroxide (N ₂ O ₄) Oxidizer
ODC	Ozone Depleting Chemical
ODP	Ozone Depletion Potential
ODS	Ozone Depleting Substance
OSHA	Occupational Safety and Health Administration
P _{HCl}	Partial Pressure of HCl
PBAN	Polybutadiene Acrylonitrile Acrylic Acid, Polymeric binders and catalysts
PEL	Permissible Exposure Limit
PEG	Polyethylene Glycol
PGN	Polyglycidyl Nitrate

APPENDIX A
List Of Acronyms & Abbreviations (Continued)

PIM	Plume <i>In-Situ</i> Measurement Experiment
PKM	Perigee Kick Motor
PLA	Payload Adapter
PLE	Plume LIDAR Experiment
PLF	Payload Fairing
ppb	Part per billion (1 in 10 ⁹)
ppbv	Part per billion by volume
PSCs	Polar Stratospheric Clouds
psi	Pounds per square inch
PSLV	Polar Satellite Launch Vehicle
PSOM	PSLV Strap-On Motors
PST	Pacific Standard Time
RLV	Reusable Launch Vehicle
RISO	Rocket Impacts on Stratospheric Ozone Program
RP-1	Rocket Propellant-1, Kerosene fuel
SBUV	Solar Backscatter Ultraviolet Spectrometer
SIMS	Secondary Ion Mass Spectrometry
SMC	Space & Missile Command
SPF	Standard Plume Flowfield Model
SLLP	Sea Launch Limited Partnership
SLS	Sea Launch System
SLV	Satellite Launch Vehicle
SMM	Solar Maximum Mission
SOB	Strap-On Booster
Spelda	Structure Porteuse Externe Pour Lancements Doubles Ariane (Europe)
Speltra	Structure Porteuse Externe Pour Lancements Triples Ariane (Europe)
SRB	Solid Rocket Booster
SRM	Solid Rocket Motor
SRMU	Solid Rocket Motor Upgrade
SSME	Space Shuttle Main Engine
SSN	Space Surveillance Network
SSO	Sun Synchronous Orbit
SST	Space Shuttle
SSTO	Single-stage-to-orbit
SUS	Storable upper stage
Sylda	Systeme de Lancements Double Ariane (Europe)

APPENDIX A
List Of Acronyms & Abbreviations (Continued)

T3B	Titan IIIB rocket
TEGDN	Triethyleneglycol Dinitrate
TOMS	Total Ozone Mapping Spectrometer
TOS	Transfer Orbit Stage
TSPS	Tank Sampling and Pressurization System
UCI	University of California Irvine (United States)
UDMH	Unsymmetrical Dimethylhydrazine
UNEP	United Nations Environment Program
UNI	Ultraviolet Network Instrumentation
U.S.	United States of America
USSR	Union of Soviet Socialist Republic, hereafter CIS
UV	Ultraviolet
UVA	Ultraviolet-A (400 – 320 nm)
UVB	Ultraviolet-B (320 – 290 nm)
X-33	Experimental-33 RLV
v	Frequency
VAFB	Vandenberg Air Force Base, California
WMO	World Meteorological Organization

APPENDIX B

List of Chemical Formulae and Nomenclature

HALOCARBONS

Chlorofluorocarbons (CFCs)

Symbol	Name
CFC-10	CCl_4
CFC-11	CCl_3F
CFC-12	CCl_2F_2
CFC-13	CClF_3
CFC-14	CF_4
CFC-113	$\text{CCl}_2\text{FCClF}_2$
CFC-114	$\text{CClF}_2\text{CClF}_2$
CFC-115	CClF_2CF_3
CFC-116	CF_3CF_3

Hydrofluorocarbons (HFCs)

Symbol	Name
HFC-23	CHF_3
HFC-32	CH_2F_2
HFC-41	CH_3F
HFC-125	CHF_2CF_3
HFC-134	CHF_2CHF_2
HFC-134a	CH_2FCF_3
HFC-143	$\text{CHF}_2\text{CH}_2\text{F}$
HFC-143a	CH_3F_3

Hydrochlorofluorocarbons (HCFCs)

Symbol	Name
HCFC-21	CHCl_2F
HCFC-22	CHF_2Cl
HCFC-30	CH_2Cl_2
HCFC-40	CH_3Cl
HCFC-123	CF_3CHCl_2
HCFC-124	CF_3CHFCl
HCFC-141b	CFCl_2CH_3
HCFC-142b	CF_2ClCH_3

APPENDIX B
List of Chemical Formulae and Nomenclature (Continued)

Hydrochlorofluorocarbons (HCFCs)

Symbol	Name
HCFC-225ca	CF ₃ F ₂ CHCl ₂
HCFC-225cb	CF ₃ ClCF ₂ CHFCI
HCFC-152a	CH ₃ CHF ₂
HCFC-227ea	CF ₃ CHF ₂ CF ₃
HCFC-236cb	CF ₃ CF ₂ CH ₂ F
HCFC-236ea	CF ₃ CHFCHF ₂
HCFC-236fa	CF ₃ CH ₂ CF ₃
HCFC-245ca	CHF ₂ CF ₂ CFH ₂
HCFC-43-10mee	CF ₃ CHFCHF ₂ CF ₃

Halons

Symbol	Name
halon-1211	CF ₂ ClBr
halon-1301	CF ₃ Br
halon-2402	C ₂ F ₄ Br ₂

Fluorocarbons

Symbol	Name
C ₃ F ₈	Perfluoropropane
c-C ₄ F ₈	Perfluorocyclobutane
C ₆ F ₁₄	Perfluorohexane
CHF ₃	Fluoroform, Trifluoromethane
TFA, CF ₃ COOH	Trifluoroacetic acid
CH ₂ ClI	Chloriodomethane
CF ₃ I	Trifluoromethyl Iodide
C ₂ F ₅ I	Iodopentafluoroethane

APPENDIX B
List of Chemical Formulae and Nomenclature (Continued)

Hydrocarbons (HC)

Symbol	Name
NMHC	Non-methane hydrocarbon
VOC	Volatile Organic Compound
CH ₄	Methane
C ₂ H ₆	Ethane
C ₃ H ₈	Propane
C ₂ H ₄	Ethene, Ethylene
C ₂ H ₂	Ethyne, Acetylene
C ₅ H ₈	Isoprene, 2-methyl-1,3-butadiene
C ₆ H ₆	Benzene
CH ₃ CN	Methyl Cyanide, acetonitrile
PAN	Peroxyacetylnitrate
CO	Carbon Monoxide
CO ₂	Carbon Dioxide
CS ₂	Carbon Disulfide
COS, OCS	Carbonyl Sulfide
CH ₂ O	Formaldehyde
CH ₃ CHO	Acetaldehyde
(CH ₃) ₂ CO	Acetone
CH ₃ O ₂ H	Methyl Hydroperoxide
CH ₂ CHCHO	Acrolein

Others

Symbol	Name
Br	Bromine atom
BrO	Bromine Monoxide
Br _x	Odd Bromine, Inorganic Bromine
BrNO ₂	Bromine Nitrite
BrONO ₂	Bromine Nitrate
HBr	Hydrogen Bromide
HOBr	Hypobromous acid
CH ₃ Br	Methyl Bromide
CH ₂ Br ₂	Methylene Bromide
CHBr ₃	Bromoform, tribromomethane
C ₂ H ₄ Br ₂	1,2-Dibromoethane
CHBr ₂ Cl	Dibromochloromethane

APPENDIX B
List of Chemical Formulae and Nomenclature (Continued)

Others

Symbol	Name
Cl	Chlorine atom
ClO	Chlorine Monoxide
Cl _x	Odd Chlorine, Inorganic Chlorine
ClNO ₂	Chlorine Nitrite
ClONO ₂ , ClNO ₃	Chlorine Nitrate
HCl	Hydrogen Chloride
HOCl	Hypochlorous acid
CH ₃ Cl	Methyl Chloride
CH ₂ Cl ₂	Methylene Chloride
CHCl ₃	Chloroform
CCl ₄	Carbon Tetrachloride
C ₂ H ₄ Cl ₂	1,2-Dichloroethane
CH ₃ CCl ₃	Methyl Chloroform
C ₂ HCl ₃	Trichloroethylene
C ₂ Cl ₄	Tetrachloroethylene
COCl ₂	Phosgene, Carbonyl Chloride
F	Fluorine atom
FO	Fluorine Monoxide
HF	Hydrogen Fluoride
COFCl	Fluorophosgene
H	Atomic Hydrogen
H ₂	Molecular Hydrogen
OH, HO	Hydroxyl radical
H ₂ O	Water vapor
HO ₂	Hydroperoxyl radical
H ₂ O ₂	Hydrogen Peroxide
HO _x	Odd Hydrogen (H, HO, HO ₂ , H ₂ O ₂)
I	Atomic Iodine
IO	Iodine Monoxide
HI	Hydrogen Iodide
IONO ₂	Iodine Nitrate
CH ₃ I	Methyl Iodide

APPENDIX B
List of Chemical Formulae and Nomenclature (Continued)

Others

Symbol	Name
N	Atomic Nitrogen
N ₂	Molecular Nitrogen
N ₂ O	Nitrous Oxide
NO	Nitric Oxide
NO ₂	Nitrogen Dioxide
NO ₃	Nitrogen Trioxide, Nitrate radical
NO _y	Odd Nitrogen (NO, NO ₂ , NO ₃ , N ₂ O ₅ , ClONO ₂ , HNO ₄ , HNO ₃)
NO _x	Oxides of Nitrogen (NO, NO ₂ , NO ₃)
N ₂ O ₄	NTO, Nitrogen Tetroxide
N ₂ O ₅	Dinitrogen Pentoxide
HNO ₂ , HOHO	Nitrous acid
HNO ₃ , HONO ₂	Nitric acid
HNO ₄ , HO ₂ NO ₂	Peroxynitric acid
NH ₃	Ammonia
O	Atomic Oxygen
O ₂	Molecular Oxygen
O ₃	Ozone
O _x	Odd Oxygen (O, O ¹ (D), O ₃)
O(¹ D)	Atomic Oxygen (first excited state)
SF ₆	Sulfur Hexafluoride
SO ₂	Sulfur Dioxide
H ₂ SO ₄	Sulfuric acid
HCN	Hydrogen Cyanide

APPENDIX C.

Compilation of Launch Vehicles and Their Descriptions by Country of Origin. All of the Following Data Was Retrieved and Condensed From AIAA, Isakowitz, 1994. See this Reference for a Complete Compendium of Data Relating to These Launch Vehicles.

China

- CZ-1 Three stage vehicle derived from the CSS-2 ICBM. First two stages are nitric acid/UDMH propellant and the third stage is solid. One engine for each first and second stage, both controlled by jet vanes*
- CZ-2 Two stage vehicle derived from the CSS-4 IBM. Both stages use N₂O₄/UDMH. Four first stage engines with gimbal control and one second stage engine with four verniers for control*
- FB-1 Two stage liquid vehicle. Similar to CZ-2*
- CZ-2C Same as CZ-2 except upgraded for improved reliability and performance.**
- CZ-3 Same as CZ-2C except aerodynamic fins on first stage, and the addition of a LOX/LH₂ four-nozzle third stage.**
- CZ-4 Same as CZ-2C except aerodynamic fins on first stage, stretched first and second stages and addition of a UDMH/N₂O₄ third stage**
- CZ-2E Same as CZ-2C except stretched stages and four UDMH/N₂O₄ strap-ons for increased performance.**
- CZ-3A Same as CZ-3 except stretched first two stages and a new LOX/LH₂ third stage with two engines derived from the CZ-3.**
- CZ-1D Same as CZ-1 except a UDMH/N₂O₄ second stage and higher orbit injection accuracy.**
- CZ-3B Same as CZ-2E first stage with strap-ons, CZ-3 second stage, and CZ-3A LOX/LH₂ third stage.**

Europe

Ariane

- 1 Stage 1 and 2 storable propellant, stage 3 cryogenic propellant.*
- 2 Same as Ariane-1, except increased thrust for stage 1 and 2 engines, stretched stage 3 for 25% more propellant, 4 sec specific impulse increase in stage 3 engine, increased volume in fairing.*

Appendix C. Description of Launch Vehicles by Country of Origin, AIAA, 1994 (Continued).

Europe

Ariane (Continued):

- 3 *Same as Ariane-2, except two solid strap-on boosters are added.*

- 4 Same as Ariane-3 except stretched and strengthened stage 1 for 61% more propellant, new water tank and new propulsion bay layout; strengthened stage 2 and 3; and a mix of boosters either solid strap-ons (30% more propellant than Ariane-3 solids) or liquid strap-ons.

- 5 Lower composite, which is mission independent, consisting of two large solid strap-ons, and cryogenic propellant core, and upper composite comprised of a final stage.

Example Designations for Ariane-4 and Ariane-5 Launch Vehicles, read from left to right:

Example Designation: 42P021

Designation	Definition	Configuration here
4 is:	Rocket is:	Ariane-4
2 is:	Boosters (0,2,4)	2 Boosters
P is:	Sol. or Liq.	Solid
0 is:	Sylda (0,1)	1 is Sylda 4400
2 is:	Fairing (1,2,3)	2 is 9.6m long Fairing
1 is:	Spelda (0,1,2,3)	0 is No Spelda

India

- SLV-3** *Satellite Launch Vehicle (SLV) is a four stage, solid-propellant vehicle based on earlier sounding rockets.*

- ASLV** Augmented Satellite Launch Vehicle (ASLV) is an upgraded version of the SLV-3 with the first stage motor used as two strap-ons.

- PSLV** Polar Satellite Launch Vehicle (PSLV) has six solid strap-ons similar to the ASLV, a solid-propellant first and third stage, and liquid second and fourth stages.

- GSLV** **Geostationary Satellite Launch Vehicle (GSLV) is derived from PSLV by replacing the six solid strap-ons of PLSV with four liquid strap-ons similar to the second stage of PSLV. A cryogenic upper stage will replace the last two stages of PSLV**

Appendix C. Description of Launch Vehicles by Country of Origin, AIAA, 1994 (Continued).

Israel

Shavit A three-stage solid-propellant vehicle. It is a modified version of the Jericho II intermediate range ballistic missile.

Japan

N-1 Derived from a version of the Thor-Delta launcher, three solid Castor II strap-ons, LOX/RJ-1 first stage, NTO/A-50 second stage.

N-2 Same as N-1, except nine solid Castor II strap-ons, first stage tank extended, second stage engine improved.

H-1 Same as N-2, except new LOX/LH₂ second stage and engine and higher mass fraction third stage.

H-2 New vehicle fully developed with Japanese technology; two large solid strap-ons, LOX/LH₂ first stage, and a LOX/LH₂ derived H-1 second stage.

J-1 Combination of the H-2 Solid Rocket Booster (SRB) and the M-3SII upper stages (second and third stages with the payload fairing).

L-4S This Lambda rocket was first to orbit a payload. Four-stage solid-propellant, with first three stages unguided and fourth stage with attitude control.

M-4S First member of the M-Family. Four stage solid propellant vehicle utilizing fins and spinning for attitude stabilization.

M-3C Same as M-4S, except stage 2 was improved, stage 3 motor was replaced by enlarged M-4S stage 4, and stage 2 used liquid injection thrust vector control (LITVC) and hydrazine side jets for roll control.

M-3H Same as M-3C, except longer stage 1, fairing was lengthened, and option existed for a stage 4.

M-3S Same as M-3H, except added stage 1 LITVC and small motors for roll control (SMRC).

M-3SII Same as M-3S, except enlarged strap-on boosters with steerable nozzles, lengthened stage 2, enlarged stage 3, and wider and longer fairing.

M-V New development with larger diameter stage motors and fairing.

Appendix C. Description of Launch Vehicles by Country of Origin, AIAA, 1994 (Continued).

Russia/Ukraine/CIS

Commonwealth of Independent States (formerly the USSR) or CIS vehicles are identified either by their CIS, U.S., or Sheldon name. In the Soviet Union, it was standard practice to name a launch vehicle after its original payload (e.g., Kosmos, Proton). The U.S. names (developed by the U.S. Department of Defense) are alphanumeric designations roughly on chronological appearance. The Sheldon names, a most commonly used system that was published by Dr. Charles Sheldon of the U.S. Library of congress in 1968, emphasize the basic families of launch vehicles with special indicators for variants within a family.

Example Designation: D-1-e

Designation	Definition	Configuration here
D is:	Family (A,B,C,D,F,G,J,K)	D
1 is:	Upper Stage (1,2)	D1
e is:	e - earth escape or fourth stage	e
	m - maneuverable stage	
	r - reentry stage	

Energia

K-1, SL-17 LOX/LH₂ cryogenic core vehicle with four LOX/kerosene liquid strap-ons based on Zenit first stage. Payloads are located in a side-mounted carrier. The Buran Space Shuttle can also be attached for manned launches. An LOX/LH₂ Energia Upper Stage (EUS) and LOX/kerosene retro and correction stage (RCS) are being developed for high energy and low energy orbit changes, respectively.

Ikar

- 1 Based on the SS-18 "Satan" ICBM (Russian designation RS-20), it is composed of three stages (2 boost stages plus a small insertion stage) utilizing storable propellants.
- 2 **Stages 1 and 2 are identical to those of Ikar-1. Tsyklon stage 3 (designated "S5M") replaces insertion stage.**

Kosmos

C-1, SL-8 Based on the Skean SS-5, it has two stages with storable liquid propellant.

Proton

D, SL-9 *Two stage vehicle using N₂O₄ and UDMH liquid propellant. The first stage has six liquid strap-ons that provide all the thrust. Second stage has four liquid engines.*

Appendix C. Description of Launch Vehicles by Country of Origin, AIAA, 1994 (Continued).

Russia/Ukraine/CIS

Proton (Continued):

D-1, SL-13 Same as D, except the addition of a N₂O₄ and UDMH third stage for increase performance.

D-1-e, SL-12 Same as D-1, except the addition of a LOX and kerosene fourth stage for GEO and interplanetary missions.

Rokot Based on the SS-19 Stiletto (Russian designation RS-18) ICBM. The SS-19 is silo-based, liquid-propellant two stage missile. Rokot consists of the SS-19 first and second stages, plus an additional third stage designated Briz. Briz is apparently a new stage; other applications of this stage have been proposed including use as a fifth stage for Proton.

Soyuz/Molniya

A, SL-1/2 *Based on the Sapwood SS-6 ICBM, it has four symmetrically arranged strap-ons around a core stage, all burning LOX/kerosene propellants.*

Vostok *Same as "A", except addition of a LOX/kerosene core second stage.*

A-1-m, SL-5 *Same as Vostok, except addition of a maneuverable stage.*

Soyuz A-2, SL-4 Same as Vostok, except replacement of the core second stage with a more powerful second stage. The second stage is also LOX/kerosene.

Molniya A-2-e, SL-6 Same as Soyuz, except addition of a LOX/kerosene third stage.

Tsyklon

F-1-r, SL-10 *Based on the Scarp SS-9 ICBM, it has two stages with storable liquid propellant. Includes a reentry rocket which is actually part of the payload*

F-1-m, SL-11 Same as the F-1-r, except includes a maneuverable stage which is actually part of the payload.

F-2, SL-14 Same as F-1-m, except addition of small liquid third stage.

Zenit

Zenit-2 J-1, SL-16 Two stage vehicle using LOX and kerosene liquid propellant. The first stage is also used on Energia as strap-ons. (The "-2" in Zenit-2 refers to the number of stages)

Appendix C. Description of Launch Vehicles by Country of Origin, AIAA, 1994 (Continued).

Russia/Ukraine/CIS

Zenit (Continued):

Zenit-3 Same as Zenit-2, except for addition of a third stage using LOX and
J-1, SL-16 kerosene propellants. The third stage is based on the Proton's Block DM
fourth stage

United States of America

Atlas

A ICBM single stage test vehicle.
B,C ICBM 1-1/2 stage test vehicle.
D ICBM and later space launch vehicle.
E,F First an ICBM (1960), then a reentry test vehicle (1964), then a space launch vehicle
(1968).
LV-3A Same as D, except Agena upper stage.
LV-3B Same as D, except man-rated for Mercury Project.
SLV-3 Same as LV-3A, except reliability improvements.
SLV-3A Same as SLV-3, except stretched 117 inches.
LV-3C Launched with Centaur D upper stage.
SLV-3C Same as LV-3C, except stretched 51 inches.
SLV-3D Same as SLV-3C, except Centaur up-rated to D-1A.
G Same as SLV-3D, except longer by 81 inches.
H Same as SLV-3D, except no Centaur upper stage.
I Same as G, except strengthened for 14 ft. payload fairing
II Same as I, except Atlas lengthened 108 in., engines up-rated, add hydrazine roll
control, and Centaur stretched.
IIA Same as II, except Centaur RL-10s engines up-rated to 20K lbs thrust and 6.5 sec I_{sp}
increase from extendable RL-10 nozzles.
IIAS Same as IIA, except 4 Castor IVA strap-ons added.

Conestoga (first launch in mid-1995)

The booster stage rockets consist of one core CASTOR solid rocket motor (SRM) surrounded by two to six strap-on CASTOR IVA and/or IVB SRMs. An upper stage combination of one to two motors from the STAR 37, 48 or 63 series can be added directly above the core booster SRM. The four digit designator used to identify Conestoga configurations is explained below.

Potential Configurations:

1620
1229
1379
1679

Appendix C. Description of Launch Vehicles by Country of Origin, AIAA, 1994 (Continued).

United States of America

Conestoga (Continued):

Example Designation: 1620

Designation	Definition
1 is:	Vehicle Series by Core SRM type
	1 is CASTOR IVB
	2 is CASTOR IVA
	3 is CASTOR IV AXL (8'8" extension to CASTOR IVA)
6 is:	Number of Strap-on CASTOR IVA/B SRMs
2 is:	Midstage SRM Type
0 is:	Upper Stage Motor Type
	1 - STAR 37FM
	2 - STAR 48V
	3 - Orion 50
	5 - STAR 48A
	6 - STAR 63D
	7 - STAR 63F
	9 - Liquid Transfer Stage
	0 - Upper Stage Only (no mid stage)

Delta

Current Four Digit Designation

Delta II 6925

Delta II 7925

Delta III

Example Designation: 6925

Designation	Definition
6 is:	First Digit - First Stage Type of Augmentation
	0 - Castor II, Long Tank, MB-3 Engine
	1 - Castor II, Extended Long Tank, MB-3 Engine
	2 - Castor II, Extended Long Tank, RS-27 Engine
	3 - Castor IV, Extended Long Tank, RS-27 Engine
	4 - Castor IV, Extended Long Tank, MB-3 Engine
	5 - Castor IVA, Extended Long Tank, RS-27 Engine
	6 - Castor IVA, Extra Extended Long Tank, RS-27 Engine
	7 - GEM, Extra Extended Long Tank, RS-27A Engine
9 is:	Second Digit - Number of Augmentation Motors
	3 - Three Augmentation solid rocket motors
	9 - Nine Augmentation solid rocket motors

Appendix C. Description of Launch Vehicles by Country of Origin, AIAA, 1994 (Continued).

United States of America

Delta (Continued):

- 2 is: Third Digit - Type of Second Stage
0 - AJ10-118 (Aerojet)
1 - TR-201 (TRW)
2 - AJ10-118K (Aerojet)
- 5 is: Fourth Digit - Type of Third Stage
0 - No Third Stage
3 - TE-364-3
4 - TE-364-4
5 - PAM-D Derivative (STAR 48B)

EELV

X-33 **Venturestar™ is the Lockheed Martin version of the Evolved Expendable Launch Vehicle or EELV.**

Delta IV **The Boeing Companies version of the EELV.**

Pegasus/Taurus

Pegasus Three stage, solid-propellant, inertially guided, all-composite winged-launch vehicle carried aloft by an aircraft.

Pegasus XL Growth version of the Pegasus with lengthened Stage 1 and Stage 2, allowing for an increase in propellant of 24% and 30%, respectively.

Taurus Four-stage, inertially guided three-axis stabilized solid-propellant launch vehicle that is fully road mobile. Stages two through four are derived from Pegasus

Space Shuttle

The Space Shuttle consists of a reusable delta-winged space-plane called an orbiter; two solid propellant rocket boosters, which are recovered and reused; and an expendable external tank containing liquid propellants for the orbiter's three main engines.

Appendix C. Description of Launch Vehicles by Country of Origin, AIAA, 1994 (Continued).

United States of America

Titan

- II, Gemini Titan II ICBM converted to a man-rated space launch vehicle.*
IIIA Same as Titan II Gemini except stretched stage 1 and 2 and integral Transtage upper stage.
IIIB Same as Titan IIIA, except Agena upper stage instead of Transtage.
34B Same as Titan IIIA, except stretched stage 1.
IIIC Same as Titan IIIA, except five-segment solid rocket motors.
IIID Same as Titan IIIC, except no upper stage.
IIIE Same as Titan IIID, except Centaur upper stage.
34D Same as Titan 34B, except a 5-1/2-segment solid rocket motor. Uses either Transtage or IUS upper stage.
- II SLV Refurbished Titan II ICBM with 10 ft. payload fairing
- III Same as Titan 34D, except stretched stage 2, single or dual carrier enhanced liquid rocket engines and 13.1 ft. diameter payload fairing. Can use either a PAM-D2, Transtage, or TOS upper stage.
- IV Same as Titan 34D, except stretched stage 1 and stage 2, 7-segment solid rocket motor or three-segment solid rocket motor upgrade. Can use either a IUS or Centaur upper stage.

Out of Production
Current Production
In Development